Multi-level Energy Management Framework with Flexibility Provision in Distribution Networks

Sadam Hussain

A Thesis

in the Department

of

Electrical and Computer Engineering

Presented in Partial Fulfillment of the

Requirements for the Degree of

Doctor of Philosophy (Electrical and Computer Engineering)

at Concordia University

Montreal, Quebec, Canada

February 2024

CONCORDIA UNIVERSITY

School of Graduate Studies

This is to certify that the thesis

prepared By: **Sadam Hussain**

Entitled: **Multi-level Energy Management Framework with Flexibility Provision in Distribution Networks**

and submitted in partial fulfillment of the requirements for the degree of

Doctor of Philosophy (Electrical and Computer Engineering)

complies with the regulations of this University and meets the accepted standards with respect to originality and quality. Signed by the Final Examining Committee:

_____ Chair
Dr. Jun Yan

_____ External Examiner
Dr. Ahmed Mohamed

_____ Arm's Length Examiner
Dr. Hua Ge

_____ Examiner
Dr. Pragasen Pillay

_____ Examiner
Dr. Luiz A. C. Lopes

_____ Supervisor
Dr. Chunyan Lai

_____ Co-supervisor
Dr. Ursula Eicker

Approved by _____
Dr. Yousef R. Shayan, Chair
Department of Electrical and Computer Engineering

_____ 2024

_____
Mourad Debbabi, Dean
Faculty of Engineering and Computer Science

Abstract

Multi-level Energy Management Framework with Flexibility Provision in Distribution Networks

Sadam Hussain, Ph.D.

Concordia University, 2024

Renewable energy sources are variable and pose new challenges for power systems. A flexible energy management framework is needed for distributed energy resources (DERs) to improve power system performance. Although home energy management systems (HEMSs) can control household appliances, they can not address the issues that may arise due to high DER penetration levels on a distribution network. A multi-level energy management system (ML-EMS) is necessary to improve the techno-economic performance of the distribution system and satisfy the objectives of end-users, aggregators, electricity retailers, and the distribution system operator (DSO). With the rise of DERs, consumers are progressively shifting towards the role of "prosumers," serving as flexible energy resources for DSOs. This work proposes a novel ML-EMS coordination framework in which prosumers provide upward and downward flexibility to the DSO. The DSO optimizes the whole system with the optimal flexibility request sent to the aggregator. The suggested methodology considers the conflicting techno-economic objectives of the DSO and prosumers. To evaluate the proposed method, we compare two scenarios: without flexibility and with flexibility provision. The results show that our proposed strategy improves the voltage profiles and reduces power losses, power generation costs, and peak demands from the DSO's perspective.

To motivate consumers to participate in the proposed coordination framework, an adaptive incentive program is proposed based on the flexibility of the end-user. The prosumer will receive incentives to provide more flexibility to the DSO. To evaluate the proposed methodology, a comparative analysis is conducted involving five scenarios: ML-Framework (a) without HEMS (base case), (b) without flexibility and an incentive program, (c) with flexibility and no incentive, (d)

with flexibility and a fixed incentive, and (e) with flexibility and an adaptive incentive program. The results show that our proposed strategy has increased the monetary benefits for prosumers for their flexibility services provided to the DSO compared to other scenarios. Moreover, the proposed method improves the voltage profiles and reduces the peak load and power losses of a 33-bus radial distribution system.

Taking flexibility to the next level, we propose peer-to-peer (P2P) energy trading to buy and sell energy from neighbors using a smart transformer as an aggregator in our ML-EMS. This part of the work presents a new coordination framework for HEMS-integrated P2P trading, focusing on the impact of such trading on a distribution transformer. The proposed framework provides a comprehensive solution to manage power distribution within a smart grid environment by enabling HEMS to engage in P2P trading. This work also examines optimal energy management in a smart neighborhood to minimize the total cost of energy usage. In addition, to prevent power peaks – that could create overloading and damage the top pole transformer, an adaptive cap within the flexibility bound of the household is placed on the total power households that can draw/penetrate from/to the power grid. To validate the proposed method, we consider three scenarios: a) HEMS directly with transformer. b) HEMS with integration of rule-based P2P with transformer, c). HEMS With fixed power limit on transformer. The result shows that the proposed method reduces the electricity cost of the prosumers and extends the life expectancy of the transformer.

To include the three-phase unbalanced distribution system in the proposed framework, we develop another strategy, which includes four-stage optimization for a three-level coordination framework. A mixed integer linear programming (MILP)-based HEMS is formulated in the first stage to perform home energy management effectively. At the aggregator level, in the second stage, a MILP-enabled P2P trading mechanism is designed. At the same level, a third-stage loss of life optimization is performed pertaining to the optimal power status of the HEMS and P2P trading. In the last stage, a three-phase optimal power flow-based optimization is proposed to maintain the operational constraints of the unbalanced distribution network. This work compares the proposed P2P-based method with a local energy market community with a HEMS-based smart home neighborhood with a distribution transformer. Optimizing HEMS and P2P trading while addressing transformer

limitations, our proposed method reduces peak power and life loss of distribution transformers. Additionally, our method substantially lowers electricity costs for P2P prosumers. Thus, our proposed method outperforms other existing mechanisms from both financial and physical network operation suitability perspectives.

Acknowledgments

In the name of Allah, the Most Gracious and the Most Merciful.

All praises are to Allah and to Him alone. Foremost, I extend my heartfelt gratitude to the Almighty Allah, my Creator and Sustainer, for endowing me with intelligence, skills, resilience, and the determination to embark on this profound journey toward my PhD

I wish to express my deepest appreciation to my esteemed principal advisor, Professor Chunyan Lai, and my co-advisor, Professor Ursula Eicker. Their exceptional guidance, unwavering mentorship, invaluable insights, and constant encouragement have been the cornerstones of this research endeavor. Despite their demanding schedules, Professors Lai and Eicker generously devoted time to meet with me on a regular basis throughout my PhD candidature. Their unwavering support motivated me to embrace challenges that contribute to the realization of a renewable-driven energy future.

I also would like to express my deepest appreciation to my examination committee for their useful and constructive feedback, valuable comments, and support.

A highly deserved thank you goes to all my teammates in both CERC and PEER groups, especially Dr. Ramanunni Menon, who assisted me in difficult situations.

My absolute love and thanks to my parents, my lovely sisters and brothers for all their support and encouragement during this journey, which helped me to stand again in challenging situations.

Last but not least, an exceptional thanks to my lovely wife, who I couldn't have accomplished this thesis without her endless support, love, and encouragement

I dedicate this thesis to my respected parents and lovely wife

Contents

List of Figures

List of Tables

LIST OF ABBREVIATIONS

CPP critical peak pricing

COP coefficient of performance

DERs distributed energy resources

DR demand response

DRP demand response program

DRA demand response aggregator

DSO distribution system operator

DSM demand side management

EV electric vehicle

ESS energy storage system

EMS energy management system

EWH electric water heater

FiT feed-in-tariff

FER flexible energy source

HVAC heating, ventilation, and air conditioning

HEMS home energy management system

HP heat pump

HST hot spot temperature

LEM Local energy market

LV low-voltage

MILP mixed integer linear programming

ML-EMS multi-level energy management system

NLP non-linear programming

OPF optimal power flow

PV photovoltaic

PYOMO python optimization modeling library

PCC point of common connection

P2P peer-to-peer

RES renewable energy source

RTP real time price

RC resistance-capacitance

SoC state-of-charge

ToU time of Use

TAM transactive meter

Chapter 1

Introduction

1.1 Background and Motivation

With the continuously increasing demand for energy globally, which is expected to grow by 12% from 2019 to 2030 [10], there have been serious concerns about the long-term adequacy, availability, and supply of energy. Traditional fossil fuel-based energy sources are detrimental to the environment and are not the preferred option by governments for new capacity. Thus, it is necessary to investigate other eco-friendly energy resources and solutions to meet the demand in the long run. Recent research also shows substantial power losses in the current power grid are due to distribution and long-distance transmission systems [11]. Failures on the power grid transmission and distribution lines cause about 90 percent of power outages. The conventional power grid has been redesigned into a smart, highly efficient, and fully integrated system in the last few years, the so-called smart grid. Traditional electricity consumers have become prosumers who can produce and consume electricity with the development of distributed energy resources (DERs) such as photovoltaic (PV), ESS, and EV [12]. At the house level, the use of DER increase for an instant global market of rooftop solar PV panels is expected to grow by 11% over the next six years, with an additional increase in residential storage systems from 95 MW in 2016 to 3700 MW by 2025 [13]. The prosumer seeks cost-effective and reliable renewable energy technologies, requiring a robust control system. An energy management system (EMS) is needed to keep the balance between generation and consumption. EMS can also mitigate the increasing penetration of DERs on

the distribution network. With advanced DERs, a bidirectional power flow and communication are required between the prosumers and the DSO.

Furthermore, electric power systems have traditionally operated on a demand-following basis. The generation side of a power network is responsible for electric energy supply-demand matching. In contrast, the demand side is considered uncontrollable and must be met regardless of cost. Demand following can be quite costly, particularly during peak demand periods when the least efficient generators must be engaged to meet the increased demand [14]. As a result, DSO began to see the potential benefits of demand response (DR), which differs from typical generation-side decisions. DR is a subset of demand side management (DSM) that aims to modify demand by offering customers various financial incentives. Many factors attracted researchers' attention to the topic of EMS, including cost minimization of consumers and DSO by exploiting the flexibility of controllable loads and energy resources using demand response. The development of a demand response program (DRP) and the smart use of consumers' flexibility can help the DSO to enhance grid reliability and operational efficiency. The display of electricity tariffs in real-time, such as time of use (ToU) rates, can boost load shifting on average days from 3.7 % to 5.5 %, while on hot days, up to 8.5 percent, and result in a 13 % decrease in energy consumption, according to a study by Hydro One [15].

Similarly, as Quebec strives to electrify the majority of the transport sector, the existing renewable hydro-electricity pool of Hydro Quebec will reach capacity limits by 2026, requiring investment from multiple stakeholders in new wind or solar resources [16]. As the number of EVs increases, the electricity demand required to charge their batteries increases. When the EV load is plugged in, the required demand almost doubles on a typical residential circuit [17]. The high penetration of EVs and large-scale DERs' deployment can cause problems in the distribution system, such as, but not limited to, increased load demand, system losses, additional voltage drops, and power quality. Such a problem could create a blackout, which may cost billions of dollars [18]. A proper coordination framework is necessary for a demand-side EMS. In the present distribution networks, prosumers are crucial. Prosumers can interact with one another in local markets directly through peer-to-peer (P2P) marketplaces or indirectly through community-based marketplaces. Local energy market (LEM) provide prosumers with a competitive environment where they

may exchange power services, including energy and network flexibility [19]. To do this, novel methods must be developed to coordinate prosumer energy and flexibility trading in LEMs, considering the limitations of the distribution network and the autonomous choices prosumers make for local energy trading. However, the decisions of participating prosumers on their actions in the market may not be technically feasible for the physical distribution system to support. Thus, DSOs need flexibility services to resolve these issues and keep the network within safe operational limits. Therefore, we need a coordination framework that helps the smart homes have home energy management system (HEMS) and P2P energy trading capability with distribution networks.

1.2 Problem Statement and Research Questions

End-users always want to have lower electricity costs. Therefore, the HEMS tries to minimize the cost of end-users (prosumers hereafter), while the DSO is concerned about the minimization of operation costs, power losses, peak shaving, and voltage regulation. Due to the inherent conflict between the primary goals of HEMS, which prioritize the economic interests of prosumers, and distribution energy management systems, which are primarily focused on the technical concerns of distribution system operators, it is challenging to satisfy both sets of objectives simultaneously. In addition to the economic objectives, there is an essential need for technical objectives. Ignoring the technical aspect of the system may result in optimizing economic outcomes while exposing the system to potential power failures, leading to blackouts and damage to distribution system equipment. Hence, a robust coordination framework is indispensable to harmonize the objectives of prosumers and the DSO effectively.

Moreover, the DRP alone cannot provide the combined objectives of the prosumers and DSO. For example, a price-based program is not an ideal option for high penetration levels of EVs, which shifts the high peak load to off-peak hours. The simultaneous charging of multiple EV loads under low pricing will cause an even higher increase in off-peak demand. Additional voltage drops could result during off-peak hours [20]. Hence, a multi-level energy management system (ML-EMS) seems necessary to improve the techno-economic performance of the distribution network while satisfying prosumers, aggregators, electricity retailers, and the DSO. Due to the high penetration of

DERs, the power system, especially the distribution system, must be flexible to take any uncertainty and condition from DERs.

Flexibility provision is essential nowadays because of the DER penetration in the power system. These flexible resources provide ancillary services that must be appropriately managed to achieve prosumer and distribution-level benefits. The uncoordinated DRP might affect the distribution network operation negatively, whereas a proper coordination framework with DRP can reduce the adverse impact of demand-side behavior [21]. DRP can assist prosumers in rescheduling their loads based on the DSO's electricity pricing. However, even if DRPs are built, the high penetration level of EVs or DERs in the network may cause serious challenges. It is necessary to find a coordination framework based on prosumers' flexibility to limit the impact of high energy-demanding elements such as EVs and other controllable DERs by prosumers' participation. Only price-based DRP is neither an effective nor a motivational way for prosumers to shift their load to off-peak time. A fixed incentive program for all prosumers does not encourage enough prosumers to take part in flexibility service. There is a need for adaptive incentive programs for the prosumers based on the flexibility provided to the grid. The aggregator emerges as a critical player, allowing small customers to participate in DRP and take advantage of their flexibility. The smart transformer could be a natural aggregator to which the consumer is connected. In conventional grids, distribution transformers were considered passive elements in the power system. The smart transformer can facilitate P2P energy exchanges while also resolving the physical constraints of the transformer and DSO.

In general, P2P energy trading research focuses on either the virtual (pricing mechanism and market operation) or physical (grid integration, smart meter, and distribution transformer) layer of the P2P operation [22]. Indeed, previous studies and trials have opened the road for P2P trading to be recognized as an appealing mechanism and a viable alternative to the feed-in tariff (FiT) system. However, when the physical layer feasibility study is performed in reality, the scalability assumption of the low-voltage (LV) distribution networks - to accommodate the prosumer may affect the virtual layer decisions of the P2P prosumers. In contrast, some studies [23], [24] are very limited compared to the virtual layer, focusing primarily on the physical layer complexity of P2P trade. As a result, there is potential to expand these investigations of a unified model of virtual layer and physical layer P2P trading operations.

The aforementioned challenges pose the following underlying research questions:

- *How to satisfy the techno-economical objectives of prosumers and distribution network?*
- *How to mitigate the impact of high penetration of DERs in the distribution networks even if DRP is implemented?*
- *How to incentivize the prosumers to participate in the flexibility provision?*
- *How a P2P energy trading can be modeled considering the LV distribution network constraints?*
- *How a P2P trading can be modeled considering the distribution transformer with adaptive power limit?*
- *How a P2P trading can be modeled considering the distribution transformer and LV three-phase unbalanced distribution network constraints?*

1.3 Research Objectives

The primary objective of the research is developing a robust and smart coordination framework for the flexibility provision using ML-EMS that could benefit different stakeholders simultaneously, like prosumers, aggregators, and DSOs.

The main objective of this thesis is divided into sub-objectives as below:

- ***Modeling of ML-EMS:*** Augment the mathematical model of the residential customer's constraints to represent it as a HEMS considering detailed characteristics of ESS, EV, EWH, and PV units. The developed model will consider the detailed interactions, data, and information exchanges between different entities within the HEMS and between the aggregator and the DSO.
- ***Flexibility-based coordination framework using the ML-EMS:*** This work proposes a novel concept of the HEMS aggregator to quantify the upward and downward flexibility of the flexible energy resources (FERs) available from a household. Thereafter, develop a coordination

scheme that can consider distinctly individual objectives of each HEMS and that of the DSO, seeking to enhance grid operational efficiency and hence create an aggregated DR service for the distribution networks. This will involve a DSO operations model, determining the optimal peak reduction requests based on flexibility from the individual HEMS through an aggregator.

- ***Incentive program based on the flexibility of the prosumer with DSO using ML-EMS:*** This part of the work develops a novel adaptive incentive program for the prosumer based on their flexibility. The prosumers get incentives for how much flexibility they provide to the DSO. Such a system will motivate prosumers to participate in the flexibility provision.

- ***A unified model of P2P energy trading through the smart transformer as an aggregator:*** This work proposes a unified model with the virtual layer that includes a pricing scheme, market strategies, and an energy management system. Also, this model will have the physical layer, which consists of physical and operational constraints of the top pole transformer. The transformer also acts as an aggregator for the flexibility provision.

- ***Multi-stage optimization for Smart Home P2P trading considering DSO constraints:*** In this part, a four-stage optimization methodology is introduced and implemented within a three-level framework. This framework addresses transformer lifespan optimization, P2P energy trading facilitated by LEM, and optimal power flow for a three-phase unbalanced distribution network. The objective is to compare the implications of HEMS with mixed integer linear programming (MILP)-based P2P energy trading on the distribution transformer and the three-phase unbalanced distribution network.

1.4 Thesis Structure

This thesis is organized into seven chapters, each contributing to exploring and enhancing a coordination framework for energy management and flexibility provision in smart grids.

- **Chapter 2: Literature Review:**

  This chapter presents a comprehensive review of prior studies in control architecture, flexibility management, demand response, and peer-to-peer energy systems in the context of smart

grids. It establishes the foundational knowledge upon which the subsequent chapters build.

- **Chapter 3: Multi-level Energy Management System and Flexibility Provision:**

  This chapter outlines the methodology of ML-EMS, covering home, aggregator, and distribution levels. The coordination framework for flexibility provision is discussed, serving as a crucial basis for the subsequent chapters.

- **Chapter 4: Incentive program based on the flexibility Using ML-EMS:**

  In Chapter 4, we explore the novel incentive program based on the flexibility of ML-EMS. The design and implementation of this program are detailed, highlighting its potential benefits and impact on the distribution network.

- **Chapter 5: Smart Home P2P Energy Trading with Dynamic Flexibility Limit Considering Distribution Transformer:**

  Chapter 5 introduces a new coordination framework for rule-based P2P trading in smart homes with smart transformers. The primary focus of this framework is to evaluate the distribution transformer loads resulting from HEMS and P2P energy trading under different flexibility provisions. This chapter extensively investigates the effectiveness and adaptability of the proposed approach in comparison to other scenarios.

- **Chapter 6: Smart Home P2P Energy Trading Considering Three-Phase Unbalanced Distribution Network Optimization:**

  Chapter 6 provides a comprehensive four-stage optimization framework for ML-EMS. This framework combines HEMS, MILP-based P2P energy trading, a transformer model, and three-phase unbalanced distribution network optimization. The integration of these components facilitates a holistic approach to energy system enhancements.

- **Chapter 7: Conclusion and Future Directions:**

  The final chapter, Chapter 7, summarizes the key findings and contributions of this thesis. It also offers valuable insights into potential areas for future research and development, providing a road map for further advancing the smart grid energy management field.

This structured arrangement ensures a logical progression through the research, building a coherent narrative that addresses the complex challenges associated with energy management and flexibility provision in smart grids.

Publications included in this thesis

Peer-reviewed Journals:

- **Hussain, S.**, Lai, C., & Eicker, U. (2023). Flexibility: Literature review on concepts, modeling, and provision method in smart grid. *Sustainable Energy, Grids and Networks*, 101113. (incorporated significantly in **chapter 2**).

- **Hussain, S.**, El-Bayeh, C. Z., Lai, C., & Eicker, U. (2021). Multi-level energy management systems toward a smarter grid: A review. *IEEE Access*, 9, 71994-72016. (incorporated significantly in **chapter 2**).

- **Hussain, S.**, Alrumayh, O., Menon, R. P., Lai, C., & Eicker, U. (2023). Novel Incentive-based Multi-level Framework for Flexibility Provision in Smart Grids. *IEEE Transactions on Smart Grid*. (incorporated significantly in **chapter 3 and 4**).

- **Hussain, S**, Azim, M. I., Lai, C., & Eicker, U. (2023). New coordination framework for smart home peer-to-peer trading to reduce impact on distribution transformer. *Energy*, 284, 129297. (incorporated significantly in **chapter 5**).

- **Hussain, S.**, Azim, M. I., Lai, C., & Eicker, U. (2023). Multi-stage optimization for energy management and trading for smart homes considering operational constraints of a distribution network. *Energy and Buildings*, 113722.(incorporated significantly in **chapter 6**)

Peer-review conference

- **Hussain, S.**, El-Bayeh, C. Z., Menon, R. P., Lai, C., & Eicker, U. (2022, August). Flexibility based Coordination Framework For Three-Level Energy Management System. In 2022 19th

International Bhurban Conference on Applied Sciences and Technology (IBCAST) (pp. 568-572). IEEE. (incorporated significantly in **chapter 3**).

- **Hussain, S.**, Menon, R. P., Fatima,A., Lai, C., & Eicker, U. (submitted). Optimization of Energy Systems using MILP and RC Modeling: A Real Case Study in Canada. In the 18th Annual IEEE International Systems Conference *SYSCON 2024* (incorporated significantly in **chapter 3**).

Chapter 2

Literature Review

This chapter demonstrates an up-to-date literature review regarding different energy management architecture, a detailed literature review on flexibility and P2P energy trading [1]. Governments introduce new policies, dynamic pricing tools, and new strategies to reduce the peak load to address the increasing energy demand globally. For instance, flex rate-D in Quebec [25] and global adjustment program in Ontario, Canada [26] aims to reduce the peak demand. The development of the demand response program will help the power system reliability and operation efficiency. Such features allow end-users to participate in the solution of distribution network problems through the use of home-appliance flexibility [27]. According to the US Federal Energy Regulatory Commission, a DRP is defined as [28] "*Changes in electric usage by end-use customers from their normal consumption patterns in response to changes in the price of electricity over time, or to incentive payments designed to induce lower electricity use at times of high wholesale market prices or when system reliability is jeopardized.*" The capacity to adjust, shift, reduce, or curtail the load over time, known as energy flexibility, constitutes a fundamental component of the evolving energy market model [29]. To delve deeper into the concepts of flexibility and flexibility provisioning, these elements require an architectural framework to facilitate their provision. An effective energy management framework is essential for harnessing consumer flexibility, and the subsequent section explores three control

[1]This chapter has significant materials from the following papers published by the PhD candidate:
Hussain, S., El-Bayeh, C. Z., Lai, C., & Eicker, U. (2021). Multi-level energy management systems toward a smarter grid: A review. IEEE Access, 9, 71994-72016.
Hussain, S., Lai, C., & Eicker, U. (2023). Flexibility: Literature review on concepts, modeling, and provision method in smart grid. Sustainable Energy, Grids and Networks, 101113.

architectures for energy management systems.

2.1 Control Architecture for Energy Management System

Many control strategies were used to optimize and schedule the controllable loads and the power flow of DERs to overcome the negative impact of the high penetration of DERs on the distribution network [30, 31, 32]. The efficiency of EMS depends on the control architecture; commonly used architectures are centralized, decentralized (distributed), and hierarchical control architectures [33].

A centralized control architecture comprises a single controller with high computation performance capability and will need a secure communication infrastructure to collect information and manage different system entities. This strategy is usually used in the charging station and parking lot. This control system can provide optimal performance, reduce the overall operation cost, and is easy to implement, but it has some disadvantages. Since this system relies on one controller, the computational burden on the system increases by one controller. It can also cause single-point failure, making this architecture less effective for a real-time system. Furthermore, expanding or integrating new components in such a system is very hard.

Unlike the centralized architecture, in the decentralized EMS strategy, each entity has its local controller and communicates with other nodes. They share information with neighbors to send and receive the data from different local controllers [34]. Hence, the decentralized control architecture overcomes the shortcomings of the centralized system by developing expandability flexibility and preventing single-point failure. It distributes the computational burden on different controllers, making this architecture more reliable than the centralized control architecture. However, suppose the decentralized control architecture is implemented in the home. In that case, it might only consider the home's objectives and not care about the effect on the distribution system and vice versa, as shown in table 2.1. For example, in [31], the authors implement a decentralized EMS architecture to minimize energy consumption and operation costs. This system does not fulfill the technical objectives of the distribution system. Such a control strategy has only one objective and will also cause a rebound and second peak effect during low tariffs on the distribution system, as presented in reference [35].

Based on these discussions, it can be concluded that both available distributed and centralized EMS methods may fail to simultaneously cover the main requirements of the distribution system operators (DSO) and the prosumer [1]. It is crucial to create an effective strategy for involving customers in DR programs to enhance the operation of the distribution system. The expanded geographic areas of these systems and extensive communication and computational burden make it impossible to incorporate centralized approaches completely. Because of the high coupling of various local controllers, they require a maximum coordination level that cannot be achieved by decentralized EMS architecture. Multi-level EMS (ML-EMS) architecture is a compromise between centralized and decentralized control architectures [32].

Table 2.1: Comparison of Different Control Architectures [1]

Control Architecture	Advantages	Disadvantages
Centralized	Provides optimal performance. Reduces overall operation cost. Simple architecture, easy to implement. Suitable for small scale with internal control system. Offers optimal global solutions for all entities. Secure communication infrastructure.	Computation burden increases on one controller. Single-point failure is less effective for real-time systems. Hard to expand and integrate new components for plug-and-play. Requires a high level of connectivity and processing. Less reliable for real-time applications.
Decentralized	Enhances expandability with plug-and-play functionality. Flexible architecture due to peer-to-peer communication. Prevents single-point failure. Distributes computation burden on different controllers. More reliable due to redundancy in communication.	Single objective control architecture. Provides only optimal local solution, not optimal global solution. Higher implementation complexity compared to centralized control. Local controllers require robust synchronization.
Hierarchical	Each level sends optimal solutions to a higher-level controller. Level-wise control increases the accuracy and reliability. Scalability. Flexible architecture due to peer-to-peer communication. Prevents single-point failure. Distributes computation burden on different controllers. Less processing time due to distributed operation constraints. Achieves optimal global solution.	Coordination of different levels is required. Adjacent layers coordination required; Communication fault at the upper level disrupts information. Privacy and data security concerns across different levels. Complex architecture due to coordination platform for different levels.

2.2 Multi-Level Energy Management System

In the ML-EM framework, the system can be divided into different levels with objectives and constraints. Each local controller manages its appliances at different levels and sends the optimal solution to the higher-level controller [36]. The higher-level controller acts as the central controller to collect and analyze all data of the local controllers. Based on the global solution, it orders all the local controllers to modify their optimal targets. The conceptual architecture overview of ML-EMS is presented in Fig. 2.1 [1]. Such a system can be used to benefit both prosumers and DSO. Such level-wise control can increase accuracy and reliability and might be the best for future smart grids.

Different optimization algorithms have been used for ML-EMS, which are categorized in table 2.2.

The deployment of ML-EMS strategies requires different objective functions; details of the technical and economic objectives used in different levels of EMSs are shown in Fig. 2.1. The main economic objective functions are to minimize electricity usage costs, operation, maintenance, operation, investment, project planning, technical, and component, and maximize aggregator and DSO profit. Many researchers used different methods for cost minimization in ML-EMS. For instance, the authors in [37] used flexible loads such as electric water heater (EWH), heating, ventilation, and air conditioning (HVAC), refrigerators, and EVs to minimize costs. Similarly, authors in [38] used controllable appliances like air conditioners, washing machines for flexibility within user comfort level, and energy storage systems (ESSs) for energy trading to reduce costs. The PV and ESS were used with the controllable appliance to reduce the electricity usage cost [39]. Also, in [40], the authors used controllable loads, PV, and ESS with DRP to minimize the electricity cost. The technical objective is more related to the DSO, such as but not limited to minimization of power losses, total harmonic distortion, power stability, power (active and reactive) deviation, voltage, and frequency deviation in the distribution system, as depicted in Fig. 2.1. For example, in reference [40], the authors used volt-VAR optimization (VVO) to minimize the power losses on the distribution line. Similarly, Omar et al. [39] used system-level optimization to reduce the losses and increase the system's efficiency at DSO. The details of the objective functions used in each level of EMSs are illustrated in Fig. 2.1.

The details of the objective function used in the different levels and some of the constraints used in each level are presented in appendix A.1 and A.2 [1]. The constraints used in HEMSs are appliance operation constraints such as indoor temperature constraints, ESS operation constraints, EV operational constraints, and PV operational constraints. Constraints used at the aggregator level are total electricity cost, active and reactive power balance, and power limit on the distribution transformer. Voltage drop limit constraints, OLTC, capacitor bank, smart inverter operation constraints, and active and reactive power consumption limits are constraints used on the distribution level. The ML-EMS can be two, three, or four levels depending on the objective and architecture of the proposed system.

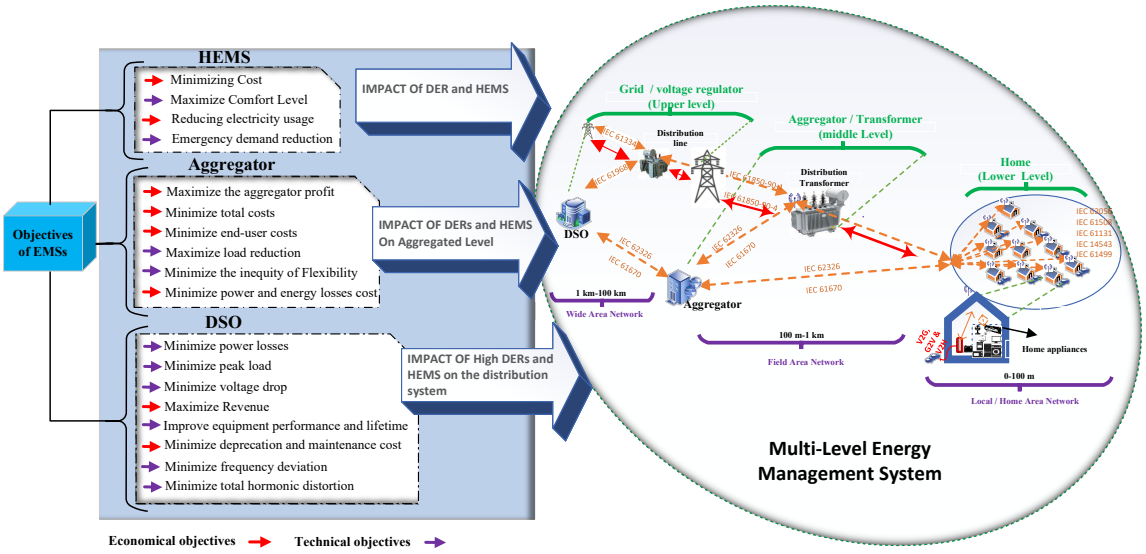

Figure 2.1: Architecture overview of Multi-level EMS [1].

2.2.1 Two-Level Energy Management System

Two different EMS levels are needed to optimize prosumers' usage and satisfaction levels and minimize the expense without raising the detrimental effects on the grid. In ML-EMS, having two EMS levels can be HEMS at the home level and another EMS on the aggregator level to which multiple homes are connected. Keeping in mind the consumer and DSO' combined objectives, there are various studies done on the two-level framework for ML-EMS [37, 38, 41]. Sarker et al. [8] presented an EMS for EV at the aggregator level. In their model, the consumer gives the aggregator permission to control the charging and discharging of their EV to co-optimize the transformer's damage cost. The aggregator obtains profits from the transformer owner for maintaining a lifetime, and some portion of these profits must be given to prosumers for their services. The DSO also benefits from the transformer's maintenance cost, so it is a win-win situation for the end-user to minimize their cost in response to DRP. Additional incentives should be offered to reduce the overload of the distribution network. They concluded that a high penetration of EVs can be handled without violating the capability of the distribution network. The two-level EMS may not be limited to the HEMS and aggregate EMS. It can be a coordination framework between home and grid EMS. For instance, Kikusato et al. [42] proposed a two-level EMS that is home and Grid EMS (GEMS) to utilize PV and EV effectively. Based on voltage information from the GEMS, it reduces operation costs and

PV curtailment without disturbing EV usage for driving. Hamid et al.[43] proposed two-level EMS to implement the bidding strategy based on the weighted distribution of excess power among end-users. The lower level in an energy hub reduces its energy cost. At the same time, the upper-level EMS focuses on building coordination between home energy hubs and making attractive deals for all stakeholders. Rastegar et al. [37] developed a two-level framework for residential EMS. In the first level, they took the economic objectives in their objective functions, such as payment cost, system operator cost, and operational constraints of the home appliances. In the second level, a technical objective, such as load demand deviation, given the least desired payment cost of each customer, is considered in the multi-objective optimization function to modify the house's desired demand profiles. They compare the centralized, distributed, and ML-EMS framework. In [41], a framework was proposed in which the aggregator seeks to maximize the income through a bidding strategy to maximize monetary benefit. The study concluded that consumers could buy energy at a very low price from their neighborhood and reduce their dependency on the grid. Similarly, Joo et al. [38] divided the optimization into local HEMS and GEMS. The local HEMS controls the home appliances such as washing machines and air conditioners with consumers' comfort level preference, and the GEMS performs the energy trading and scheduling between houses and ESS.

Suppose we have a two-level system on the home level (HEMS) and the grid level (GEMS). In that case, the system operator may face a considerable optimization problem in the second level because of thousands of prosumers, which existing solvers might not solve. Also, if the generation side directly communicates with customers, numerous information exchanges will delay the system response time. Meanwhile, the generation side is designed for a large spatial scale and cannot negotiate directly with each customer. The DSO uses distribution system management to control the medium and low-voltage (LV) distribution systems operations. The DSO allows the consumer to participate in the various DRPs using a residential load aggregator (called an aggregator) connected to the multiple HEMSs. HEMSs can be essential for aggregator EMS to manage multiple households in LV distribution networks efficiently. The flexibility of prosumers measured from the HEMS can be correctly estimated and aggregated by the aggregator and communicated to the DSO, which increases the efficiency of the management system handled by the DSO.

2.2.2 Three-Level Energy Management System

A three-level framework consists of HEMS for a prosumer at the first level, an aggregator at the second level, and GEMS at the third level, as shown in Fig. 2.1 [1]. In such a system, the HEMS schedules the home appliances according to the consumer's comfort level. The aggregator recalculates the optimized schedules of multiple HEMSs and sends them to the higher level, i.e., GEMS, for global optimization. In the first level, the HEMS calculates each house's prosumer energy usage and electricity cost and sends them to the HEMS aggregator. In the second level, the HEMS aggregator performs mainly two tasks, namely, but not limited to, gathering the data of electricity costs and the energy consumption schedules of multiple households delivered from the lower level and sending them to the upper level, and rescheduling the aggregated energy consumption for the multiple households based on the optimal solutions from the HEMS and GEMS. The GEMS conducts an efficient and cost-effective operation at the upper level using optimal power flow.

Li et al. [44] integrated renewable energy source (RES) with a day-ahead three-level DSM model. The three levels were upper, middle, and lower levels for the utility, the demand response aggregator (DRA), and prosumers management, respectively. The operator wants to minimize the operation cost and gives part of the profit to the DRA as a bonus. The DRA gets a bonus from the utility and provides some rewards to end-users for modifying their energy usage pattern. They concluded that using the proposed model reduces the generation cost, the DRA can make revenue by supplying DRP service, and prosumers can reduce their electricity cost. Different optimization techniques are used for each level, as shown in table 2.2 [1]. Recently, Davye et al. [40] developed a coordination framework for a three-level ML-EMS with a HEMS (first level), a HEMS aggregator on the LV distribution network (second level), and volt-var optimization at the medium voltage distribution network (third level). They concluded that such coordination further reduces the consumer's electricity price within their comfort zone and reduces the network losses on medium and LV distribution networks. As per the authors' best knowledge, the EMS of the three-level framework is new and needs further analysis for the combined objectives of all stakeholders.

The architectures/frameworks mentioned above provide a foundation for the prosumer and grid to participate in the demand and grid side flexibility (change in demand and generation profile),

respectively. More details of the flexibility will be discussed in the next section.

Table 2.2: Some notable algorithmic approaches used for different levels of the EMS [1]

Algorithmic approach	HEMS	Aggregator	Distribution system
Mixed integer linear programming	✓	✓	✓
Mixed integer non-linear programming	✓	✓	✓
Mixed integer quadratic programming	✓	✓	
Particle swarm optimization	✓	✓	✓
Volt-var optimization			✓
Genetic algorithm	✓		✓
Model prediction control	✓		

2.3 Flexibility

It has been acknowledged that traditional operation methods are insufficient to handle the fluctuations in net load due to the substantial penetration of RESs [45]. Therefore, flexibility has emerged as a critical aspect in the design of future power systems dominated by RESs. The key sources of flexibility in such systems include flexible power plants, distributed generation, consumer-side resources, virtual flexibility solutions, and ESS. [46].

Flexibility in buildings is an essential resource for managing energy demand to maintain a balance with the instantaneous and increasingly unpredictable energy generation from renewable sources. The International Energy Agency defines energy flexibility as *the ability of a building to manage its demand and generation in response to local climatic conditions, user needs, and grid requirements* [47]. This is exemplified by changing the amount and timing of building energy use in response to system costs, emissions, and operational requirements, as shown in Fig. 2.2. Flexibility can also be defined as *a power system that can manage variability and uncertainty in both generation and demand while maintaining reliability at a reasonable cost over different time horizons* [48]. It might be considered that this definition is the more comprehensive of the two since it emphasizes satisfying needs (variability and uncertainty) while specifically mentioning reliability and applicability across time horizons.

The timeline in Fig. 2.3 shows the required activation time for the different types of flexibility,

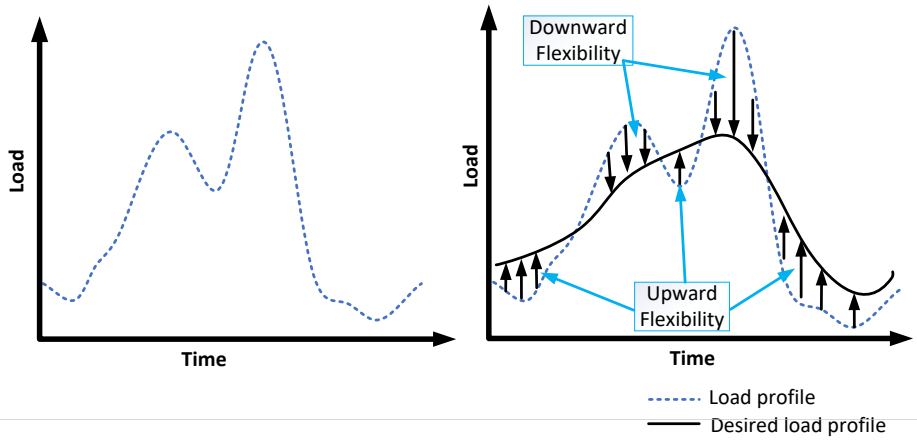

Figure 2.2: Concept of flexibility [2].

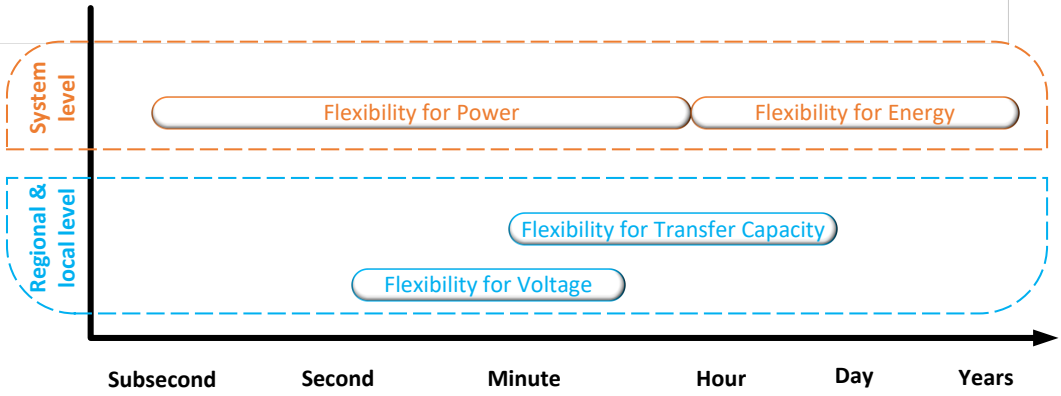

Figure 2.3: Flexibility requirements in terms of space (local/regional to system level) and time [2]

which include flexibility for power, flexibility for energy, flexibility for transfer capacity, and flexibility for voltage. These categories have approximate ranges that depend on the system's physical behavior, requirements, and regulations. Local or regional demands for flexibility for transfer capacity and flexibility for voltage are distinguished from system-wide needs for flexibility for power and flexibility for energy. Flexibility for power refers to the short-term equilibrium between power supply and demand and is a system-wide requirement for maintaining frequency stability. Flexibility for energy is the medium to long-term balance between energy supply and demand and is a system-wide requirement for demand scenarios over time. Flexibility for transfer capacity refers to the short to medium-term ability to transfer power between supply and demand, where local or regional limitations may cause bottlenecks resulting in congestion costs. It increases utilization levels with increased peak demands and increased peak supply. Flexibility for voltage refers to the

short-term ability to keep the bus voltages within predefined limits.

Quantifying energy flexibility has been a challenge in prior research due to a lack of standardization. Various parameters from time, cost, electrical, and comfort domains have been utilized to measure flexibility, as outlined in table 2.3 [49]. Flexibility can be measured using three primary dimensions: power, energy, and time. The power dimension quantifies the capacity of flexible loads, incorporating metrics such as instantaneous power flexibility and maximum power capacity. The energy dimension is the primary parameter for shiftable and storage devices with parameters such as shiftable energy and storage capacity. The time dimension is crucial for schedulable flexible loads, with duration and regeneration time. In addition to these dimensions, other methods of quantifying flexibility include combined (shiftable power and cost curve) [50, 51], relative (self-consumption and storage efficiency) [52, 52, 53, 50, 54, 55, 55], and other parameters, such as ramping rate, consistency of operation, potential score [55, 56, 57, 57, 57, 57] etc., as mentioned in table 2.3.

Overall, flexibility refers to the capacity of a power system network to sustain supply reliably during transient and significant imbalances. The work in IEA-EBC Annex 67 and 82 [47] has shown that to offer an aggregate quantity sufficient for the operation of electricity grids, energy flexibility of buildings must be harnessed across a cluster of buildings or at a district scale. Flexibility can be characterized by five distinct attributes: (a) the orientation, either upward or downward; (b) the velocity of change or magnitude of power capability; (c) the initiation moment and triggering event; (d) the duration, and (e) the geographical position or point of the distribution network. Other qualities like controllability, predictability, time availability, and delivery time are also listed in [59].

Several pilot projects have been conducted to manage the functioning of electric power systems. Table 2.4 summarizes a few exemplary initiatives. For instance, to reduce the congestion in the local distribution system, iPower project [60] established a "clearinghouse" for local flexibility trading at the DSO level. PeerEnergyCloud project [61] focuses on building a microgrid's virtual market platform for trading electricity. Similarly, the purpose of the ECO-Grid project [62] was to utilize market forces and smart power consumption management to engage individual consumers in balancing an energy system with abundant renewable. Piclo project's [63] object was to provide data visualization for consumers. EMPOWER project [64] develops a local market paradigm that includes three financial market platforms for trading in local electricity, local flexibility, and other

Table 2.3: Quantifying Flexibility Parameters

Type	Parameter	Descriptions as given in literature	Ref
Power [kW]	Maximum power	Thermal energy storage and power-to-heat flexibility in various modes.	[53]
	Mean power	Peak response to a trigger signal.	[58]
	Instantaneous power	Mean power during activation.	[58]
	Curtailed power	Maximum EV charging power.	[54]
	Power capacity	Average power reduction for lighting during the curtailable period.	[55]
	Charging power	Flexible power delivery capability.	[56]
Energy [kWh]	Storage capacity	Energy shifted during optimal control	[53]
	Shiftable energy	Energy added to storage system without affecting comfort	[50]
	Energy capacity	Energy content below the curve, consumable by the pool during activation	[58]
		Energy reduction during a day	[55]
		Energy delivered during flexibility action	[56]
		Energy added to building thermal mass during demand response (DR) action.	[52]
Time [h]	Duration	Time until electricity consumption drops below normal	[58]
	Interval	Time until power consumption returns to normal	[58]
	Regeneration time	Time EV can be used flexibly	[54]
	Available period	Total time of curtailment possible per day	[55]
	Curtailment duration	Duration of sustainable response before comfort limits reached	[56]
	Comfort capacity/recovery	Time required to restore nominal comfort in the building	[56]
Combine	Shiftable power	The relationship between heating power changes and the duration that changes can be sustained under boundary conditions	[50]
	Cost curve	The level of flexibility (shiftable energy) and its corresponding cost	[51]
Relative	Self consumption (%)	Percentage of increased energy demand met by generation during DR action	[52]
	Storage efficiency (%)	Energy cost related to DR action	[52]
		Ratio of energy discharged to energy charged during 24-hour control period	[53]
		Fraction of stored heat used to reduce heating power during DR	[50]
		EV battery charge level	[54]
		Comparison of lighting power with base case	[55]
		Comparison of power deviation from base case	[55]
Other	Coefficient of power	Stability of power curtailment capacity (stable/fluctuating)	[55]
	Ramping rate (kW/min)	Building's reaction speed	[56]
	Frequency of operation	Ratio of days appliance is active to total historical days	[57]
	Consistency of operation	Predictability of user behavior over time	[57]
	Peak time operation	Energy consumption during DR period	[57]
	Potential score	Flexibility score based on three parameters.	[57]

services. The emerging field of research known as energy flexibility focuses on examining the capabilities of various grid services concerning real-world fidelity factors such as building thermal dynamics, service systems and appliances, occupant influences, and weather impacts, taking into account different temporal considerations.

From the above literature, we can deduce that the definition of flexibility is very subjective. It depends on the context of the project or research. However, incorporating flexibility, whether system-side flexibility or demand-side flexibility, can significantly improve the system's resilience, efficiency, and sustainability while providing benefits to end-users and reducing the need for a costly upgrade. In this work, we only focus on the demand side flexibility, which will be discussed in the

Table 2.4: Industrial projects on flexibility

Project name	iPower project [65]	PeerEnergyCloud [66]	ECO-Grid project [62]	Piclo [63]	Horizon 2020-project EMPOWER [64]
Start year	2011	2012	2013	2014	2015
Country	Denmark	Germany	Denmark	United Kingdom	Europe
System size	Regional	Microgrid	Regional	National	Regional

below sections.

2.3.1 Demand Side Flexibility

Flexibility on the demand side is being recognized as a key facilitator for the quick transition to a low-carbon energy system that replaces traditional fossil fuels with RESs while maintaining, if not improving, the system's functionality.

Flexibility, which is sometimes referred to as demand flexibility in publications, is frequently taken into account within a broader ML-EMS framework, where DSM techniques can be generally divided into energy efficiency, DR, and energy flexibility approaches [67]. Energy usage reduction describes energy efficiency methods compared to a baseline or reference system. These can be accomplished by enhancing building envelope or energy conversion systems, control algorithm improvements, or building system optimization techniques [68]. A technique for exploiting energy flexibility in buildings (or other end-users) without requiring a significant capital investment may be seen as DR that reduces building electrical demand during grid stress [69].

2.3.2 DSM for Flexibility Service

An essential aspect of demand-side flexibility is DSM. DSM, as the name suggests, includes changing demand side behavior. It is the concept for the voluntary changes in grid electricity demand triggered by some incentives or administrative actions [70]. Only voluntary consumer-side flexibility, in which customers actively contribute to supplying demand-side flexibility, is considered in this definition. Due to demand-side flexibility, customers adjust their consumption in response to changing pricing signals. DSM can reduce energy costs, optimize energy use, and contribute to keeping the power system more reliable. DSM also delays the investment in upgrading the electrical grid by altering or lowering demand. Based on the timing and the influence on the customer process quality, DSM can be classified into four categories, as illustrated in Fig. 2.4 [71]: Energy efficiency,

ToU, DR (market and physical), and spinning reserve.

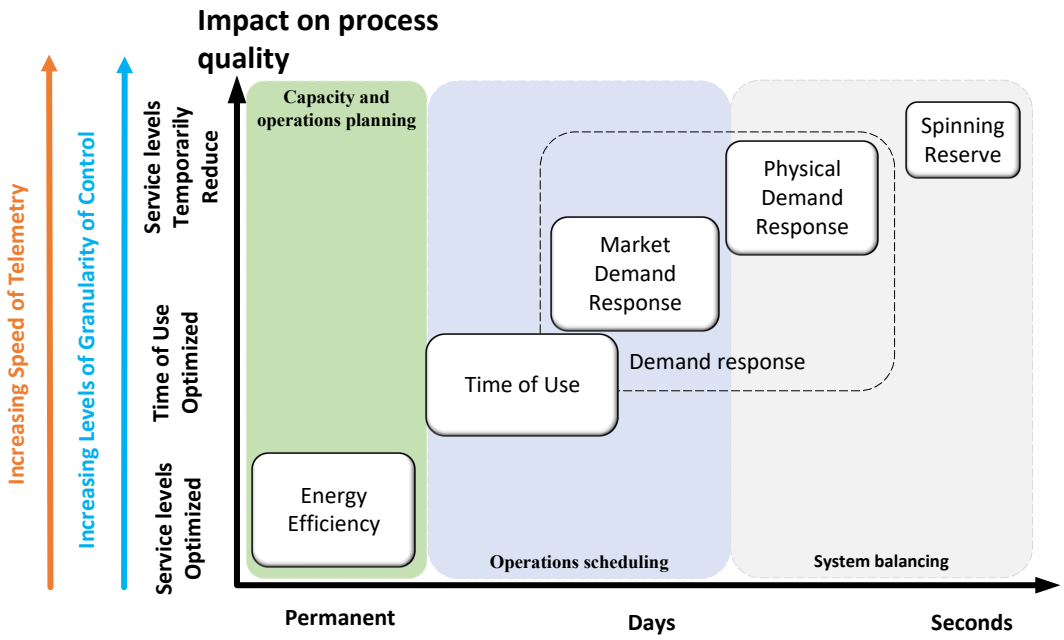

Figure 2.4: Classification of DSM.

- *Energy efficiency* can be improved through permanent and temporary measures that fall under the umbrella of the DSMs. The frequency at which changes are made to energy systems can impact the processes of customers, such as manufacturing output or building comfort. The most desirable method for reducing energy consumption is through energy efficiency measures, such as upgrading equipment or improving the physical properties of a system.

- *Time of Use* tariffs can also encourage customers to shift their energy usage to less peak periods. However, it can lead to the "rebound effect", where energy consumption may not be reduced or even increase.

- *Spinning reserve* represents the upper end of the DSM spectrum, providing quick support to traditional providers of ancillary services. Loads can act as virtual spinning reserves by adjusting their power consumption in response to changes in grid frequency [72].

- *Demand response* can be a market or physical demand response program. The detailed demand response is discussed in subsection 2.4.

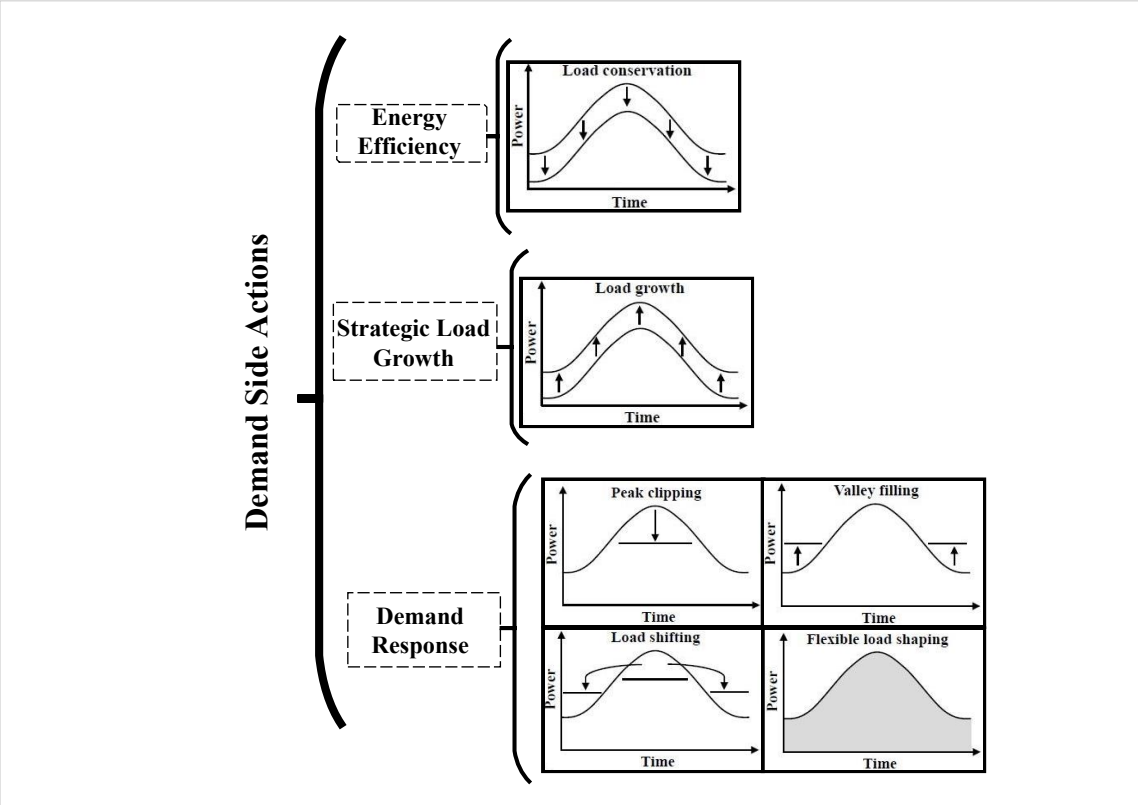

Figure 2.5: Demand side action.

As demonstrated by [73], combining other DSM techniques with time of Use (ToU) tariffs can significantly increase security and decrease costs and emissions in energy systems with high shares of wind and solar power. Achieving these DSMs requires some action known as a demand-side action, as shown in Fig. 2.5 [74]. Energy efficiency can be achieved using demand side action "load conservation". Similarly, the DR program includes actions such as but not limited to peak clipping, valley filling, load shifting, and flexible load shaping, as shown in Fig. 2.5.

2.4 Demand Response Program

The DR is an effective DSM solution that can be implemented at a particular time [75]. Depending on the consumer process's impact, DR programs are divided into price-based and incentive-based, as shown in Fig. 2.6 [1].

2.4.1 Price or Time Based

Dynamic pricing-based programs form the basis of price-based programs, where the power tariff is not constant and fluctuates in response to prevailing energy costs. This approach aims to even out energy consumption by offering higher tariffs during periods of high demand and lower tariffs during periods of low demand. These programs can be implemented in industrial sectors, where energy expenses are a crucial component of production costs. With the widespread deployment of information and communication technology in residential sectors, price or time-based DR programs are becoming increasingly accessible for smart homes and communities [76]. End users can adjust their energy consumption in response to external signals, such as price signals, which may encourage them to participate in system improvements. Four types of price-based demand response programs are ToU rates, critical peak pricing (CPP), inclining block rate, and Real-Time Pricing schemes, as presented in Fig. 2.6 [1].

The advantages and disadvantages of price-based DR schemes have been discussed in reference [76]. There are two main benefits to the ToU programs. First, because ToU pricing maintains the same price structure, participants can quickly comprehend its portfolios and create plans for their daily energy usage. Second, the program's participation percentages are consistently compared to the other two DR programs. The drawback is that a new peak may be generated when ToU pricing DR techniques lower the peak load.

Three benefits can be found with the CPP programs. First, the CPP portfolio is simple to comprehend and follow. Second, CPP programs can assist the operator in shifting the peak load demand. Third, it is possible to estimate the incentive payment for the participant. Nevertheless, there are drawbacks to this technique. Since the system only deals with extreme situations sometimes, CPP applications cannot be used regularly. Therefore, the CPP schemes will not successfully lower the costs of energy bills. Similarly, the real time price (RTP) is suitable for real-time power balance. Still, it is challenging to implement and hard for the end-user to plan their schedule their activities regarding the RTP tariff.

2.4.2 Incentive Based

In incentive-based DR schemes, end users could be eligible for financial incentives, rewards, payments in cash, or discounted prices if they can adjust or decrease their energy usage to the system's needs. Market-based and classical programs are the two additional categories for incentive-based programs. According to [77, 78], two main types of incentive programs for managing energy demand are available. The first type, known as traditional programs, includes methods such as direct load control (DLC) and interruptible/curtailable programs. On the other hand, market-based programs involve emergency DR, capacity market, demand bidding/buyback, and supplementary market services programs, as shown in Fig. 2.6 [1]. Using DLC, grid operators, and utilities can immediately and directly access electrical equipment from a distance. Residential or small-scale commercial consumers have also used this type of DR program [79]. Interruptible/curtailable rate programs are those in which the end-users consent to receive incentives, bill discounts, or cash payments to reduce power consumption or shift their load to another time interval. All these DR and DSM require some asset on the demand side that is flexible and controllable. Such systems are called flexible energy resources.

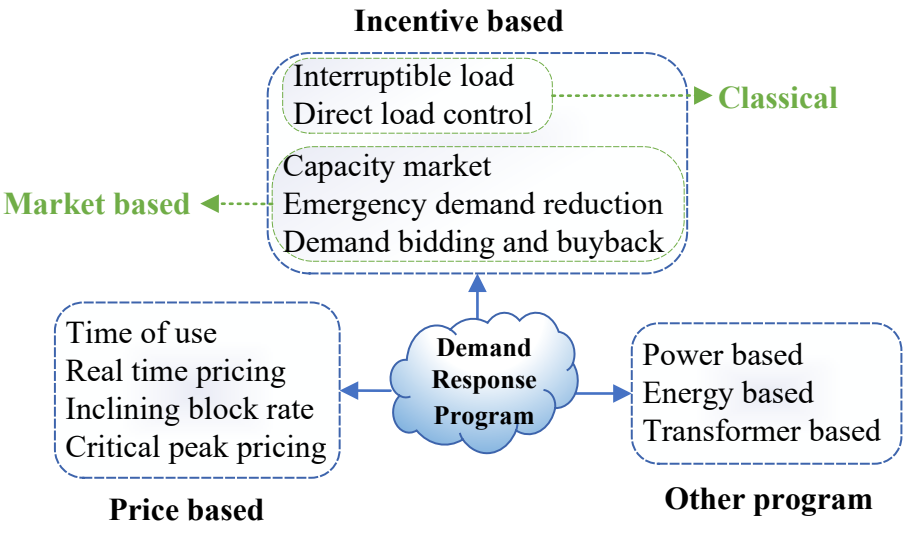

Figure 2.6: Classification of demand response program [1].

2.4.3 Flexible Energy Resource

Flexible energy resources (FERs) are typically located on the distribution system, where most customers are often found in residential and communities at energy hubs. These flexible resources can also be found at the generation, aggregator, or demand side of the distribution network, as shown in Fig. 2.7. Different optimization techniques are used for flexibility forecasting using FERs, as shown in table 2.5 [2]. Generation side FERs include different power plants such as solar, wind, and hydropower plants. The aggregator side can consist of large battery capacity, EV parking lots, etc. The demand side energy resources can include smart households, HVAC systems, rooftop PV systems, EVs, home batteries, and other smart devices.

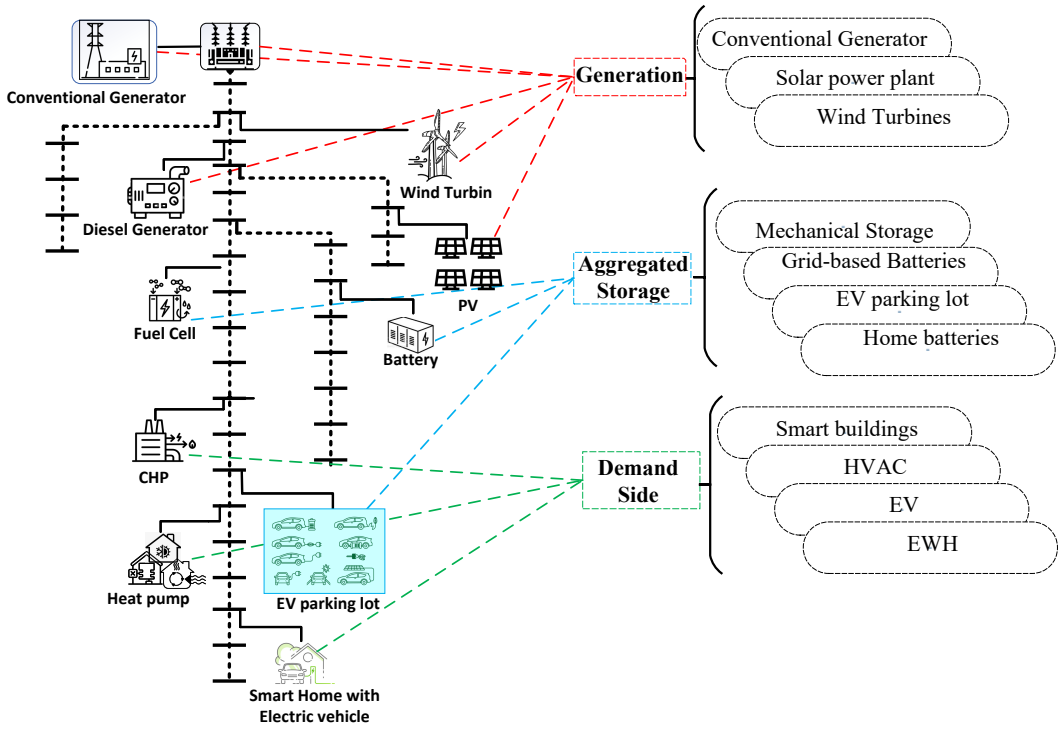

Figure 2.7: Different sources of flexibility in the LV distribution network.

Demand-side FERs are broadly categorized into storage and load-based resources that can adjust their power output to support various local and system-wide flexibility services, as shown in Fig. 2.8. Many appliances at the house or in a community can participate in DR or energy management programs by reducing or adjusting their usage over time [99]. However, the FERs that can offer power-based flexibility services to the distribution systems or local communities are the main focus of this

Table 2.5: Optimization for Flexibility forecasting and FERs used in the literature [2]

Model type	Specific models	Ref.	Price signal response	Base on historical data	Shiftable loads	TCL	ESS	EV
Machine learning models	Neural networks	[80]		✓	✓	✓		
		[81]		✓		✓		
	Support vector machine	[82]	✓	✓	✓	✓		
	Support vector data description	[83]				✓	✓	
	Logistic regression	[84]	✓	✓	✓			
	Piece-wise linear regression	[85]		✓		✓		
Probabilistic models	Chance constrained	[86]	✓	✓	✓	✓	✓	✓
		[40]	✓	✓				
	Auto-regressive integrated moving average	[87]		✓		✓		
		[88]	✓	✓				✓
		[89]		✓		✓		
	Data analysis base	[90]		✓		✓		
Deterministic models	Mixed integer linear programming	[91]	✓		✓	✓	✓	✓
		[92]	✓	✓		✓		
		[86]	✓					
		[93]	✓			✓		✓
		[94]	✓		✓			✓
		[95]	✓	✓	✓	✓	✓	✓
		[96]	✓	✓	✓	✓	✓	✓
		[1]	✓			✓		
	Mixed integer non-linear programming	[97]	✓	✓	✓	✓	✓	✓
	Algorithmic method	[98]		✓		✓		

section. These resources may be managed for output power and often respond quickly to necessary adjustments. Load-based resources are further divided into interruptible and non-interruptible flexible loads. Interruptible loads such as EWH, refrigerators, electric pool pumps, and HVAC systems can be turned off or adjusted their power rating during operation. Non-interruptible loads, such as washing machines, dishwashers, electric stoves, dryers, and microwave ovens, cannot be interrupted during operation. These non-interruptible loads only provide upward flexibility but can not offer downward flexibility [100]. The storage base resources are further divided into movable and immovable storage, shown in Fig. 2.8. The flexible portable storage resources for flexible are electric transportation such as EVs, electric buses, electric bikes, etc. The immovable storage-based resource can be electric, mechanical, or electro-chemical energy storage, as shown in Fig. 2.8.

Other appliances such as the refrigerator, lighting system, dishwasher, washer, and dryer can be used as FER but do not provide complete upward/positive and downward/negative flexibility to the distribution grid [100]. The EV, ESS , and EWH are considered the three target appliances for FERs in this study for modeling to utilize the storage capability of these DERs in the DR program for flexibility provision because they can provide upward and downward flexibility [101]. However, it can be extended to integrate other appliances.

2.5 Type of Electricity Markets for Flexibility

To account for fluctuations and uncertainties in energy markets, describing the required ramping capabilities and implementing a fair payment system that incentivizes consumers to participate is crucial. There may be difficulties in determining the appropriate payment for demand-side flexibility, but it is essential to ensure consumers' participation and avoid price spikes. A fair payment system that incentivizes consumers to engage in the market is the best incentive for providers of demand-side flexibility. Despite the benefits of intra-hour and real-time markets in reducing ramp shortages, the lack of a sufficient day-ahead market can still impact real-time markets by increasing the likelihood of contingencies [102]. There may be some difficulties in integrating the flexibility market with related markets. Effective markets must have specific essential characteristics, including the ability for new suppliers to enter the market, the provision of incentives and assurances, and

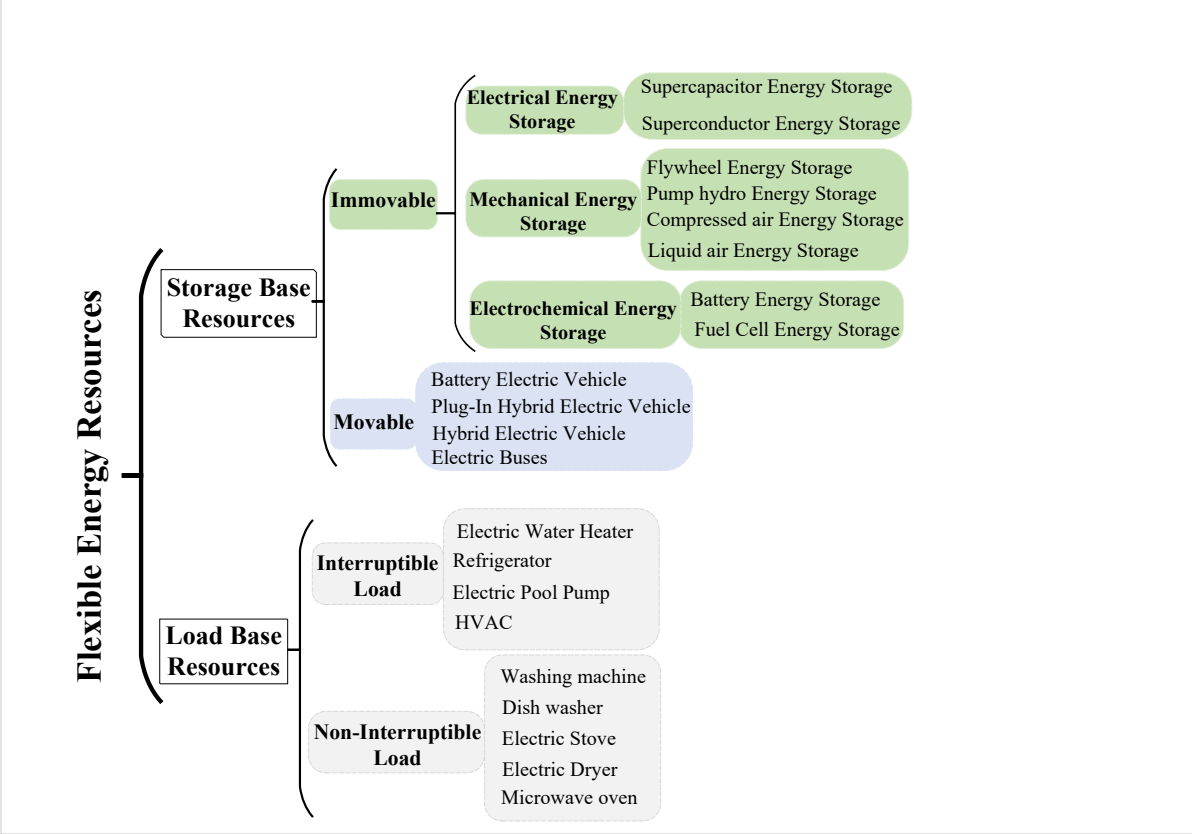

Figure 2.8: Demand side flexible energy resources.

the potential for them to overtake incumbents in terms of market share [102]. All time frames, from very short-term to long-term, can be impacted by demand-side flexibility [103]. Fig. 2.9 provides an overview of the electricity market with the time of delivery that is typically present. Different types of flexibility markets are as follows:

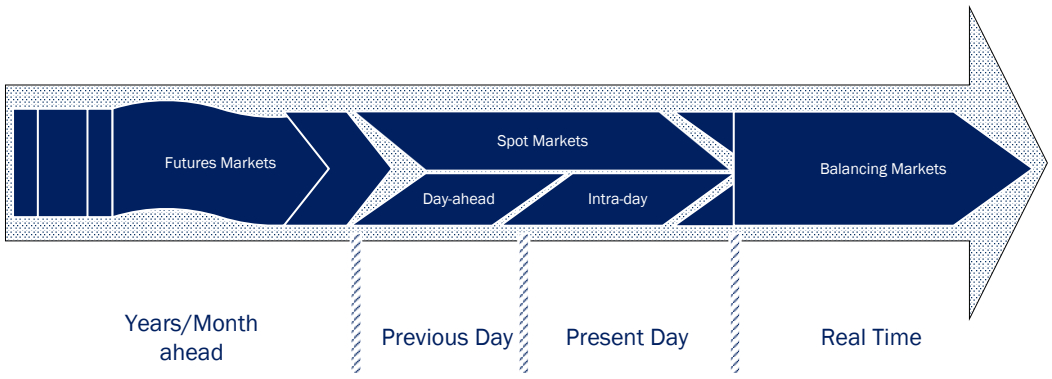

Figure 2.9: Different electricity market with respective time [2].

2.5.1 Day-ahead Market

There are two types of demand-side flexibility in the day-ahead market: proactive and reactive. According to Alvehag et al., [104], reactive demand-side flexibility occurs once the day-ahead market prices have been disclosed. In contrast, proactive demand-side flexibility has an instant effect on price determination. For proactive demand-side flexibility to participate in the day-ahead market, it is essential to furnish the customer with hourly price signals, as this type of flexibility significantly impacts price formation [105].

2.5.2 Intra-day Market

The day-ahead market's correction for flexibility trading is employed mainly by aggregators. Stakeholders in this market, such as electricity users, DSOs, and aggregators, can demonstrate their adaptability and change any prior trading if the earlier projections are inaccurate.

2.5.3 Balancing power market

The balancing power market is critical in ensuring the grid's stability and reliability in the flexibility electricity market. The market mechanism allows the system operator to procure enough flexibility to respond rapidly to short-term electricity supply or demand fluctuations, ensuring that the grid frequency remains within acceptable limits. The market's design and operation can significantly impact the overall performance and efficiency of the electricity system.

The cost savings drive the increased adoption of self-consumption installations compared to energy purchased from the grid, as fees, margins, and taxes are eliminated [106]. The regulation of self-consumption in many territories further supports this trend, leading to a paradigm shift in the electricity system and markets where consumers become active participants, referred to as prosumers [107]. These prosumers can form energy communities, which are set to play an increasingly important role in the energy system. Within these communities, prosumers can engage in P2P energy exchanges, maximizing their resources through the recently developed P2P trading technology in smart grids [108].

2.6 Peer-to-Peer Energy Trading

Transactive energy is a framework for managing power generation and consumption within an electric network by taking reliability constraints into account [109]. This framework uses two-way information exchange and price signals to connect buyers and sellers into the transactive energy market protocol. It allows them to participate in various financial transactions with each other or energy retailers [110]. The subset of transactive energy that focuses on prosumers is called P2P energy trading [111, 112, 113].

The implementation of P2P energy trading has been shown to have numerous positive impacts on the community, including lifestyle and cultural changes related to electricity supply and demand, job creation and local training, increased social trust, transparency in transactions, reduced fraud, and a greater sense of community attachment [114, 115].

2.6.1 Market Structure of P2P Energy

The P2P energy trading framework uses a bottom-up approach to include prosumers in the market, in contrast to the top-down approach used in the current electricity market. The P2P market can be divided into three structures, as outlined in the Fully Decentralized P2P market, Community-based P2P market, and Hybrid P2P market. These structures differ in how prosumers are coordinated for the energy exchange. The advantages and challenges of these different P2P markets are shown in table 2.6.

Table 2.6: P2P energy market Structure

Ref	P2P Market	Benefits	Challenges
[116, 117, 118, 119] [120, 121, 122, 123, 124]	Fully Decentralized	Autonomous	No central control
		Prosumer-centric	Reliability issue
			Slow convergence to the final value
			High maintenance and investment costs.
[125, 126, 127, 128, 129] [130, 131, 132, 133, 134]	Community based	Common interest	Proper coordination
		Collaborative and competitive	Unbiased and fair energy trading
[135, 136, 113, 137, 138]	Hybrid	Suitable design	Inclusion of stakeholder
		Predictive to the grid	Coordination of communities
		Scalable	Capable for future gird

2.6.2 Operation layers of P2P Energy

The operation of P2P trading is divided into two layers, the virtual layer and the physical layer [139]. The physical layer includes the grid connection, smart metering, and distribution asset, for instance, the distribution transformer, as shown in figure 2.10. The virtual layer has an information system, market operation, pricing mechanism, and energy management system, as mentioned in figure 2.10.

Virtual Layers of P2P Energy

Prosumers can access the energy-related information of other prosumers through the virtual layer's protected information platform, which is part of a P2P network [133]. A prosumer's transactive meter (TAM), a separate smart meter from the traditional energy meter to track P2P trading, transmits price information, energy surplus, and deficit data through a secure communication channel [140]. Orders for selling and purchasing energy are made based on this data. Then, depending on the selling and purchasing orders, a robust P2P market mechanism is developed to carry out energy exchange between prosumers [108]. The three main components of virtual P2P trading are the information-sharing platform, local market setup, and decision-making technique.

Physical Layers of P2P Energy

On a real distribution network, energy transmission and adjustment are the responsibility of the physical layer [133]. When the virtual layer's financial settlement is complete, sellers may reduce the contractual energy demand or export the agreed-upon energy to the distribution network. The TAMs monitor both actions. On the other hand, buyers use the exact amounts of energy from the physical network, similarly noted in TAMs as energy quantities traded through the P2P framework [139]. The energy used by a specific customer does not always correspond to the energy added to or decreased by the seller with whom it has a contract. This is so because physics governs how electricity moves across a physical network. As a result, neighboring purchasers closer to the seller than the target buyer might use the energy exported or lowered by this seller to make up for their energy shortage [141].

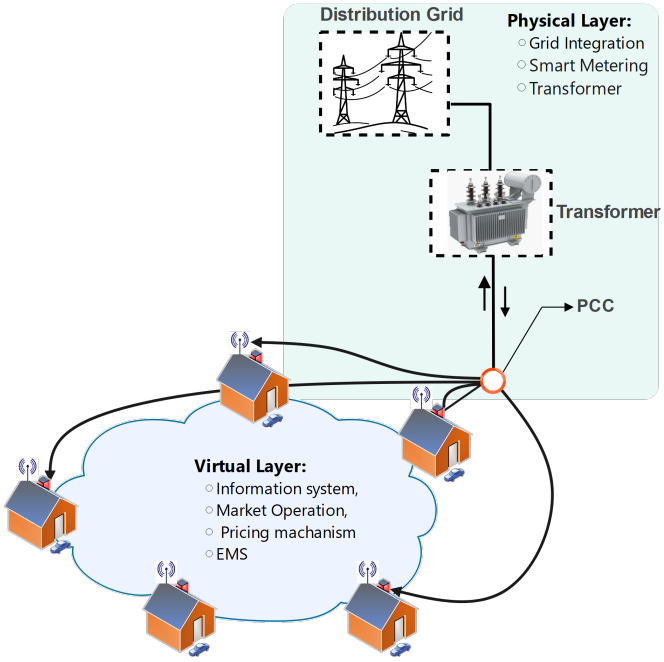

Figure 2.10: Virtual and physical layer of P2P energy trading.

2.6.3 Optimization Approach for P2P Energy Trading

P2P energy trading systems have been developed using various methodologies, broadly categorized into four main categories: game theory, auction theory, constrained optimization, and blockchain. Table 2.7 summarizes the different technical approaches used in current investigations.

Game theory is a mathematical methodology developed to investigate the decision-making strategies of rational agents operating in competitive environments. In such situations, the actions of one participant influence and are influenced by the actions of other participants, and game theory provides a means of analyzing these interactions [172]. In recent years, game theory has been widely employed in P2P energy trading due to its ability to model the diverse interests of multiple agents in a decentralized and computationally efficient manner [151]. Two distinct categories of game theory are typically considered: non-cooperative and cooperative games [173].

Auction theory deals with multiple buyers and sellers trying to exchange goods or services [174]. Buyers present their offers to an auctioneer, soliciting prices from potential sellers. The four steps involved in the process are: (a) the sellers submit their reservation prices in ascending

Table 2.7: Summary of optimization approaches for P2P energy trading

Technical approach	Game theory	Auction theory	Constrained optimization	Block chain
Virtual P2P Layer	[142, 120, 143, 144, 145, 146, 147, 148, 149, 150, 151, 152, 153]	[116, 152, 154, 155]	[156, 157, 118, 158, 159, 160]	[161, 162, 163, 164, 165, 166]
Physical P2P Layer	[167]	[168]	[169, 170, 171]	Not found
Popular method	Non-cooperative and cooperative game, Stackelberg game, Canonical coalition game, Coalition formation game	Double auction, Iterative auction	LP, MILP, ADMM, NLP	Elecbay, Smart Contract, Ethereum, Hyperledger, Consortium blockchain

order, (b) the buyers are arranged in descending order based on their reservation bid values, (c) the demand and supply curves are constructed and intersect at a specific point, and (d) the intersection determines the auction price and the number of buyers and sellers who ultimately participate in the market transaction. In P2P energy markets, the application of auction theory enables the capture of interactions between multiple vendors and buyers, facilitating a step-by-step power exchange. All these methodologies need a specific place to trade their power or energy, known as the flexibility market. The detail of the flexibility market is in the next section.

Constrained optimization involves optimizing the objective function of P2P markets under operational constraints. Various constrained optimization techniques have been used to design P2P energy trading schemes, such as linear programming (LP), mixed-integer linear programming (MILP), alternating direction method of multipliers (ADMM), and nonlinear programming (NLP) as mentioned in table 2.7.

Blockchain technology was first introduced by [175] as a fast, accurate, and reliable decentralized data structure for P2P energy transfers. Blockchain is a distributed data structure replicated and distributed among network participants. With blockchain, programs that previously could only run through a trusted intermediary can now operate in a decentralized way, without a central authority, and accomplish the same functionality with the same level of assurance [176]. P2P trading's characteristics make blockchain technology a valuable tool for future energy networks.

Chapter 3

Multi-level Energy Management System and Flexibility Provision

NOMENCLATURE

Indices, Sets and Functions

h_j	Index of houses h at j bus
j, k	Index of buses in distribution system; $(j, k) \in \mathcal{N}$
t	Index of time; $t \in \mathcal{T}$
$t_{h_j}^{\boldsymbol{EV}}$	Index of time EV connected to house; $t_{h_j}^{EV} \in \mathcal{T}$
$t_{h_j}^{\boldsymbol{AR}}$	Index of time EV arrived to house; $t_{h_j}^{AR} \in \mathcal{T}$
$t_{h_j}^{\boldsymbol{DEP}}$	Index of time EV depart from house; $t_{h_j}^{DEP} \in \mathcal{T}$
J_{1,h_j}	Cost minimization objective function
J_{2,h_j}	Energy minimization objective function
J_4	Loss minimization with optimal flexibility request objective function

Parameters

C^f	Weight function assigned by the DSO
C_{h_j}	Thermal capacitance; $kWh/^\circ C$
$E_h^{\textbf{ESS,min}}$,$E_{h_j}^{\textbf{EV,min}}$	Minimum energy level of an ESS , EV; kWh
$E_h^{\textbf{ESS,max}}$,$E_{h_j}^{\textbf{EV,max}}$	Maximum energy level of ESS , EV; kWh
$E_{h_j}^{\textbf{EV,AR}}$, $E_{h_j}^{\textbf{EV,DEP}}$	Arrival and departure energy of EV; kWh
$E_{h_j}^{\textbf{EV,AR}}$, $E_{h_j}^{\textbf{EV,DEP}}$	Arrival and departure energy of EV; kWh
$E_{\textbf{ESS}}^{\textbf{initial}}$, $E_{\textbf{ESS}}^{\textbf{final}}$	Initial and final energy of ESS ; kWh
$G_{j,k}$	Conductance between buses; $p.u$
M	Very large number
M_{h_j}	Water tank capacity; L
$m_{h_j,t}$	Hot Water usage; L
$P_{C_{h_j}}^{\textbf{ESS,max}}$,$P_{C_{h_j}}^{\textbf{EV,max}}$	Maximum charging power of ESS , EV; kW
$P_{D_{h_j}}^{\textbf{ESS,max}}$,$P_{D_{h_j}}^{\textbf{EV,max}}$	Maximum discharging power of ESS , EV; kW
$P_{h_j,t}^{\textbf{flex}^+}$, $P_{h_j,t}^{\textbf{flex}^-}$	Upward, downward flexibility of house; kW
$P_{j,t}^{\textbf{flex}^+_{\textbf{agg}}}$, $P_{j,t}^{\textbf{flex}^-_{\textbf{agg}}}$	Upward, downward aggregated flexibility; kW
$P_{h_j,t}^{\textbf{BL}}$	Base load; kW
$(P_{h_j,t}^{\textbf{con}})_{J_1}$	Power demand using J_{1,h_j}; kW
$(P_{h_j,t}^{\textbf{con}})_{J_2}$	Power demand using J_{2,h_j}; kW
$P_{j,t}^{\textbf{flex}_{\textbf{agg}}}$	Total flexibility at bus j; kW
$P_{h_j,t}^{\textbf{flex}}$	The flexibility of each household; kW
$P_{h_j,t}^{\textbf{max}}$	The maximum power demand of household; kW
$P_{j,t}^{d_{\textbf{agg}}}$, $P_{j,t}^{\textbf{sell}_{\textbf{agg}}}$	Aggregated power buy, sell from, to DSO; $p.u$
$P_{g_j}^{\textbf{min}}$, $P_{g_j}^{\textbf{max}}$	Lower, upper limit active power generation; $p.u$
$Q_{g_j}^{\textbf{min}}$, $Q_{g_j}^{\textbf{max}}$	Lower, upper limit reactive power generation; $p.u$
PF	Power factor

$Q_{j,t}^{d_{agg}}$	Aggregated reactive power demand; $p.u$
Q_{h_j}	Thermal capacity; kW
R_{h_j}	Thermal resistance; $^\circ C/kW$
$T_{h_j,t}^{a}$	Ambient temperature; $^\circ C$
$T_{h_j}^{EWH,min}$	Minimum limit of water temperature; $^\circ C$
$T_{h_j}^{EWH,max}$	Maximum limit of water temperature; $^\circ C$
V_j^{min}, V_j^{max}	Minimum, maximum voltage at bus j; $p.u$
$Y_{j,k}$	Admittance of line of the electrical network; $p.u$
ξ^{+}, ξ^{-}	Percentage peak reduction, increase
$\eta_{C_{h_j}}^{ESS}$, $\eta_{D_{h_j}}^{ESS}$	Charging, discharging efficiency of ESS
$\eta_{C_{h_j}}^{EV}$, $\eta_{D_{h_j}}^{EV}$	Charging, discharging efficiency of EV
$\gamma_{h_j,t}^{flex}$	Flexibility index of each household
$\theta_{j,k}$	Angle of complex Y-Bus matrix; rad
τ	Time step; $15min$
π_t^{Buy}, π_t^{Sell}	Buying, selling price; $\$/kWh$

Variables

$E_{h_j,t}^{EV}$, $E_{h_j,t}^{ESS}$	Energy level of EV, ESS , kWh
$P_{h_j,t}^{Buy,DSO}$	Buying power of household from DSO; kW
$P_{h_j,t}^{Sell,DSO}$	Selling power of household to DSO; kW
$P_{C_{h_j,t}}^{EV}$, $P_{C_{h_j,t}}^{ESS}$	Charging power of EV, ESS ; kW
$P_{D_{h_j,t}}^{EV,H}$,$P_{D_{h_j,t}}^{EV,DSO}$	Discharging power of EV to home, DSO; kW
$P_{D_{h_j,t}}^{ESS,H}$,$P_{h_j,t}^{ESS,DSO}$	Discharging power of ESS to home, DSO; kW
$P_{D_{h_j,t}}^{EV}$,$P_{D_{h_j,t}}^{ESS}$	Total discharging power of EV, ESS ; kW
$P_{h_j,t}^{PV}$	Total power of PV; kW

$P^{\boldsymbol{PV,ESS}}_{D_{h_j,t}}$	Power of PV supply to ESS ; kW
$P^{\boldsymbol{PV,H}}_{D_{h_j,t}}$,$P^{\boldsymbol{PV,DSO}}_{D_{h_j,t}}$	Power of PV supply to home, DSO; kW
$P^{\boldsymbol{EWH}}_{h_j,t}$	Power demand of EWH; kW
$P^{g}_{j,t}$, $Q^{g}_{j,t}$	Active, reactive power generation; $p.u$
$P^{f_{DSO}}_{j,t}$, $Q^{f_{DSO}}_{j,t}$	Active, reactive flexibility signal; $p.u$
$T^{\boldsymbol{EWH}}_{h_j,t}$	Water temperature; $^{\circ}C$
$V_{j,t}$, $V_{k,t}$	The voltage level at bus j and k; $p.u$
$\delta_{j,t}$, $\delta_{k,t}$	Voltage angle at bus j, k; rad

Binary Variables

$X^{\boldsymbol{ESS}}_{h_j,t}$,$X^{\boldsymbol{EV}}_{h_j,t}$	Charging and discharging status of ESS , EV; ON/OFF
$X^{\boldsymbol{EWH}}_{h_j,t}$	Status of EWH; ON/OFF
$X_{h_j,t}$	Status of buying and selling power; ON/OFF

3.1 Background

This chapter focuses on the multi-level energy management modeling and flexibility provision. [1] The contribution of residential flexibility demand for power system flexibility providers has been studied in the literature [177, 178, 179]. With the increasing penetration level of DERs in the system, flexibility provisions have become a crucial topic in power systems. These flexible resources provide DRP services that must be appropriately managed to achieve prosumer and system-level benefits. The energy sector's evolution is pushing for more sustainable electricity infrastructure. In this perspective, energy flexibility becomes critical to achieving sustainable energy goals, as it provides

[1]This chapter has significant materials from the following papers published by the PhD candidate:
Hussain, S., El-Bayeh, C. Z., Menon, R. P., Lai, C., & Eicker, U. (2022, August). Flexibility based Coordination Framework For Three-Level Energy Management System. In 2022 19th International Bhurban Conference on Applied Sciences and Technology (IBCAST) (pp. 568-572). IEEE.
Hussain, S., Menon, R. P., Fatima,A., Lai, C., & Eicker, U. (submitted). Optimization of Energy Systems using MILP and RC Modeling: A Real Case Study in Canada. In the 18th Annual IEEE International Systems Conference SYSCON 2024
Hussain, S., Alrumayh, O., Menon, R. P., Lai, C., & Eicker, U. (2023). Novel Incentive-based Multi-level Framework for Flexibility Provision in Smart Grids. IEEE Transactions on Smart Grid.

an efficient means of balancing supply and demand under more varied energy usage patterns (such as renewable and electric vehicles). Prosumers have been suggested as a potential source of power grid flexibility. However, the individual flexibility that small prosumers can provide may not be enough to solve power grid issues. As a result, the function of the ”aggregator” emerges to collect total flexibility quantities from small prosumers, allowing them to access larger markets. We assume the required infrastructure for achieving management and control (e.g., smart metering systems, communication lines, HEMS) is available [180]. A few researchers investigated the integration of EVs and RESs and noticed substantial changes in residential load profiles and consumers' monthly costs. Very little research has examined how distribution operations are affected by the flexibility of residential loads and DR provisions [181, 39, 21]. Hence, the inherent benefits of managing flexible resources to facilitate the integration of RES and EV calls for in-depth research on this subject. The authors of [39, 40] used prosumers' flexibility to improve the system's operational efficiency, reduce network losses, peak power, and the prosumers' energy expenses. However, these studies did not study downward flexibility, making the coordination framework infeasible and less attractive for the prosumer. For this reason, this chapter developed a novel flexibility (downward and upward) based coordination framework for ML-EMS.

3.2 Mathematical Modeling of Multi-level EMS

This section introduces the assumptions and mathematical modeling of the multi-level EMS. We assume that the required infrastructure is available, such as smart metering systems, communication networks, and HEMS. The mathematical formulation is a three-stage EMS: first, second, and third stages, as shown in figure 3.1. In this study, each household has an EV, PV, ESS, and EWH controlled by a HEMS, accommodating each customer's preferences and objectives. Other appliances such as the refrigerator, water heater, lighting system, dishwasher, washer, and dryer do not provide full flexibility (upward and downward) to the distribution grid [100] and are referred to as base loads or uncontrolled loads. The HEMS manages the EV and ESS charging and discharging. The EV and ESS are charged from the distribution grid or PV and may be used to earn profits by discharging power to the grid during high peak demand. The objectives of HEMS are the

minimization of electricity costs and energy consumption. The aggregator calculates the flexibility and aggregated power bought/sold from/to the DSO in the second stage. The third stage is the DSO model, which minimizes the power losses of the system using optimal power flow (OPF) and calculates the signals, providing information on the optimal flexibility required.

The proposed method is rooted in the idea that the DSO can request flexibility from the aggregator. The aggregator, in turn, can provide flexibility provisioning based on special contracts between prosumers and aggregators. These contracts allow the prosumers' system flexibility to provide benefits to the grid and the end-users simultaneously. This concept has been examined in other works, such as the universal smart energy framework [182], which studies a contractual connection between the aggregator and the DSO to exchange flexibility. The following sections discuss the detailed modeling of each level and the flexibility provisions.

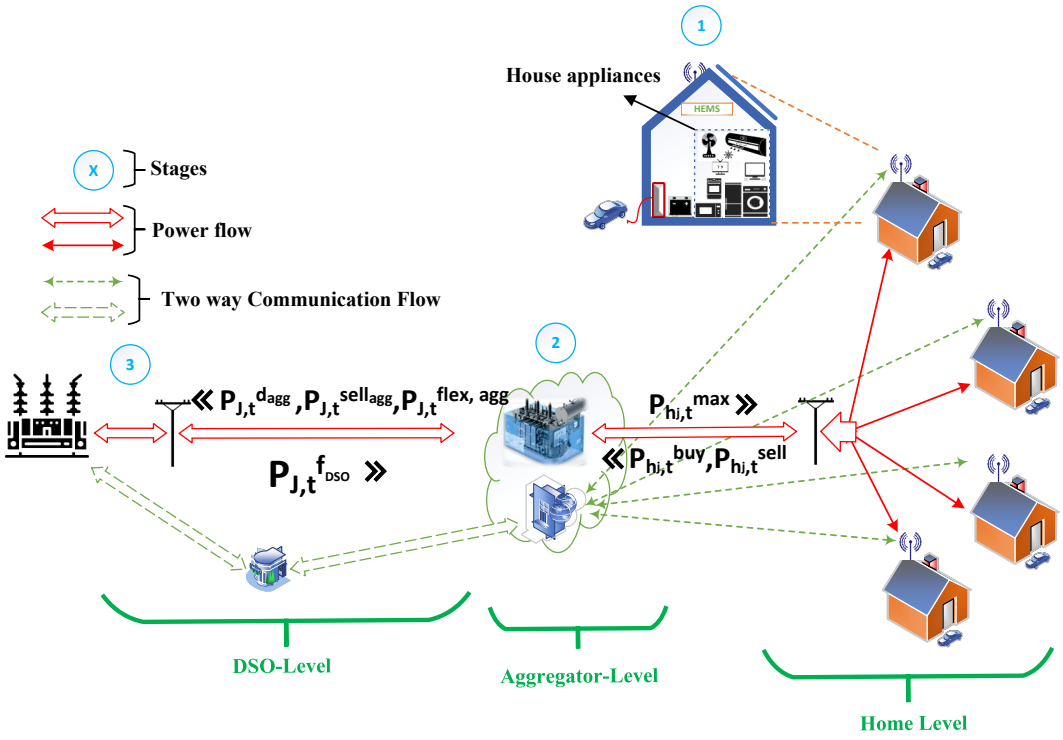

Figure 3.1: Conceptual diagram of three-level EMS.

3.2.1 Home (lower level)

The goal of the HEMS in each household is assumed to optimize the operation schedule of home appliances and DERs by minimizing the electricity cost, minimizing the energy consumption, maximizing the conforming level, etc., as mentioned in table A.1 [1]. With these objectives, HEMS will satisfy the operational constraints of appliances, DERs, and the prosumer's preferences.

Objective Function

The main objectives of the HEMS are cost, as follows:

$$J_{1,h_j} = \sum_{t \in T} (P_{h_j,t}^{Buy,DSO} \cdot \pi_t^{Buy} - P_{h_j,t}^{Sell,DSO} \cdot \pi_t^{Sell}) \tau \tag{3.1}$$

Equation (3.1) is the objective function to minimize the energy cost of a household. In equation (3.1), the first term $P_{h_j,t}^{Buy,DSO}$ is power buying/demand from the grid by the prosumers with buying price π_t^{Buy} of electricity from the DSO. The second term of right-hand side in equation (3.1) is power selling to the grid from the home's DERs corresponding to the selling price.

The objective function to minimize the energy is used to make a baseline for the prosumer to minimize the energy as low as possible. The optimal power of the home using objective function used in (3.2) to make a reference/baseline for calculating flexibility in section 3.2.2. To minimize the energy consumption or maximizing local energy consumption as follows:

$$J_{2,h_j} = \sum_{t \in T} (P_{h_j,t}^{BL} + P_{h_j,t}^{EWH} + (P_{C_{h_j,t}}^{EV} - P_{D_{h_j,t}}^{EV,H}) + (P_{C_{h_j,t}}^{ESS} - P_{D_{h_j,t}}^{ESS,H}) - P_{D_{h_j,t}}^{PV,H}) \tau \tag{3.2}$$

Equation (3.2) minimizes the energy consumption of household appliances such as base load, EWH, EV, and ESS . The right-hand side of equation (3.2) is the power demand of the base load, the power demand of EWH, charging of EV and ESS at home, and the power supply to the house from the EV, ESS , and PV, respectively

HEMS Constraints

Power Balance Constraints

Equation (3.3) ensures that the net power consumption of the appliances is equal to the power bought from the DSO as below:

$$P_{h_j,t}^{Buy,DSO} = P_{h_j,t}^{BL} + P_{h_j,t}^{EWH} + (P_{C_{h_j,t}}^{EV} - P_{D_{h_j,t}}^{EV,H}) + (P_{C_{h_j,t}}^{ESS} - P_{D_{h_j,t}}^{ESS,H}) - P_{D_{h_j,t}}^{PV,H}, \quad \forall t \in \mathcal{T}; \forall h_j \in \mathcal{H} \tag{3.3}$$

In equation (3.3), the different terms represent the power demand of the base load, the power demand of EWH, the charging of EV and ESS at home, and the power supply to the house from the EV, ESS , and PV, respectively. According to the FiT, the HEMS can also sell power to the DSO and reduce the electricity cost.

$$P_{h_j,t}^{Sell,DSO} = P_{D_{h_j,t}}^{EV,DSO} + P_{D_{h_j,t}}^{ESS,DSO} + P_{D_{h_j,t}}^{PV,DSO}, \forall t \in \mathcal{T}; \forall h_j \in \mathcal{H} \tag{3.4}$$

In (3.4), the first term of the right-hand side is EV supply power to DSO, the second term is ESS supply excess power to DSO, and the last term is PV supply surplus power to the DSO. Equation (3.5) and (3.6) ensure that the process of selling and buying power does not occur simultaneously. In these equations, M is a very large number, and $X_{h_j,t}$ is a binary variable.

$$0 \leqslant P_{h_j,t}^{Buy,DSO} \leqslant M \cdot X_{h_j,t}, \qquad \forall t \in \mathcal{T}; \forall h_j \in \mathcal{H} \tag{3.5}$$

$$0 \leqslant P_{h_j,t}^{Sell,DSO} \leqslant M \cdot (1 - X_{h_j,t}), \qquad \forall t \in \mathcal{T}; \forall h_j \in \mathcal{H} \tag{3.6}$$

EWH Operational Constraints

Equation (3.7) shows the thermal energy charging/discharging of EWH, which considers the heat exchange of cold water inflows with environment [3].

$$T^{EWH}_{h_j,t} = T^{a}_{h_j,t} + R_{h_j} \cdot Q_{h_j} \cdot X^{EWH}_{h_j,t} - (\frac{M_{h_j} - m_{h_j,t}}{M_{h_j}}) \\ (T^{a}_{h_j,t} - T^{EWH}_{h_j,t-1}) e^{\frac{\tau}{R_{h_j} C_{h_j}}}, \quad \forall t \in \mathcal{T}; \forall h_j \in \mathcal{H} \quad (3.7)$$

In equation (3.7), EWH's heat transfer rates are determined as a function of hot water usage, ambient temperature, thermal parameters, and the EWH's ON/OFF status. Equation (3.7) models the water temperature inside the tank while adjusting for the heat exchanged with the outside environment and the heat produced by the EWH resistance. It should be noted that the EWH tank is assumed to be placed in a space that is directly affected by the changes in the ambient temperature of air [183].

$$T^{EWH,min}_{h_j} \leq T^{EWH}_{h_j,t} \leq T^{EWH,max}_{h_j}, \quad \forall t \in \mathcal{T}; \forall h_j \in \mathcal{H} \quad (3.8)$$

Equation (3.8) ensures that the hot water temperatures of EWH are within the limit set by the household.

PV Operational Constraint

The HEMS distributed power generated by the PV to the DSO, battery, and house is described below in the form of the following equation:

$$P^{PV}_{h_j,t} = P^{PV,DSO}_{D_{h_j,t}} + P^{PV,ESS}_{D_{h_j,t}} + P^{PV,H}_{D_{h_j,t}}, \forall t \in \mathcal{T}; \forall h_j \in \mathcal{H} \quad (3.9)$$

EV Operational Constraints

When EV is at home at time $t^{EV}_{h_j}$, the energy level of the EV will be affected by the charging and discharging as follows:

$$E^{EV}_{h_j,t} = E^{EV}_{h_j,t-1} + \tau \left(P^{EV}_{C_{h_j,t}} \cdot \eta^{EV}_{C_{h_j}} - P^{EV}_{D_{h_j,t}} \right), \forall t \in t^{EV}_{h_j}; \forall h_j \in \mathcal{H} \quad (3.10)$$

In equation, (3.10), the first term is the energy level for the previous time step, and the second term represents the charging and discharging of the EV. When the EV is plugged in at home (and not charging), it will either discharge to the house or can sell electricity to the DSO as follows:

$$P^{EV}_{D_{h_j,t}} = \frac{P^{EV,DSO}_{D_{h_j,t}} + P^{EV,H}_{D_{h_j,t}}}{\eta^{EV}_{D_{h_j}}}, \quad \forall t \in t^{EV}_{h_j}; \forall h_j \in \mathcal{H} \tag{3.11}$$

Equations (3.12) and (3.13) limit EVs' charging and discharging power, ensuring that charging and discharging does not occur at some time.

$$0 \leq P^{EV}_{C_{h_j,t}} \leq P^{EV,max}_{C_{h_j}} \cdot X^{EV}_{h_j,t}, \quad \forall t \in t^{EV}_{h_j}; \forall h_j \in \mathcal{H} \tag{3.12}$$

$$0 \leq P^{EV}_{D_{h_j,t}} \leq P^{EV,max}_{D_{h_j}} \cdot (1 - X^{EV}_{h_j,t}), \forall t \in t^{EV}_{h_j}; \forall h_j \in \mathcal{H} \tag{3.13}$$

Equation (3.14) ensures that energy level of EV's battery is within the defined lower and upper bounds.

$$E^{EV,min}_{h} \leq E^{EV}_{h_j,t} \leq E^{EV,max}_{h_j}, \quad \forall t \in t^{EV}_{h_j}; \forall h_j \in \mathcal{H} \tag{3.14}$$

The equation (3.15) defines the energy level within the device at the time of arrival:

$$E^{EV}_{h_j,t} = E^{EV,AR}_{h_j}, \quad \forall t \in t^{AR}_{h_j}; \forall h_j \in \mathcal{H} \tag{3.15}$$

At the time of departure, the energy of the EV should equal the desired energy level as follows:

$$E^{EV}_{h_j,t} = E^{EV,DEP}_{h_j}, \quad \forall t \in t^{DEP}_{h_j}; \forall h_j \in \mathcal{H} \tag{3.16}$$

ESS Operational Constraints

Equation (3.17) presents the energy level of ESS during charging and discharging time.

$$E^{ESS}_{h_j,t} = E^{ESS}_{h_j,t-1} + \tau(P^{ESS}_{C_{h_j,t}} \cdot \eta^{ESS}_{C_{h_j}} - P^{ESS}_{D_{h_j,t}}), \forall t \in \mathcal{T}; \forall h_j \in \mathcal{H} \tag{3.17}$$

In E-q. (3.17), the first term is the energy level of ESS for the previous time step, and the second represents the charging and discharging of the ESS . ESS charges from PV or DSO are as follows:

$$P^{ESS}_{C_{h_j,t}} = P^{ESS,DSO}_{D_{h_j,t}} + P^{PV,ESS}_{D_{h_j,t}}, \quad \forall t \in \mathcal{T}; \quad \forall h_j \in \mathcal{H} \tag{3.18}$$

In (3.18), the first term represents the charging of ESS from the DSO, and the second term represents the charging of ESS from PV. The equation (3.19) ensures the discharging of ESS to the house or the DSO.

$$P^{ESS}_{D_{h_j,t}} = \frac{P^{ESS,DSO}_{D_{h_j,t}} + P^{ESS,H}_{D_{h_j,t}}}{\eta^{ESS}_{D_{h_j}}}, \quad \forall t \in \mathcal{T}; \forall h_j \in \mathcal{H} \tag{3.19}$$

Equation (3.20) sets the initial energy of ESS at the start of the time horizon, and (3.21) ensures that the energy stored within the ESS stays at the desired level at the end of the day.

$$E^{ESS}_{h_j,t} = E^{initial}_{ESS} \quad \forall t = 0, \forall h_j \in \mathcal{H} \tag{3.20}$$

$$E^{ESS}_{h_j,t} = E^{final}_{ESS} \quad \forall t = 95, \forall h_j \in \mathcal{H} \tag{3.21}$$

Equations (3.22) and (3.23) limit the charging and discharging power of ESS between the minimum and maximum allowable limits, respectively. Also, equations (3.22) and (3.23) limit the charging and discharging and ensure that charging and discharging should not occur simultaneously.

$$0 \leq P^{ESS}_{C_{h_j,t}} \leq P^{ESS,max}_{C_{h_j,t}} \cdot X^{ESS}_{h_j,t}, \quad \forall t \in \mathcal{T}; \forall h_j \in \mathcal{H} \tag{3.22}$$

$$0 \leq P^{ESS}_{D_{h_j,t}} \leq P^{ESS,max}_{D_{h_j,t}} \cdot (1 - X^{ESS}_{h_j,t}), \quad \forall t \in \mathcal{T}; \forall h_j \in \mathcal{H} \tag{3.23}$$

The energy stored within ESS also remains within their upper and lower bounds due to the following constraint:

$$E^{ESS,min}_{h} \leq E^{ESS}_{h_j,t} \leq E^{ESS,max}_{h_j}, \quad \forall t \in t^{ESS}_{h_j}; \forall h_j \in \mathcal{H} \tag{3.24}$$

3.2.2 Aggregator Model for Flexibility Management (Middle level)

Currently, the DSO that owns and manages the distribution network carries out functions analogous to an aggregator. The aggregator sums the buying and selling power of the houses as follows:

$$P_{j,t}^{d_{agg}} = \sum_{h}^{H} P_{h_j,t}^{Buy,DSO}, \qquad \forall t \in \mathcal{T}; \forall j \in \mathcal{N} \tag{3.25}$$

$$P_{j,t}^{sell_{agg}} = \sum_{h}^{H} P_{h_j,t}^{Sell,DSO}, \qquad \forall t \in \mathcal{T}; \forall j \in \mathcal{N} \tag{3.26}$$

Equation (3.25) calculates the aggregated power demand of the houses connected to that bus. The aggregated power includes base load, the power demand of EWH, charging and discharging of EV, and ESS . However, this information is hidden from the aggregator to protect the privacy of the end-user. Only the aggregated power demand from the house is sent to the aggregator. Similarly, the aggregated selling power constitutes excess PV power generated and power discharged from EV and ESS to the DSO. However, only the aggregated power for each time step that may be sent/received by the DSO is sent to the aggregator, as shown in (3.25) and (3.26) .

The aggregator in the proposed method provides a flexibility management service. The aggregator calculates the flexibility available to the DSO from each household at a given time interval as follows:

$$P_{h_j,t}^{flex^+} = (P_{h_j,t}^{con})_{J_1} - (P_{h_j,t}^{con})_{J_2} \quad if \quad (P_{h_j,t}^{con})_{J_1} > (P_{h_j,t}^{con})_{J_2}, \forall t \in \mathcal{T}; \forall h_j \in \mathcal{H} \tag{3.27}$$

$$P_{h_j,t}^{flex^-} = (P_{h_j,t}^{con})_{J_1} - (P_{h_j,t}^{con})_{J_2} \quad if \quad (P_{h_j,t}^{con})_{J_1} < (P_{h_j,t}^{con})_{J_1}, \forall t \in \mathcal{T}; \forall h_j \in \mathcal{H} \tag{3.28}$$

Equations (3.27) and (3.28) calculate the upward and downward flexibility, respectively. The flexibility of each prosumer is defined as the difference between power demand by each house using the objective function $J_{1,h}$ and objective function $J_{2,h}$. If the power demand of the house using $J_{1,h}$ is greater than the power demand using $J_{2,h}$, then the house can provide upward flexibility to the grid. It means that the house can reduce power demand. Similarly, if the power demand using $J_{1,h}$ is less than the power demand of $J_{2,h}$, then houses provide downward flexibility to the grid, thus requiring more power from the grid. The total upward and downward flexibility at bus j is the sum of upward

and downward flexibilities from all houses on the same bus, as in (3.29) and (3.30), respectively.

$$P_{j,t}^{flex^{+}_{agg}} = \sum_{h}^{H} P_{h_j,t}^{flex^{+}}, \quad \forall t \in \mathcal{T}; \forall j \in \mathcal{N} \tag{3.29}$$

$$P_{j,t}^{flex^{-}_{agg}} = \sum_{h}^{H} P_{h_j,t}^{flex^{-}}, \quad \forall t \in \mathcal{T}; \forall j \in \mathcal{N} \tag{3.30}$$

To calculate the flexibility index, each household's downward and upward flexibilities and the aggregated upward and downward flexibility are summed together for each time step, as described below.

$$P_{h_j,t}^{flex} = P_{h_j,t}^{flex^{+}} + P_{h_j,t}^{flex^{-}}, \quad \forall t \in \mathcal{T}; \forall h_j \in \mathcal{H} \tag{3.31}$$

$$P_{j,t}^{flex_{agg}} = \sum_{h}^{H} (P_{h_j,t}^{flex^{+}_{agg}} + P_{j,t}^{flex^{-}_{agg}}), \quad \forall t \in \mathcal{T}; \forall j \in \mathcal{N} \tag{3.32}$$

In equation (3.31), the net flexibility at the home level is calculated by taking the sum of downward and upward flexibility. Equation (3.32) sums the upward and downward flexibilities at bus j. The flexibility index is the ratio of the flexibility of each house to the aggregated flexibility, as follows:

$$\gamma_{h_j,t}^{flex} = \frac{P_{h_j,t}^{flex}}{P_{j,t}^{flex_{agg}}}, \quad \forall t \in \mathcal{T}; \forall h_j \in \mathcal{H}; \forall j \in \mathcal{N} \tag{3.33}$$

The aggregator also calculates the maximum power limit of each house based on their flexibility as follows:

$$P_{h_j,t}^{max} = (P_{h_j,t}^{con})_{J_2} - \gamma_{h_j,t} \cdot P_{j,t}^{f_{DSO}}, \forall t \in \mathcal{T}; \forall h_j \in \mathcal{H}; \forall j \in \mathcal{N} \tag{3.34}$$

In equation (3.34), the first term $(P_{h_j,t}^{con})_{J_2}$ is the power demand of the house, and the second term of the right-hand side is the flexibility index of that house and flexibility request from the DSO. The maximum power limit calculated in (3.34) will be an additional constraint at the home level to limit the power demand of the house as follows.

$$P_{h_j,t}^{Buy,DSO} \leq P_{h_j,t}^{max}, \quad \forall t \in \mathcal{T}; \forall h_j \in \mathcal{H} \tag{3.35}$$

The left side of (3.35) is the net power demand of the house. The right-hand side of the equation

(3.35) is the resulting power limit of equation (3.34). The HEMS will reschedule the appliance of the house according to the maximum power limit based on the upward and downward flexibility of that house, which will be discussed in detail in section 3.3.

3.2.3 Distribution System Operator (Upper level)

The DSO performs a system-level OPF analysis. The objective of the DSO has been defined as the minimization of total system losses and the calculation of the optimal flexibility request. The flexibility request is further scaled down at the aggregator level to limit each end-user based on the flexibility as in (3.34) . The objective of the DSO optimization is shown in the equation below:

$$J_3 = \sum_{t\in\mathcal{T}} \left(\frac{1}{2} \sum_{j=1}^{N} \sum_{k=1}^{N} G_{j,k} \Big(V_{j,t}^2 + V_{k,t}^2 - 2V_{j,t} \cdot V_{k,t} \cos(\delta_{j,t} - \delta_{k,t}) \Big) + \sum_{j=1}^{N} C^f P_{j,t}^{f_{DSO}} \right) \quad (3.36)$$

In (3.36), The first part of the equation calculates power losses, and the second part calculates the optimal flexibility request by using a weighted component of the total flexibility used.

DSO Constraints

The OPF is subjected to the active and reactive power balance equations as below:

$$P_{j,t}^{g} + P_{j,t}^{sell_{agg}} + P_{j,t}^{f_{DSO}} - P_{j,t}^{d_{agg}} = \sum_{k=1}^{N} V_{j,t} \cdot V_{k,t} \cdot Y_{j,k} \cos\left(\theta_{j,k} + \delta_{k,t} - \delta_{j,t}\right), \forall t \in \mathcal{T}; \forall (j,k) \in \mathcal{N} \quad (3.37)$$

$$Q_{j,t}^{g} + Q_{j,t}^{f_{DSO}} - Q_{j,t}^{d_{agg}} = -\sum_{k=1}^{N} V_{j,t} \cdot V_{k,t} \cdot Y_{j,k} \sin\left(\theta_{j,k} + \delta_{k,t} - \delta_{j,t}\right), \forall t \in \mathcal{T}; \forall (j,k) \in \mathcal{N} \quad (3.38)$$

In equation (3.37) and (3.38), the first term of left-hand side is active and reactive power generation of the substation, respectively. The second term in (3.37) is aggregated selling power to the DSO. The third term $P_{j,t}^{f_{DSO}}$ in (3.37), and the second term $Q_{j,t}^{f_{DSO}}$ in (3.38) are optimal flexibility request, the fourth term $P_{j,t}^{d_{agg}}$ in (3.37), and the third term $Q_{j,t}^{d_{agg}}$ in (3.38) represent aggregated active and reactive power demand of the household connected to bus j. The right-hand side of the equations in (3.37) and (3.38) are the active and reactive power losses at that bus, respectively. The aggregated reactive power and reactive flexibility are calculated with a constant load power factor of 0.85 as

follows:

$$Q_{j,t}^{d_{agg}} = \sqrt{\frac{1 - PF^2}{PF^2}} P_{j,t}^{d_{agg}}, \quad \forall t \in \mathcal{T}; \forall j \in \mathcal{N} \tag{3.39}$$

$$Q_{j,t}^{f_{DSO}} = \sqrt{\frac{1 - PF^2}{PF^2}} P_{j,t}^{f_{DSO}}, \quad \forall t \in \mathcal{T}; \forall j \in \mathcal{N} \tag{3.40}$$

In addition to the above constraints, the bus voltage and active/reactive power drawn from the grid are limited by upper and lower bounds as follows:

$$V_j^{min} \leq V_{j,t} \leq V_j^{max}, \quad \forall t \in \mathcal{T}; \forall j \in \mathcal{N} \tag{3.41}$$

$$P_{g_j}^{min} \leq P_{j,t}^{g} \leq P_{g_j}^{max}, \quad \forall t \in \mathcal{T}; \forall j = s \tag{3.42}$$

$$Q_{g_j}^{min} \leq Q_{j,t}^{g} \leq Q_{g_j}^{max}, \quad \forall t \in \mathcal{T}; \forall j = s \tag{3.43}$$

Equation (3.41) ensures the bus voltage is within the limit. Similarly, the active and reactive power drawn from the substation is limited in equation (3.42) and (3.43), respectively. The optimal flexibility request from the grid should be limited to the flexibility of the aggregator at that bus as follows:

$$\xi^{+} \cdot P_{j,t}^{d_{agg}} \leq P_{j,t}^{f_{DSO}} \leq P_{j,t}^{flex_{agg}^{+}}, \quad \forall t \in \mathcal{T}; \forall j \in \mathcal{N} \tag{3.44}$$

$$\xi^{-} \cdot (P_{j,t}^{sell_{agg}} + P_{j,t}^{g}) \geq P_{j,t}^{f_{DSO}} \geq P_{j,t}^{flex_{agg}^{-}}, \quad \forall t \in \mathcal{T}; \forall j \in \mathcal{N} \tag{3.45}$$

In (3.44), if aggregated flexibility is positive, it means that prosumers are willing to reduce their power demand. The DSO sends an optimal flexibility request to the aggregator within the upper and lower bounds of aggregated upward flexibility from the aggregator level. Where ξ^{+} and ξ^{-} are the percentage values the DSO selects according to their requirements, respectively. Similarly, equation (3.45) calculates flexibility when $P_{j,t}^{flex_{agg}}$ is negative, meaning the prosumer wants to increase their power demand at a specific time within the downward flexibility bound provided by the aggregator.

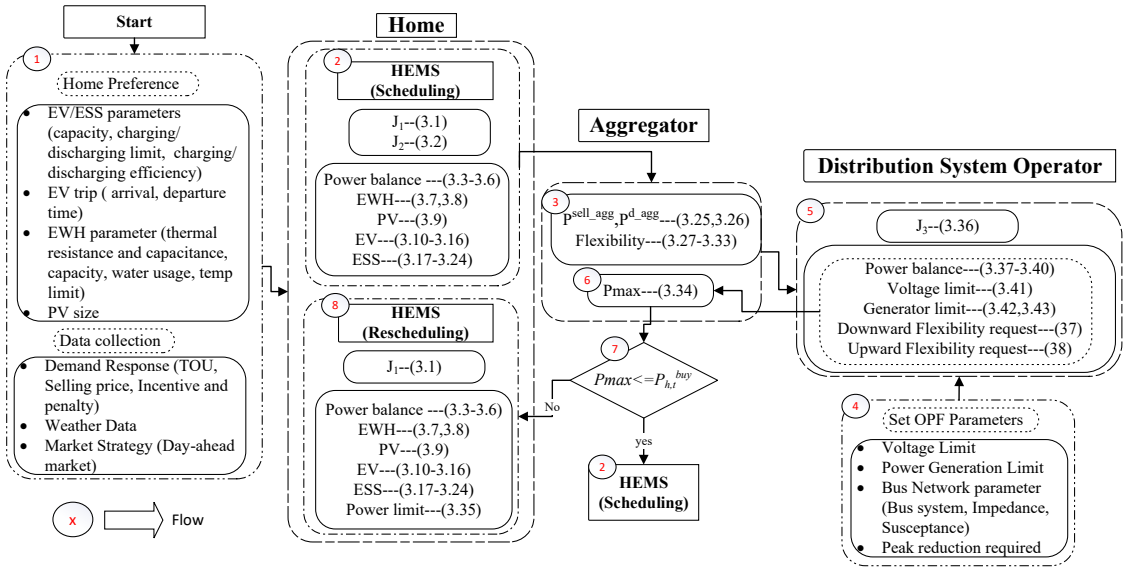

Figure 3.2: Proposed coordination framework of ML-EMS

3.3 Coordination Framework of ML-EMS for Flexibility Provision

We consider modern HEMS installed at the end-user side for managing appliances with shifting capabilities in response to a flexibility request from an aggregator. The HEMS can optimize the shifting time of various appliances and reschedule them for flexibility provision. A novel ML-EMS consists of a three-level coordination framework: home level, which performs HEMS for a prosumer at the first level, an aggregator at the second level, and OPF at the third level, as shown in figure 3.1. The proposed coordination framework comprises the following steps.

- Each house has a HEMS that receives input updates such as customer preferences, such as the desired upper and lower limit of the hot water temperature, arrival and departure time of the EV, and initial and final energy level of ESS at the beginning and end of the day, parameters of the appliances used in the house, for instance, type and built-in characteristic of the EV, ESS , EWH as in table 3.1 and 3.2, and demand response information (ToU, FiT), as shown in figure 3.2.

- The HEMS schedules the house appliances based on the prosumer's electricity costs and energy-saving objectives. Houses become flexible resources when a HEMS is incorporated

into them. The optimal load demand is determined at the house level and sent to the aggregator. To protect the privacy of the end-user, they only provide the aggregated power profile, as shown in equations (3.25)-(3.35).

- As mentioned in the literature, the individual flexibility of each prosumer will not be useful for DSO. To exploit the prosumers' flexibility, an aggregator is required to provide the bulk of the flexibility to the DSO. The aggregator acts as an intermediary between multiple houses and DSO, which exchanges information that is the decision variables from one level to another. The information flow from the end-users to the aggregator is $P_{h_j,t}^{Buy,DSO}$, $P_{h_j,t}^{Sell,DSO}$, $(P_{h_j,t}^{con})_{J_1}$, and $(P_{h_j,t}^{con})_{J_2}$. The information that goes from the aggregator to the end-users is $P_{h_j,t}^{max}$, and $\gamma_{h_j,t}$. The aggregator exchange information with DSO are $P_{j,t}^{dem_{agg}}$, $P_{j,t}^{sell_{agg}}$, $P_{j,t}^{flex^{+}_{agg}}$, $P_{j,t}^{flex^{-}_{agg}}$, and $P_{j,t}^{f_{DSO}}$.

- The aggregator performs five tasks: (a) Sums up the bus-wise optimal power demand of households while minimizing electricity costs and energy, as (3.25) and (3.26). (b) Calculates the flexibility of each prosumer as in (3.27)-(3.31). (c) Aggregates the bus-wise flexibility of all the houses, as in (3.32). (d) Calculates the flexibility index of each house, as in (3.33). The aggregator sends the aggregated upward and downward flexibility of all the prosumers to the DSO.

- The DSO minimizes overall system losses, as in (3.36)-(3.45). The DSO calculates the optimal flexibility required, $P_{j,t}^{f_{DSO}}$, from the aggregator within the upward and downward flexibility limit using (3.44) and (3.45). The DSO sends the flexibility-required signal to the aggregator.

- The aggregator receives the flexibility request from the DSO. After that, the aggregator performs two more tasks: (e) Limits each house to the maximum power they can buy from DSO based on the flexibility request and flexibility of that house, as in (3.34).

- The prosumer reruns the optimization using equation (3.1) and reschedules the appliances with new constraints of limiting the power demand to a limit as in equation (3.35).

Caapacitive Susceptance	
Line	1/2B
1-2	0.030
1-3	0.025
2-3	0.020
2-4	0.020
2-5	0.015
3-4	0.010
4-5	0.025

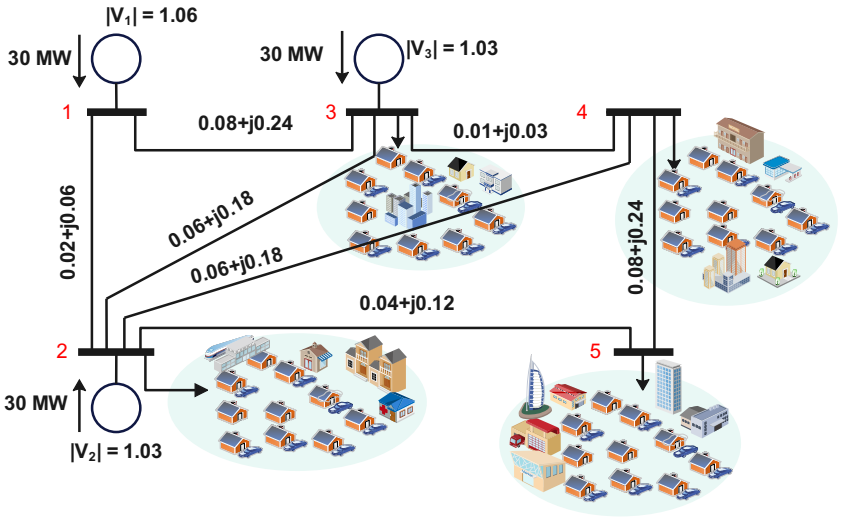

Figure 3.3: Five bus transmission network.

Table 3.1: Modeling parameters of EVs [3, 4] and ESS [3]

	Type	Capacity (kWh)	Charging rate (kW/h)	Discharging rate (kW/h)	Charging efficiency	Discharging efficiency
EV 1	Chevy Spark EV	19	3.3	2.80	0.89	0.91
EV 2	Ford Focus Electric	23	6.6	4.81	0.94	0.92
EV 3	Tesla model S	85	10	10	0.91	0.95
ESS	-	46	4.5	3.8	0.86	0.85

3.4 Result

Case Study

The proposed three-level EMS model is implemented on the Python platform using a Python-based open-source optimization modeling library known as python optimization modeling library (PYOMO) [184]. The lower level is a MILP problem solved using a CPELX solver [185]. The upper level is an non-linear programming (NLP) problem, solved using an IPOPT solver [186]. In this work, the operator is responsible for managing a 5-bus system [187] and meeting the demand of its 10000 prosumers at its various buses, as illustrated in figure 3.3. It can be implemented on large distribution networks like the 33-bus or the 123-bus distribution system.

We compare the three-level-EMS model with and without flexibility. Hereafter, we call without/before flexibility provision as "*before*" and with/after flexibility as "*after*," which is the proposed

Table 3.2: Modeling parameters of EWH [3]

	Power (kW)	Water tank capacity (L)	Thermal resistance ($^{\circ}C$ /kW)	Thermal capacitance (kWh/$^{\circ}C$)
EWH	4.5	400	1.52	863.4

model. In the proposed model, we limit the buying power of each prosumer to an adaptive maximum limit $P_{h,t}^{max}$. The green curve in figure 3.4 displays the maximum power limit $P_{h,t}^{max}$ for the prosumer from the grid based on their flexibility. The power demand of each prosumer in figure 3.4 shows that the proposed method (' *after*' flexibility) has less peak than the power demand of the previous method (' *before*' flexibility). The proposed methodology effectively reduces power consumption while simultaneously shifting buying power. We present an illustrative example of this approach in Fig 3.4, which showcases house number 12. From the load profile of each appliance in the household, we can see that the proposed method shifts the load and reduces it, as shown in Fig 3.5.

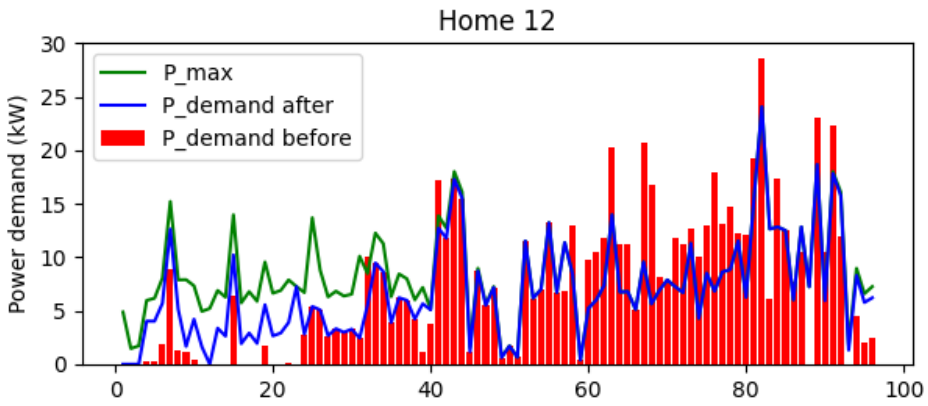

Figure 3.4: Power demand (before and after) and max power limit of home 12.

Figure 3.5 illustrates the power demand for bus 4. We can see that the proposed strategy reduces the peaks and shifts them to another period compared to without flexibility provision. Figure 3.5 shows the voltage, power demand, and power generation profiles at bus 4. The voltage profile in figure 3.5 shows that the proposed model improves the voltage. Similarly, the power demand peaks are reduced and shifted to another period, flattening the power demand as in figure 3.5b. Also, the power generation is reduced at bus 2, as shown in figure 3.5c, reducing the cost of power generation.

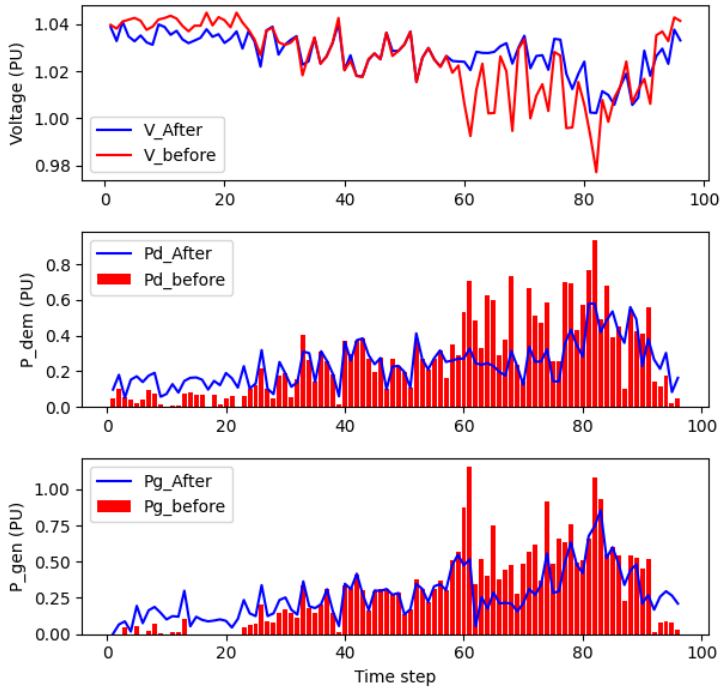

Figure 3.5: Simulation result on DSO, (a) Voltage profile, (b) power demand, and (c) power generation profile

Table 3.3: Comparison of three scenarios

	Previous Method	Proposed method
Electricity Cost of house 12, $/day	8.4	9.0
Energy demand of house 12, kWh/day	146.3	128.8
Total System losses, MWh/day	11.01	7.31
Total minimum generation Cost, $/day	24509.2	24046.8

Using the proposed method, the aggregator provides flexibility to all the prosumers connected to a specific bus. Then, the grid requests flexibility from the aggregator to minimize the losses and power generation cost, as in figure 3.5c

In our investigation, we perform a comparative analysis of electricity costs and energy consumption for prosumers. The integration of solar panel-generated power within the household significantly curtails energy consumption by offsetting grid dependency. The comprehensive assessment, including losses and generation costs of the entire system, is summarized in table 3.3. Notably, our proposed method demonstrates substantial reductions in energy demand, active power losses, and power generation costs across the entire system.

The electricity cost of house 12 is increased because the prosumer is forced to consume power at a high price. In the next chapter, we propose a novel incentive program to reduce the electricity in each house.

In conclusion, a novel three-level coordination framework is presented in this chapter, which considers the technical objectives of the system operator as well as the economic objective of prosumers. The aggregator calculates the power buy/sell from/to the grid and flexibility of the prosumers. The results demonstrate the effectiveness of the proposed method by reducing peak demand, power losses, and power generation costs and improving the voltage profiles at the system level. As the electricity cost of the prosumer is higher in the proposed method, there is a need for an adaptive incentive program that will provide monetary benefit for the prosumer who will take part in the flexibility. Optimizing the DERs (PV, heat pumps in this case) operation of big buildings to provide flexibility to the grid or neighborhood.

3.5 Optimization with RC Modeling For Varennes Library

In this subsection, we are calculating the flexibility of the institutional building. For this, we use the same two objectives (cost and energy minimization) with reference to the real consumption of the building.

When developing control-oriented models, finding the right balance between detailed process requirements, precise modeling, and high time resolution is crucial. At the same time, it's important to keep inputs to a minimum and ensure the model is easy to use, reliable, and computationally efficient. Many experts rely on thermal resistance-capacitance (RC) network models, which employ the heat balance equation to achieve these objectives. However, given their high computational demands, low-order models are often recommended, with their parameters identified through various system identification techniques.

This study explores effective strategies for achieving energy flexibility in a solar-powered, net-zero energy building in Quebec. It examines the correlation between a BIPV system, geothermal heat pump (HP), and radiant floor to optimize energy efficiency.

3.5.1 RC Modeling of building

The resistance-capacitance (RC) or gray-box model is a well-established method for controlling indoor temperatures in buildings. It focuses on modeling walls as a resistance between thermal zones, improving heat retention efficiency. The zone mass is represented as capacitors, which store thermal energy. This work presents a simplified version of the 10^{th}-order RC model mentioned in [188]. Figure 3.6 showcases an 11R5C (5^{th} order) model with eleven resistances and five capacitors.

The equations (3.46) to (3.53) represent the thermal model of the building. The equation (3.46), shows the zone temperature T_t^Z as below:

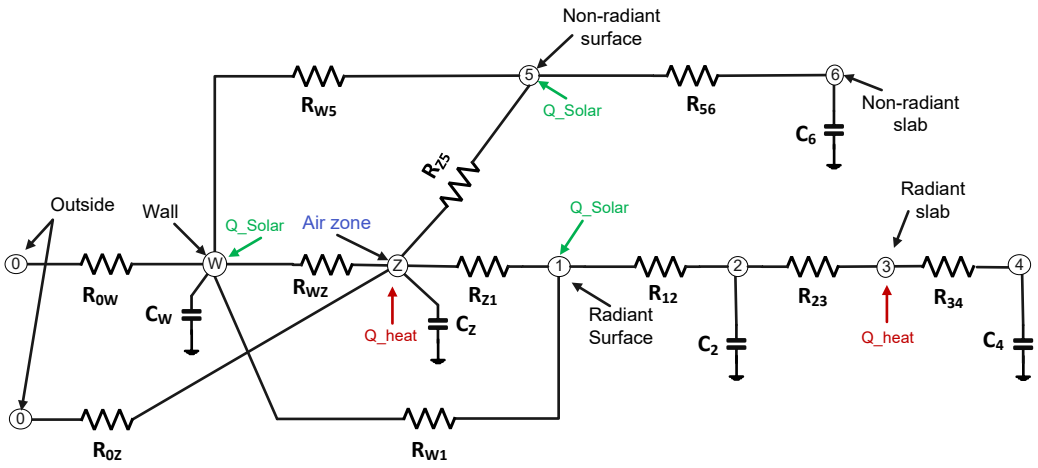

Figure 3.6: RC model of Varennes library.

C_w

$$T_t^Z = T_{t-1}^Z + (\frac{U_{WZ}(T_t^W - T_t^Z)}{k_{ef} * C_Z} + \frac{U_{Z2}(T_t^Z - T_t^2)}{k_{ef} * C_Z} + \frac{U_{Z5}(T_t^Z - T_t^5)}{k_{ef} * C_Z} + \frac{U_{0Z}(T_t^0 - T_t^Z)}{k_{ef} * C_Z}) \cdot \Delta t \tag{3.46}$$

Equation (3.47) formulates the temperature of the wall T_t^W in the building. $T_t^1, T_t^2, T_t^3, T_t^4, T_t^5$, and T_t^6 represent nodes 1-6, respectively, as shown in figure 3.6.

$$T_t^W = T_{t-1}^W + (\frac{U_{0W}(T_t^0 - T_t^W)}{k_{ef} * C_W} + \frac{U_{W6}(T_t^W - T_t^6)}{k_{ef} * C_W} + \frac{U_{WZ}(T_t^W - T_t^Z)}{k_{ef} * C_W}) \cdot \Delta t \tag{3.47}$$

$$T_t^1 = T_{t-1}^1 + (U_{Z1}(T_t^Z - T_t^1) + U_{12}(T_t^1 - T_t^2) + U_{W1}(T_t^W - T_t^1)) \cdot \Delta t \tag{3.48}$$

$$T_t^2 = T_{t-1}^2 + (\frac{U_{12}(T_t^1 - T_t^2) + U_{23}(T_t^2 - T_t^3)}{k_{ef} * C_2}) \cdot \Delta t \tag{3.49}$$

$$T_t^3 = T_{t-1}^3 + (U_{23}(T_t^2 - T_t^3) + U_{34}(T_t^3 - T_t^4)) \cdot \Delta t \tag{3.50}$$

$$T_t^4 = T_{t-1}^4 + (\frac{U_{34}(T_t^3 - T_t^4)}{k_{ef} * C_4}) \cdot \Delta t \tag{3.51}$$

$$T_t^5 = T_{t-1}^5 + (U_{W5}(T_t^W - T_t^5) + U_{Z5}(T_t^Z - T_t^5) + U_{56}(T_t^5 - T_t^6)) \cdot \Delta t \tag{3.52}$$

$$T_t^6 = T_{t-1}^6 + (\frac{U_{56}(T_t^5 - T_t^6)}{k_{ef} * C_6}) \cdot \Delta t \tag{3.53}$$

3.5.2 Building Energy Management System

For modeling the building EMS (BEMS), we used the same formulation we did in section 3.2.1. Here, we have only PV, Base load (uncontrollable load), and heat pump (HP). The only control variable is HP.

Power balance equation

The power balance equation (3.3) can be reduced as below:

$$P_t^{Dem,G} = P_t^{BL} + P_t^{HP} - P_t^{PV,B}, \qquad \forall t \in \mathcal{T} \tag{3.54}$$

In (3.54), the different terms represent the power demand of the base load, the power demand of the HP, and the power supply to the building from the PV.

Similarly, equation 3.4 where BEMS can sell power to the grid and reduce the electricity cost according to the Feed-in Tariff (FiT), as below:

$$P_t^{Expt,G} = P_t^{PV,G} \qquad \forall t \in \mathcal{T} \tag{3.55}$$

In (3.55), the right-hand side is PV supply surplus power to the grid.

Heat Pump Operational Constraint

$$P_t^{HP} = \frac{Q_t^{HP,G}}{COP^{HP}} \qquad \forall t \in \mathcal{T} \tag{3.56}$$

Equation (3.56) represents the operational constraint of an HP system at time t. It calculates the electrical power consumption P_t^{HP} of the HP as the ratio of the thermal energy output $Q_t^{HP,G}$ and the coefficient of performance (COP) (COP^{HP}) is 4.

$$Q_{min,t}^{HP} \leq Q_t^{HP} \leq Q_{max,t}^{HP}, \quad \forall t \in \mathcal{T} \tag{3.57}$$

$$P_{min,t}^{HP} \leq P_t^{HP} \leq P_{max,t}^{HP}, \quad \forall t \in \mathcal{T} \tag{3.58}$$

Equation (3.57) and (3.58) set bounds on the thermal and electrical power of HP Q_t^{HP} P_t^{HP}, respectively. It ensures that the HP output remains within the specified minimum ($Q_{min,t}^{HP}$, $P_{min,t}^{HP}$) and maximum ($Q_{max,t}^{HP}$, $P_{max,t}^{HP}$) limits.

PV Operational Constraint

The BEMS distributed power generated by the PV system to both the grid and the building, as represented in (3.9).

Temperature Constraint

$$T_{min,t}^{air} \leq T_t^{air} \leq T_{max,t}^{air}, \quad \forall t \in \mathcal{T} \tag{3.59}$$

The equation (3.59) enforces constraints on the air temperature T_t^{air} at time t. It ensures that the air temperature remains within the specified minimum ($T_{min,t}^{air}$) and maximum ($T_{max,t}^{air}$) limits for all time periods t in the set $\mathcal{T}$. These constraints are vital for maintaining comfortable and safe indoor environmental conditions.

$$T_{min,t}^{slab} \leq T_t^{slab} \leq T_{max,t}^{slab}, \quad \forall t \in \mathcal{T} \tag{3.60}$$

The equation (3.60) sets bounds on the temperature T_t^{slab} of a slab or surface at time t. Similar to the air temperature constraint, it ensures that the slab temperature remains within the specified minimum ($T_{min,t}^{slab}$) and maximum ($T_{max,t}^{slab}$) limits for all time periods t in the set $\mathcal{T}$. These constraints are relevant, for instance, in applications where maintaining surface temperatures within specific ranges is essential for operational effectiveness and safety.

Figure 3.7: Front and plan view of Varennes library.

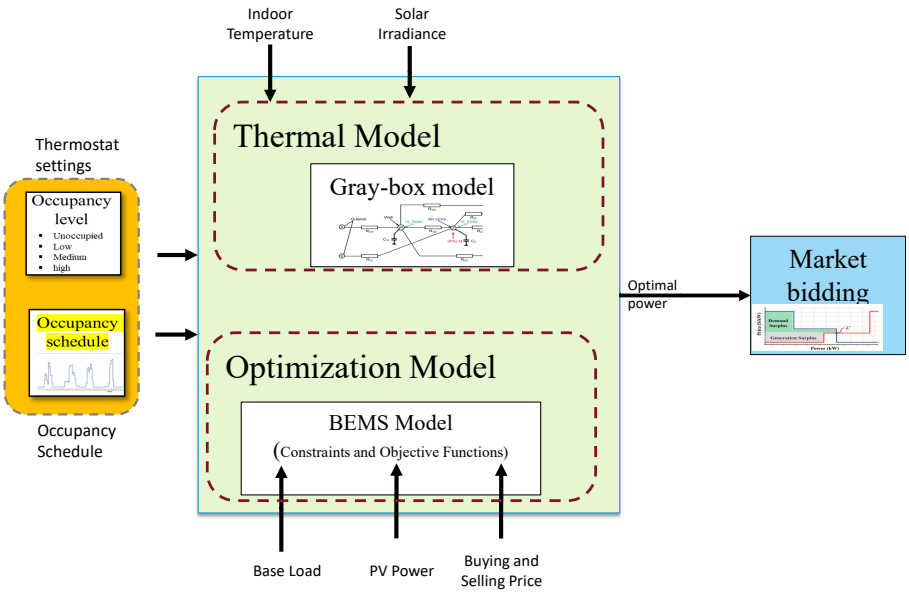

Figure 3.8: Block Diagram.

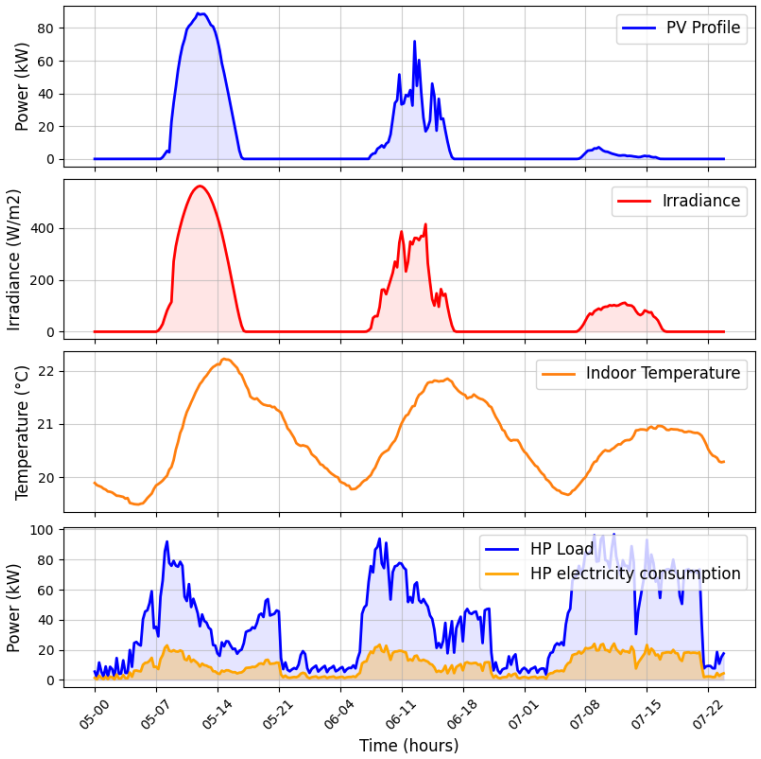

Figure 3.9: Measurement data of typical cloudy and sunny days at Varennes library.

Objective function

We use two different objectives to calculate the flexibility of the Varennes library. The two objectives are cost and energy minimization, as in equation (3.1) and (3.2). These objectives can be mathematically modeled through the application of optimization equations as follows:

Cost minimization

$$J_{11} = \sum_{t \in T} (P_t^{Buy,HQ} \cdot \pi_t^{Buy} - P_t^{Sell,HQ} \cdot \pi_t^{Sell}) \tau \tag{3.61}$$

Equation (3.61) is the objective function to minimize the energy cost of a building. In equation (3.61), the first term $P_t^{Buy,HQ}$ is power buying/demand from the hydro Quebec (HQ) by the prosumers with buying price (Flex rate) π_t^{Buy} of electricity from the HQ. The second term of right-hand side in equation (3.61) is power selling to the HQ from the building's DERs corresponding to the selling price.

Maximizing self-consumption of the building

Equation (3.62) minimizes the energy consumption of building using controllable appliances that are HP and PV. The right-hand side of equation (3.62) is the power demand of the base load, the power demand of HP, and the power supply to the building from the PV.

$$J_{22} = \sum_{t \in T} (P_t^{BL} + P_t^{HP} - P_t^{PV,B})\tau \tag{3.62}$$

3.6 Proposed Framework

In this work, we want to combine the RC model with BEMS, as shown in figure 3.8. This work is the middle block of the whole transaction framework, which means that we get the input from the library and from the occupancy behavior model, and then, after optimization, we provide the optimal output power (import/export) to the spot market. The two objectives here aim to get different optimal power and cost profiles from the library and provide these optimal profiles to the bidding market or bidding and also calculate the flexibility of the building.

3.7 Result and Discussion

Integrating thermal and electrical energy systems in building design can provide valuable flexibility services to the grid. Constructing high-performing buildings with integrated generation and storage systems, energy-efficient HVAC systems, and building automation systems can significantly reduce energy consumption and make buildings a significant source of energy flexibility. The Varennes Library is a great example of such a building and serves as a model for non-residential buildings with similar performance. The building was opened to the public in 2015 and inaugurated in May 2016 as a high-profile demonstration project that received several awards. The library has two floors with a total floor area of 2100 m^2. The first and second radiant floors serve five and six zones, with a total heated slab area of 675 m^2. Four electric ground-source HPs provide the library heating and cooling with a capacity of 105 kW (see Figure. 3.7). In addition to the air system, heating and cooling are also provided by a radiant hydronic slab system installed on the concrete floor

of the building. The slab surface temperature is typically between 18 - 29°C. The data available are PV power, radiance, HP load, and indoor and slab temperature, as shown in figure 3.9.

It is assumed that the actual measurements of total overall heating are the sum of heat into the concrete slab Q_t^{slab}, the heat to the air handling unit Q_t^{AHU}, and fan coil thermal unit Q_t^{FCU} amounts. To estimate T_t^{slab}, it is assumed that a maximum of 50% of Q_t^{Total} is supplied to the concrete slab, i.e., Q_t^{slab}. Therefore, the remaining 50 % of the total heat is provided to the air handling unit and the fan coil thermal units, i.e., Q_t^{hp}, as shown in figure 3.7.

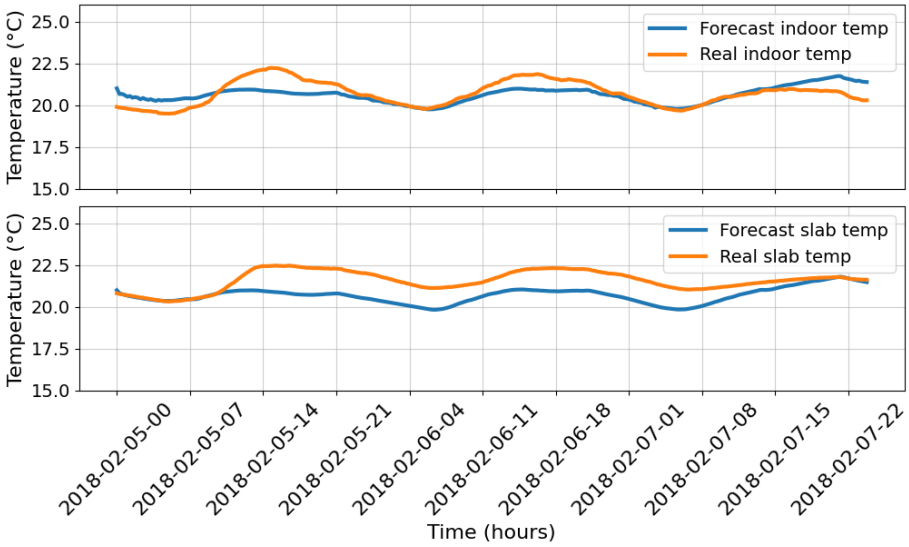

Figure 3.10: Indoor and Slab temperature using RC model.

3.7.1 RC Model

Using the proposed RC model presented in this work, the forecast indoor and slab temperatures are compared with the reference measured indoor and slab temperature as shown in figure B.3. From the second plot of figure B.3, it can be seen that the proposed RC model closely follows the actual temperature of the indoor and slab temperatures. The absolute error between them is lower than 5%.

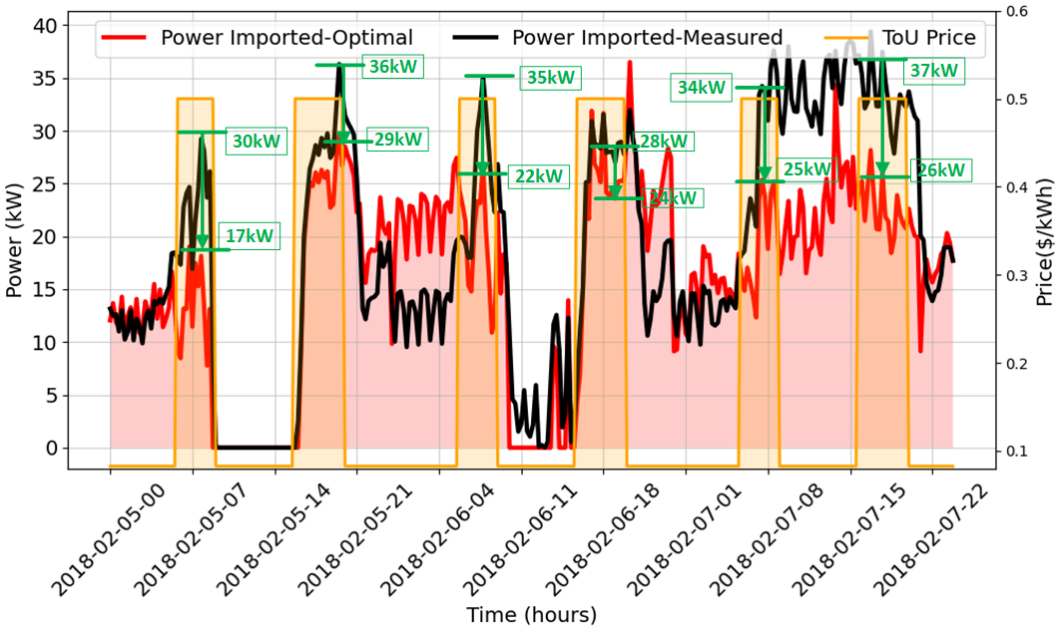

Figure 3.11: Peak reduction of imported power from the grid using Obj 1.

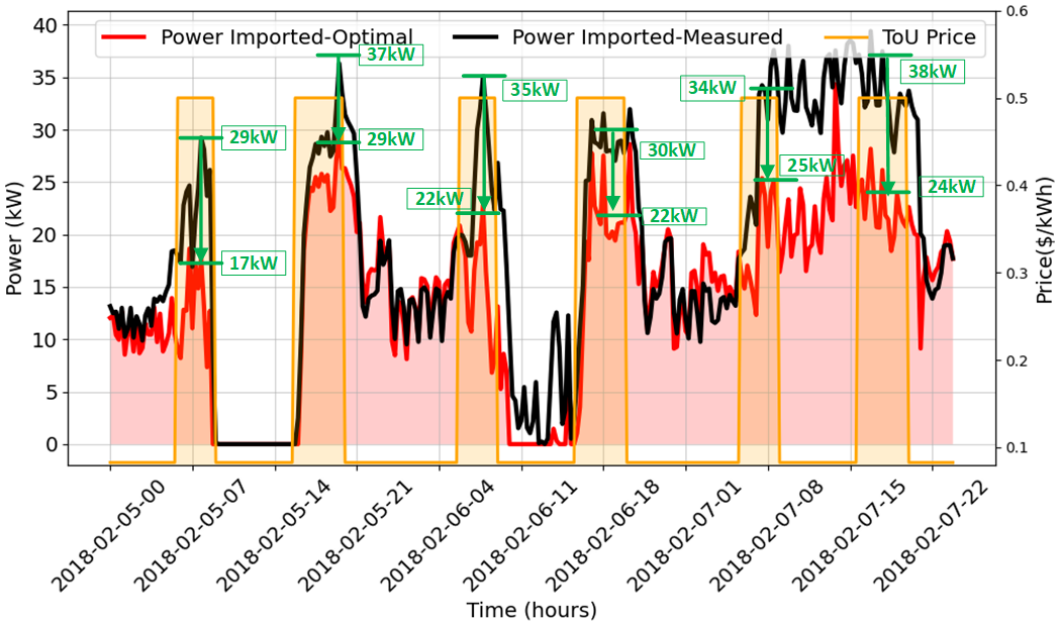

Figure 3.12: Peak reduction of imported power from the grid using Obj 2.

3.7.2 BEMS Model

The detailed analysis of the power profiles of the imported power, PV power supply to the home, HP load, electricity consumption, and indoor temperature using three objectives are in the appendix B objective. Figures 3.11 and 3.12 illustrate the net imported power under the reference with two

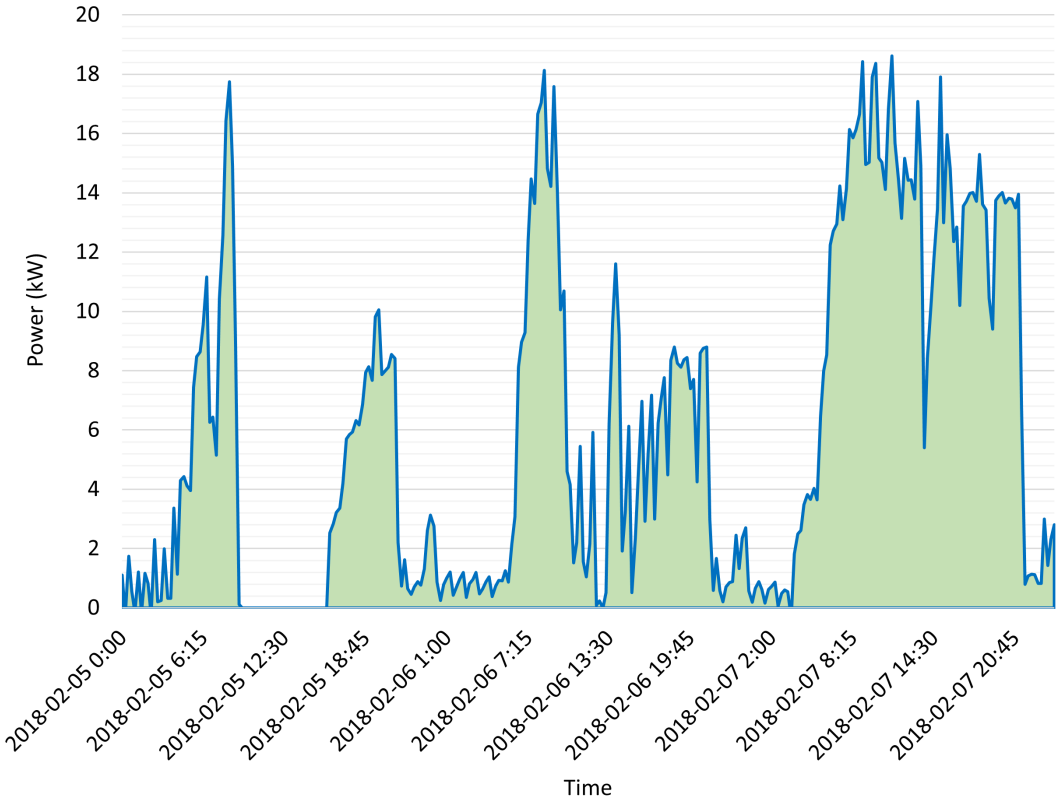

Figure 3.13: Flexibility of the Varennes Library.

objective functions: cost minimization, energy minimization, and exported power maximization, respectively. As shown in these figures, objective 2 (minimizing power demand) has remarkably decreased the net imported peak power from 29 to 17 kW, 37 to 29 kW, 35 to 22 kW, 32 to 26 kW, 37 to 25 kW, and 39 to 25 kW in the morning and evening, on sunny, partly sunny days and cloudy days of February 5th to 7th, respectively. The detailed power profile and temperature profile of the two objective functions are in Appendix B.

As in this case study, the HP is a flexible load. The HP behavior reduced morning and evening peak power using cost and energy minimization. However, the exported power maximization increases the peak power as shown in table 3.4. In table 3.4, we present a comprehensive overview of

the flexibility of imported power under varying weather conditions.

"*Cost Min*" shows cost minimization strategies for different weather scenarios. "*Energy Min*" presents findings for minimizing energy consumption. "*Export Max*" provides insights on maximizing power export under these weather conditions. Corresponding percentages of peak power reduction are presented for each case in the table 3.4. Exported power maximization increases the power consumption instead of reduction by -11.7%, -28.5%, -12.5%, -17%, and -20.9%, as shown in table 3.4.

This table shows how different optimization goals (cost minimization, energy minimization, and export maximization) reduce peak power consumption in varying weather conditions.

Table 3.4: Flexibility of imported power for three days (sunny, partly sunny, and cloudy day)

Objective Function	Days	Morning peak reduction (%)	Evening peak reduction (%)
Cost Min	Sunny Day (5th)	43	19
	Partly Sunny day (6th)	37	14
	Cloudy day (7th)	26	29
Energy Min	Sunny Day (5th)	41	21
	Partly Sunny day (6th)	37	18.5
	Cloudy day (7th)	26.4	36

Using the data extracted from figure 3.12, we have computed the flexibility, as shown in figure 3.13. Notably, the flexibility is entirely positive, indicating a decrease in power. This outcome is attributable to the exclusive presence of PV and HP as flexible loads in our case study. The absence of ESS, EWH, or EV, which could have resulted in negative flexibility, should be considered.

3.8 Summary

This chapter presents a detailed model of the multi-level energy management system. This chapter also presents a novel three-level coordination framework that considers the operational aspects and technical objectives of the system operator in conjunction with the economic objective of prosumers. The aggregator collects the flexibility of each household, and the cohort flexibility is provided to the DSO. The DSO performs optimal power flow to minimize system losses and sends the optimal flexibility reduction request to the aggregator. The aggregator then disaggregates the

flexibility requests to each participant as a peak limit on each house's consumption. The results demonstrate the effectiveness of the proposed method by reducing peak demand, power losses, power generation cost, and improving the voltage profiles at the system level.

In this chapter, we also develop a methodology that combines the RC model with the MILP-based optimization model for the Varennes library. We propose two objectives to obtain the optimal profile for bidding on the spot market and calculate the flexibility of the institutional building.

With the flexibility provision and power limit on the prosumer, the prosumers are forced to consume power at high price hour. That is why the price of the prosumer is high. Therefore, there is a need for an adaptive incentive program that will provide monetary benefit for the prosumer who will take part in the flexibility, which will be discussed in detail in the next chapter 4

Chapter 4

Incentive program based on the flexibility Using ML-EMS

NOMENCLATURE

Indices, Sets and Functions

h_j	Index of houses h at j bus
j, k	Index of buses in distribution system; $(j, k) \in \mathcal{N}$
t	Index of time; $t \in \mathcal{T}$
$t_{h_j}^{\boldsymbol{EV}}$	Index of time EV connected to house; $t_{h_j}^{EV} \in \mathcal{T}$
J_{3,h_j}	Cost minimization with optimal incentive objective function

Parameters

$P_{h_j,t}^{\boldsymbol{BL}}$	Base load; kW
$(P_{h_j,t}^{\boldsymbol{con}})_{J_1}$	Power demand using J_{1,h_j}; kW
$(P_{h_j,t}^{\boldsymbol{con}})_{J_2}$	Power demand using J_{2,h_j}; kW
$P_{j,t}^{\boldsymbol{flex_{agg}}}$	Total flexibility at bus j; kW

α, β	Maximum incentive, penalty
τ	Time step; $15min$
$\pi_t^{\textbf{\textit{Buy}}}$, $\pi_t^{\textbf{\textit{Sell}}}$	Buying, selling price; $\$/kWh$

Variables

$P_{h_j,t}^{\textbf{\textit{Buy,DSO}}}$	Buying power of household from DSO; kW
$P_{h_j,t}^{\textbf{\textit{Sell,DSO}}}$	Selling power of household to DSO; kW
$\pi_{h_j,t}^{\textbf{\textit{Inc/Pen}}}$	Incentive and penalty; $\$/kWh$

4.1 Background

This chapter focuses on a novel incentive program based on the flexibility provision using ML-EMS. [1] From a residential perspective, end-users can provide flexibility to the grid through the better scheduling and use of home appliances with capabilities to adjust their profiles by lowering or shifting their loads to other periods of the day. The role of prosumers as flexibility providers in the power system has been studied in the literature [179, 189, 190, 191, 192]. Researchers have focused on demand flexibility for energy management [179], frequency regulation [189], reverse power flow that causes voltage rise problems [190], network congestion management [191] and promoting the penetration of renewable resources [192]. More recently, a two-level coordination framework for the prosumers and system was developed in [193, 96, 41] for residential buildings. The authors in [96, 41] proposed a coordination framework that aimed to enhance the system's operational efficiency, lower energy costs for prosumers, and minimize network losses and peak power demand by utilizing the flexibility of prosumers. However, the framework presented in previous work is economically not viable due to the omission of an incentive program.

Therefore, it is necessary to find new services, incentive programs, and/or energy markets that allow for increased prosumer participation and promotion of HEMS, EVs, DERs, and other new

[1] This chapter has significant materials from the following paper published by the Ph.D. candidate:
Hussain, S., Alrumayh, O., Menon, R. P., Lai, C., & Eicker, U. (2023). Novel Incentive-based Multi-level Framework for Flexibility Provision in Smart Grids. IEEE Transactions on Smart Grid.

technology installations. This would also provide opportunities to improve understanding of the harmful effects and allow for tweaks that would curtail them. The involvement of the prosumers will greatly depend on the incentives offered. The higher the incentives, the higher the economic return is to the prosumers. In contrast, giving high incentives may increase the financial burden on the market remuneration mechanisms and skew the market towards one or more stakeholders. Therefore, considering the economic benefits for all market entities, including the utilities, DSOs, and end-users, is important. Hence, there is a need to determine the appropriate incentives to encourage prosumers to participate in such programs. In [193], the authors proposed a price-based DR program with fixed incentives to encourage prosumers to participate in peak reduction. However, the study did not consider the network constraints at the second level, and its reward function inadequately modeled the behavior and preferences of prosumers. In [194], researchers proposed a system for aggregating residential requests with incentive-based demand response, in which customers receive incentives depending on their participation. The authors primarily use thermal loads while ignoring the potential of non-thermal loads, such as ESS and EV. Also, the proper coordination framework between the end user, aggregator, and DSO was not considered.

Based on the above discussion, it can be seen that much more work is required to study how these incentive programs and flexibilities can be equitably distributed between the various stakeholders involved.

4.2 Novel Incentive/Penalty Program

The aggregator calculates the adaptable incentive for each house based on the flexibility it provides to the aggregator. Each prosumer will receive different incentive/penalty prices based on their power demand. The incentive/penalty is a function of the optimal power demand of the household using the objective functions Eq. (3.1) and (3.2), as follows:

$$\pi_{h_j,t}^{Inc/Pen} = (\alpha - \beta)\left(\frac{\exp((P_{h_j,t}^{con})_{J_2} - (P_{h_j,t}^{con})_{J_1})}{\exp((P_{h_j,t}^{con})_{J_2} - (P_{h_j,t}^{con})_{J_1}) + 1}\right) + \beta, \quad \forall t \in \mathcal{T}; \forall h_j \in \mathcal{H} \tag{4.1}$$

In Eq. (4.1), α is the maximum incentive (0.08 \$/kWh), and β is the maximum penalty (0.06 \$/kWh) for each house. The second term in (4.1) calculates incentives and penalties based on the

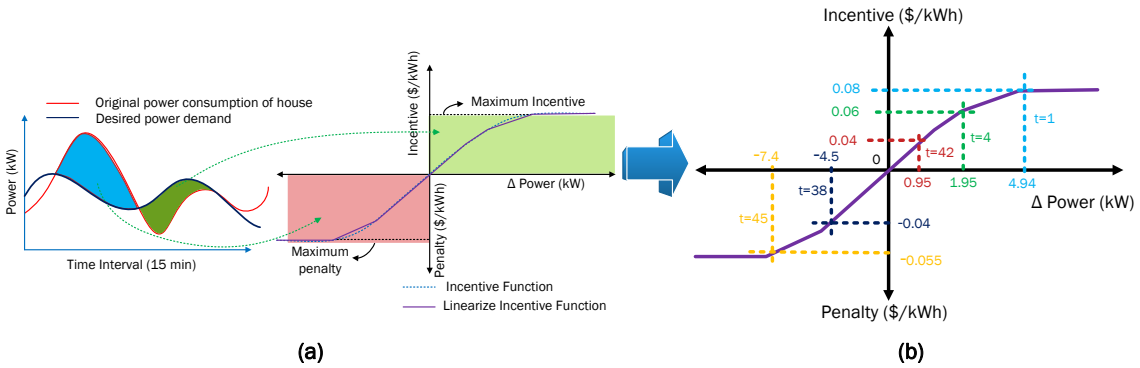

Figure 4.1: (a) Novel Incentive/penalty function. (b) Incentive/penalty value at different instances.

flexibility of the house. From Fig. 4.1a, it can be seen that if the actual power demand of the house is greater than the desired power demand of the house, the house will be penalized. Similarly, suppose the real power demand of the house is less than the desired power. In that case, the house will receive an incentive, as shown in Fig. 4.1a. The amount of the incentive and penalty depends on how much the house follows the flexibility (profile promised by the end-user) they claim to provide to the aggregator. The incentive and/or penalty are bound on α and β.

The incentive equation is decomposed using piece-wise linearization to convert the non-linear equation to linear so that it can be used to solve as part of the mixed-integer linear programming (MILP) problem at the home level in equation (4.3). Fig. 4.1b illustrates the different incentives/penalties imposed on the end-users by highlighting five instances where the incentive and penalty are given to house 86 at bus 9. The deviation between the expected optimal power consumption calculated for the house from the desired/recommended power demand (as preferred by the DSO) at time intervals 1 (9:00 AM), 4 (9:45 AM), and 42 (7:15 PM) of 4.95 kW, 1.95 kW, and 0.95 kW, leads to an incentive calculated by (4.1) of 0.08 $/kWh, 0.06 $/kWh, and 0.04 $/kWh, respectively. Similarly, at time intervals 38 (6:15 PM) and 45 (8:00 PM), the expected power consumption is higher than the desired power demand (by the DSO) by 4.5 kW and 7.5 kW, and the user is assigned a penalty of 0.04 $/kWh and 0.055 $/kWh, respectively.

The proposed method ensures that the end-user is not over-penalized. To achieve this, we have added a constraint that guarantees the electricity cost for the end-user who participates in the proposed method does not surpass that of the conventional Time of Use pricing scheme. The constraint is as follows:

$$J_{3,h_j} \leq J_{1,h_j}, \qquad \forall h_j \in \mathcal{H} \tag{4.2}$$

4.2.1 Reschedule Home Appliances

$$J_{4,h_j} = \sum_{t \in T} (P^{Buy,DSO}_{h_j,t} \cdot \pi^{Buy}_{t} - P^{Sell,DSO}_{h_j,t} \cdot \pi^{Sell}_{t} - \pi^{Inc/Pen}_{h_j,t} \cdot P^{Buy,DSO}_{h_j,t})\tau \tag{4.3}$$

Equation (4.3) minimizes the electricity cost with a novel incentive program based on flexibility provision. The first and the second term is the same as in Eq. (3.1) in addition to the adaptive incentive program, $\pi^{Inc/Pen}_{h_j,t}$ is multiplied with power imported from the DSO.

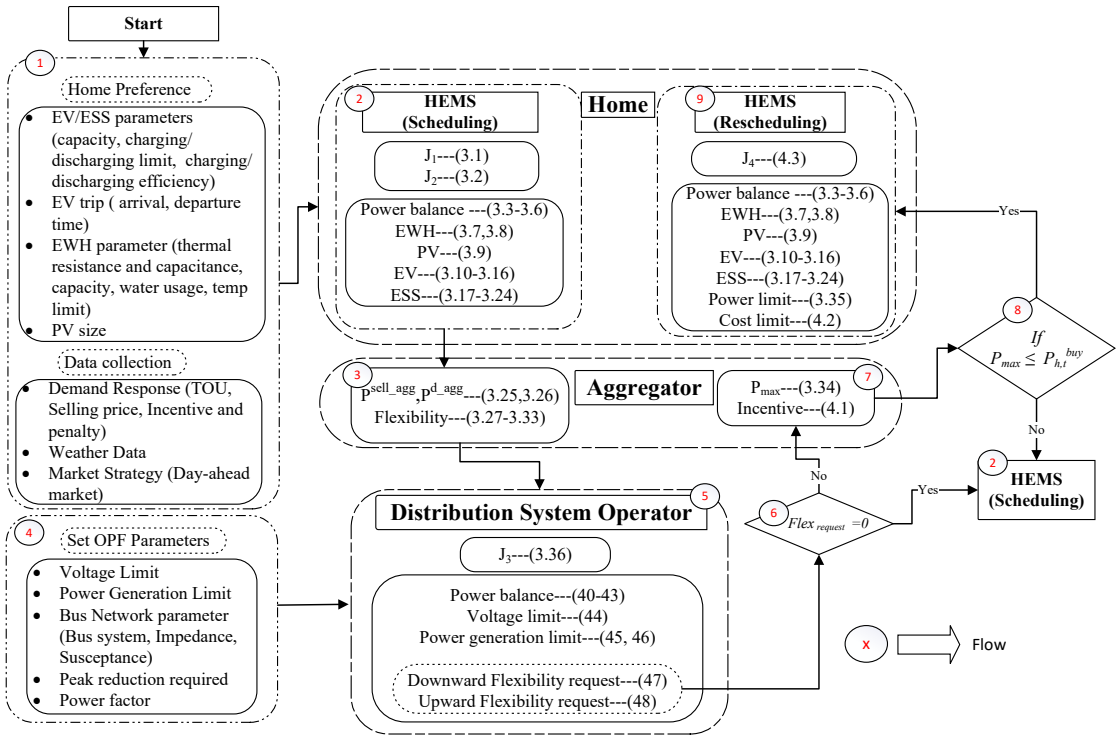

Figure 4.2: Proposed coordination framework of the three-level EMS.

4.3 Proposed Coordination Framework for Incentive program using ML-EMS

For the novel incentive program, we used the ML-EMS framework proposed in chapter 3, which consists of multiple households with HEMSs, aggregator, and DSO, as shown in Fig. 3.1. In addition to the previous coordination framework discussed in section 3.3, the proposed coordination framework comprises the following steps:

- The aggregator receives the flexibility request from the DSO. After that, the aggregator calculates the incentive/penalty price signal based on the flexibility of each prosumer, as in (4.1). The maximum power limit, $P^{max}_{h_j,t}$ and incentive/penalty, $\pi^{Inc/Pen}_{h_j,t}$ information is sent to the houses.

- The end-users re-run the HEMS optimization model with a new objective function, as in (4.3), and reschedule appliances considering two additional constraints requested from the aggregator (4.1) and (5.3).

4.4 RESULTS AND DISCUSSIONS

4.4.1 Case study

The proposed coordination framework of the three-level EMS optimization model is implemented on the Python platform using the PYOMO package [184]. The model is executed on a computer with Intel(R) Core(TM) i7-10850H CPU @ 2.70GHz 2.71 GHz processor with 32.0 GB RAM running on Windows 11 Pro 64-bit operating system. The lower level is a MILP problem that is solved using CPLEX solver [185]. The upper level is a non-linear programming problem, solved using IPOPT solver [186].

In this work, DSO is responsible for managing a 33-bus distribution system and meeting the demand of 437 prosumers on various buses, as shown in Fig. 4.3. The houses are equipped with a 5 kW PV system, ESS, EWH, and EV models for different houses. The modeling parameters of EV, ESS, and EWH are shown in table 3.1 and 3.2, respectively.

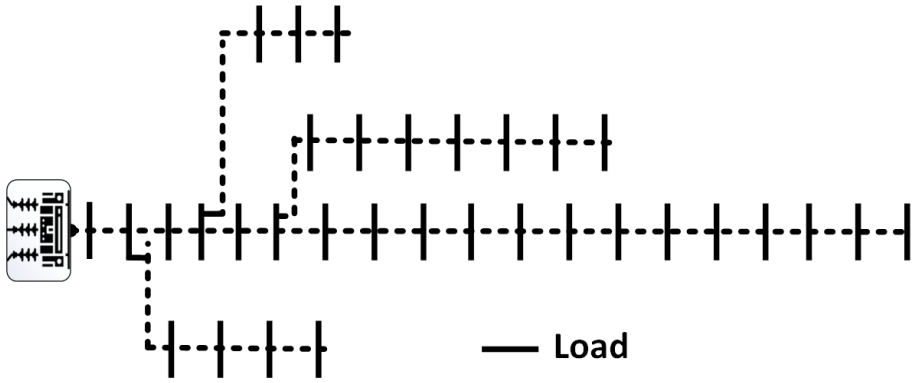

Figure 4.3: IEEE-33 bus radial distribution system.

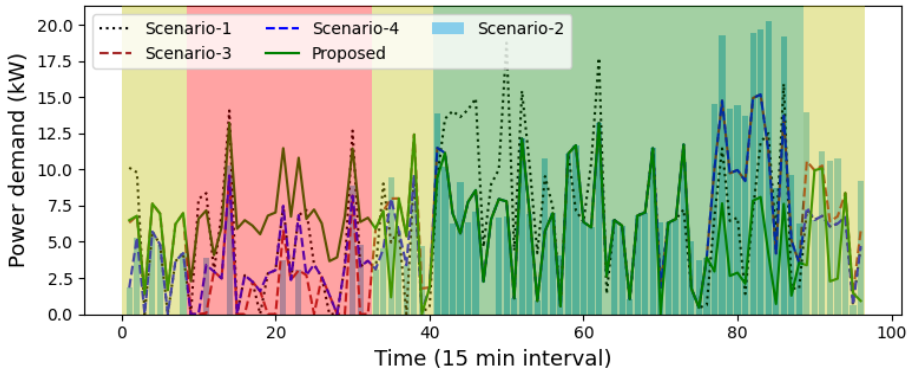

Figure 4.4: Power demand of a house.

The time step selected for the optimization is 15 min. The time horizon for the optimization is one day. Hence, the number of intervals within the optimization is 96. In this work, the interval "0" stands for 9:00 AM of day 1, and "95" stands for 8:45 AM of day 2. For simplicity, all EV's arrival and departure times are assumed to be the same for all houses: arrival time is 40 (7:00 PM), and departure time is 92 (8:00 AM). The pricing scheme used in this work is the time of use (ToU) price, and selling is a feed-in-tariff (FiT) price scheme, as used in [96]. The ToU pricing scheme consists of prices in three categories: off-peak (0.04 $/kWh), mid-peak (0.06 $/kWh), and on-peak (0.09 $/kWh), and feed-in tariff is 0.055 $/kWh, as shown in Fig. 4.5. The fixed incentives provided to the end-users is 0.08 $/kWh, as shown in Fig. 4.5. In Figs. 4.4, 4.5, 4.7, 4.9 and 4.11, the colored background is used to easily distinguish between off-peak (green shade), mid-peak (yellow shade), and on-peak (red shade) rates. Five scenarios have been considered to examine the effectiveness of the proposed method, where Scenario 1 is taken as the base case. In Scenario-1, PV generation is

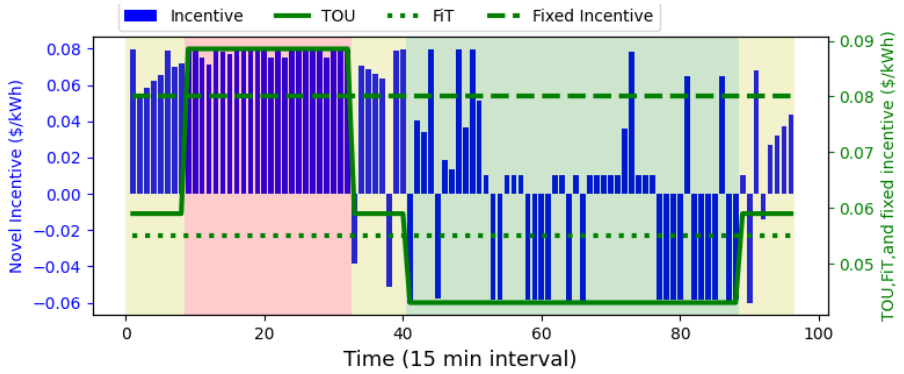

Figure 4.5: TOU, FiT, Fixed and Novel Incentive for a house.

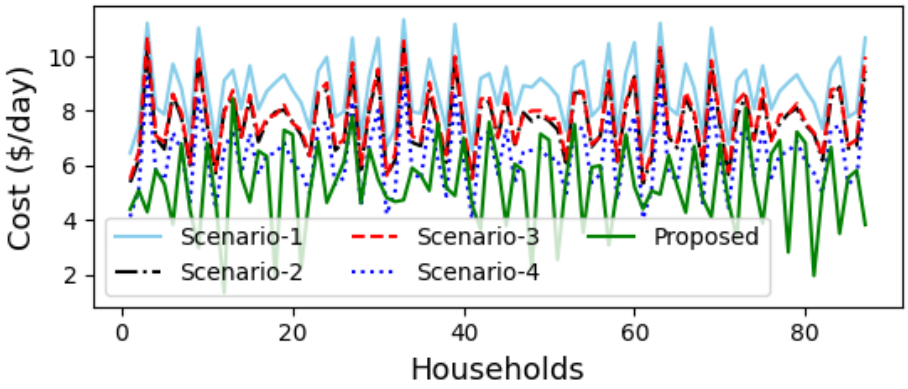

Figure 4.6: Total electricity cost of houses.

used in houses, and the surplus is sold to the grid. The EWH load is scheduled in the first stage with the key constraint of not exceeding the maximum water temperature. The EV that arrives first is charged first, keeping its energy level up to the desired level by departure time.

- Scenario-1: Rule-based EMS without flexibility and without incentive [3].
- Scenario-2: HEMS without flexibility and incentive [3].
- Scenario-3: HEMS with flexibility and no incentive [96].
- Scenario-4: HEMS with flexibility and fixed incentive [195].
- Proposed: HEMS with flexibility and adaptive incentive.

4.4.2 Home level

Household No. 85, located at bus 9, has been selected at the home level to depict the results. Fig. 4.4 presents the optimal load profile of house 85. This household has HEMS, which can schedule ESS, EV, and EWH appliances. When the grid operator provides a ToU signal, the prosumer schedules the controllable appliances to charge at a time interval where the price is low and discharge at a high pricing time to reduce the electricity cost. Consequently, there is often a rebound peak at low price hours, as shown in Fig. 4.4. The proposed strategy provides a peak limit and a novel incentive program based on flexibility to avoid a rebound peak. Thus, the end-user reschedules their appliance with additional constraints of peak limit and incentive program. The proposed technique shifted power demand from the high peak hours at time slots 41-88 (7:15 PM - 7:00 AM) to the low peak hours at time slots 0–40 (9:00 AM - 7:00 PM), reducing the peak and flatting the power demand curve. The proposed strategy also provides the incentive/penalty signal to the house based on its flexibility. It penalizes the customer at peak demand and gives incentives for low peak demand, as shown in Fig. 4.5. The proposed incentive program is hoped to encourage consumers to shift their load to off-peak hours. Fig. 4.6 shows the optimal electricity cost of the households per day. The result shows that the proposed method has a minimum electricity cost for all the households compared to the other four scenarios.

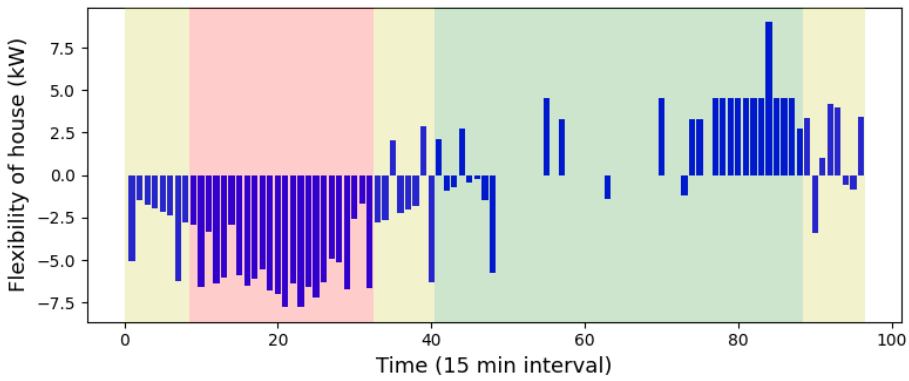

Figure 4.7: Flexibility of a house.

To fully leverage the flexibility of buildings, we need to take into account the thermal model of the buildings.

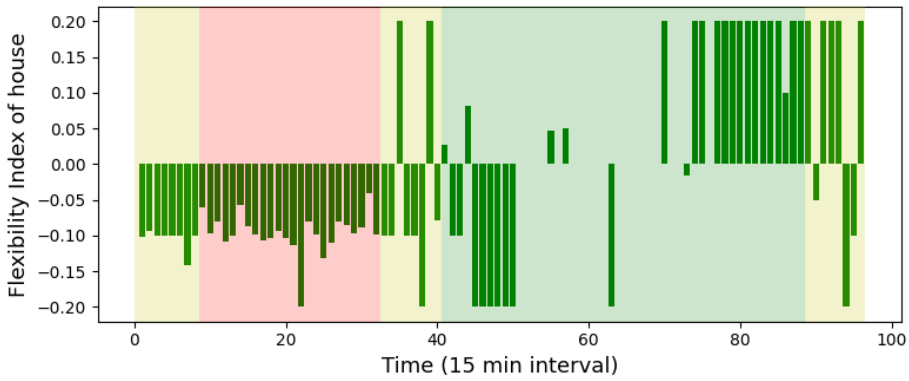

Figure 4.8: Flexibility index of a house.

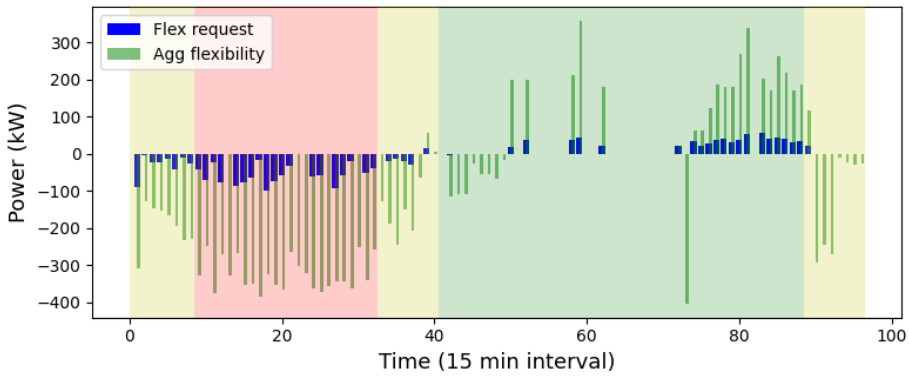

Figure 4.9: Aggregated flexibility and flexibility request from DSO at bus-23.

4.4.3 Aggregator level

The aggregator calculates the upward and downward flexibility of a household, as in Fig. 4.7. Negative flexibility represents the prosumer has the capability and willingness to increase their power demand; positive flexibility represents that prosumers are willing to decrease their power demand. These upward and downward flexibilities will help the DSO upon their flexibility request to decrease or increase the power demand for a specific time interval. Fig. 4.8 represents the flexibility index of households which is calculated at the aggregator level. The aggregator calculates the aggregated flexibility of end-users located at a bus j, as shown in Fig. 4.9.

4.4.4 DSO level

The DSO sends flexibility requests to the aggregator as shown in Fig. 4.9, which is within the bound of the aggregated flexibility of houses at a randomly selected bus-23. Fig. 4.11 depicts the

system load demand at the DSO level. The figure shows that the ToU price causes a rebound effect during low prices. However, utilizing the flexibility of the prosumers, the peak load of the overall system has been reduced and shifted to off-peak demand (high price). The result shows that the proposed approach reduces the peak load more than other scenarios. The peak reduction will avoid the thermal overload of system components, thus providing congestion management and deferring the necessity of grid reinforcement. The proposed technique also improves the voltage at each bus, as shown in Fig. 4.12. Table 4.1 presents the overview of models and solvers' statistics of home and DSO levels for all five scenarios. From Table 4.1, it can be seen that the proposed method converges almost at the same time as other scenarios. As the stopping condition for the optimization, a MIPgap of 0.04 is used at the house level, and tolerance is set at 10^{-8} for the grid level.

Table 4.1: models statistics and time of convergence

Scenarios	Level	No of Constraint	No of Variables	Tolerance/MIP Gap	Time Taken (Sec)
Scenario-1	Home	-	-	-	0.026
	Aggregator	-	-	-	0.143
	Grid	6336	6336	10^{-8}	0.173
Scenario-2	Home	2690	2304	0.04	0.259
	Aggregator	-	-	-	0.534
	Grid	9504	9432	10^{-8}	0.816
Scenario-3	Home	2978	2496	0.04	0.277
	Aggregator	-	-	-	0.634
	Grid	9504	9532	10^{-8}	0.854
Scenario-4	Home	2882	2400	0.04	0.314
	Aggregator	-	-	-	0.663
	Grid	9504	9533	10^{-8}	0.733
Proposed	Home	2978	2496	0.04	0.338
	Aggregator	-	-	-	0.673
	Grid	9504	9509	10^{-8}	0.965

The proposed methodology was evaluated by considering four different penetration levels (10%, 50%, 80%, and 100%) of ESSs, EVs, and PVs at the home level. The results, as illustrated in Fig. 4.10, demonstrate that the proposed model leads to reduced power losses, peak load, and average load and improves the minimum load, which are key indicators for flattening the load profile of the entire system. From Fig. 4.10, it can be seen that with increasing the penetration level, the proposed methodology performs better, i.e., reduces the peak load and power losses of the overall system. For the worst-case scenario of 100% penetration of EVs, ESSs, and PVs, the proposed method reduces the power losses of the overall system by 24.6%. Similarly, the peak load has been

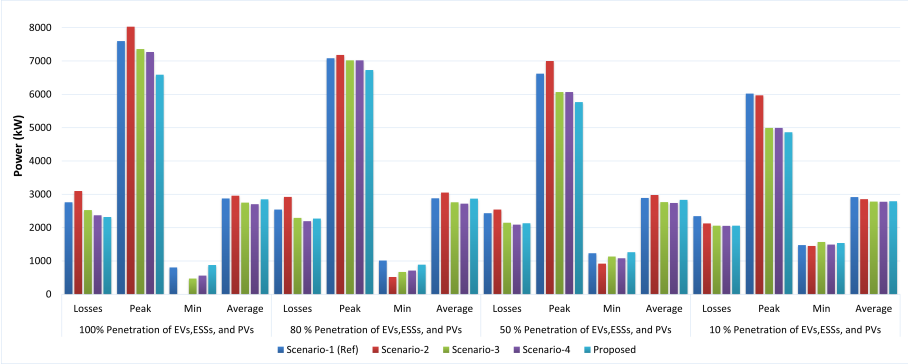

Figure 4.10: Load profile characteristics for different penetration levels of EVs, ESS s, and PVs at different scenarios.

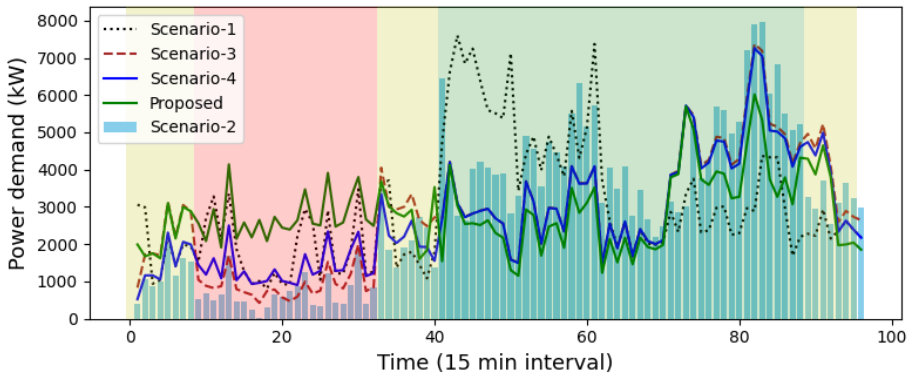

Figure 4.11: Total demand of the overall system

reduced by 20.8% compared to the base case. At the same time, the min load is increased by 42%, and the average load is reduced by 3.7% compared to scenario-1. These load profile characteristics indicate a relative flattening of the load profile compared to the base scenario. Flattening the load demand and minimizing the power losses will reduce the grid capacity investment (avoid and/or delay the grid reinforcement) and maximize the use of the network's current capacity.

4.5 Summary

This chapter illustrates a novel three-level coordination framework enabling flexibility provisioning between multiple households, aggregators, and DSOs. It proposes an adaptive incentive program based on the flexibility of the household and the interaction with DSO. This framework is a win-win situation for both households and DSO. At the home level, each house optimizes its

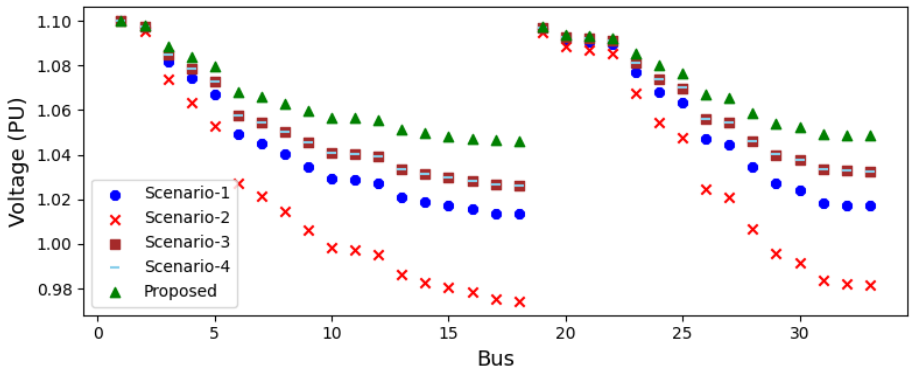

Figure 4.12: Voltage of each bus at one time instant.

appliance operation to minimize the electricity cost. The aggregator collects the flexibility of each household, and the cohort flexibility is conveyed to the DSO. The DSO performs optimal power flow to minimize system losses and sends the optimal flexibility reduction request to the aggregator. The aggregator then disaggregates the flexibility requests to each participant as a peak limit on each house's consumption and gives them incentives based on their flexibility provision. The proposed architecture significantly improves the distribution system's total load profile and reduces the electricity cost of the customers.

Upon considering a use-case of 100% penetration of EVs, ESSs, and PVs at the home level, the proposed approach was able to reduces the power losses, peak load, and average load of the overall system by 24.6%, 20.8%, and 3.7%, respectively. Furthermore, it increases the minimum load by 42%, thus flattening the load profile of the distribution network.

Chapter 5

Smart Home P2P Energy Trading with Dynamic Flexibility Limit Considering Distribution Transformer

NOMENCLATURE

Indices, Sets and Functions

h_k	Index of houses h at j bus
k	Buses where transformer located in distribution system; $(k) \in \mathcal{N}$
t	Index of time; $t \in \mathcal{T}$
C_{3k}	Loss of life transformer minimization objective function

Parameters

$\lambda_t^{\boldsymbol{P2P}}$	Mid market price; $\$/kWh$
$\lambda_t^{\boldsymbol{TOU}}$	Grid time of use price for Buying; $\$/kWh$
$\lambda_t^{\boldsymbol{FiT}}$	Feed-in tariff for selling; $\$/kWh$
j_t	Power ratio

R	Ratio of losses at rated load to losses at no load
$TX^{load}_{HEMS_t}$	Load using HEMS; kW
$TX^{\textbf{rating}}$	Transformer rating; kW
m, n	transformer's cooling parameters
$\Delta\theta^{\mathrm{HST,R}}$, $\Delta\theta^{\mathrm{TO,R}}$	Hottest-spot and top-oil at rated
$\Delta\theta^{\mathrm{HST}}$, $\Delta\theta^{\mathrm{TO}}$	Change in Hottest-spot and top-oil
$\Delta\theta^{\mathrm{HST,U}}_t$, $\Delta\theta^{\mathrm{TO,U}}$	Ultimate hottest-spot and top-oil rise over ambient temperature
τ^w	Constant time for winding
$\theta^{\mathrm{HST}}_{t,ref}$	Reference hot spot temperature
$P^{\textbf{flex}^+}_{h_j,t}$, $P^{\textbf{flex}^-}_{h_j,t}$	Upward, downward flexibility of house; kW
$P^{\textbf{flex}^+_{agg}}_{j,t}$, $P^{\textbf{flex}^-_{agg}}_{j,t}$	Upward, downward aggregated flexibility; kW
$\theta^{\textbf{a}}_{h_j,t}$	Ambient temperature; $^\circ C$
β	Normal insulating life (180,000 hours (20.5 years))
$P^{\textbf{max}}_{h_j,t}$	The maximum power demand of household; kW
ξ^{+}, ξ^{-}	Percentage peak reduction, increase
$\alpha^{\textbf{flex}}_{h_j,t}$	Flexibility index of each household
$P^{\textbf{flex}_{agg}}_{j,t}$	Total flexibility at bus j; kW
$P^{\textbf{flex}}_{h_j,t}$	The flexibility of each household; kW
$P^{d_{agg}}_{j,t}$, $P^{\textbf{sell}_{agg}}_{j,t}$	Aggregated power buy, sell from, to DSO; $p.u$
$P^{\textbf{BL}}_{h_j,t}$	Base load; kW
τ	Time step; $15min$
$\pi^{\textbf{Buy}}_t$, $\pi^{\textbf{Sell}}_t$	Buying, selling price; $\$/kWh$
$(P^{\textbf{dem}}_{h_k,t})_{C_1}$	Power consumption using obj 1; kW
$(P^{\textbf{dem}}_{h_k,t})_{C_2}$	Power consumption using obj 2; kW
$P^{\textbf{Dem,G}}_{h_k,t}$	Optimal power imported from grid; kW

$P_{h_k,t}^{\textbf{\textit{Expt,G}}}$	Optimal power exported to grid; kW

Variables

F_t^{AA}	Accelerated aging factor of transformer
F_{EQA}	Equivalent accelerated aging factor of transformer
LoL_t	Loss of life of transformer
θ_t^{HST}	Transformer winding hot spot temperature; $^\circ C$

5.1 Background

This chapter focuses on a new coordination framework for smart homes with P2P energy trading with flexibility provision and analyzing the impact of top pole transformer. [1] What if demand flexibility was taken to an entirely new level, combined with an electricity price signal and real-time, two-way communications? That's the vision for transactive energy. Transactive energy (TE) is a framework in which economic transactions are executed to manage electricity generation and consumption within an electric network, considering the reliability constraints [34]. Selling prosumers labeled as sellers and buying prosumers designated as buyers can be integrated into the TE market protocol using a two-way interchange of information and price signals. Several financial transactions can be carried out between themselves or the electricity retailers [110]. The prosumers-focused branch of the TE framework is termed P2P energy trading in [109, 113]. Under the P2P energy trading, electricity suppliers, energy markets, the power grid, homes, commercial buildings, and DERs, such as EV and ESS, would "talk" directly or indirectly to negotiate energy needs and costs. The electronic process would rapidly and automatically harmonize energy availability, consumer needs, cost preferences, and other factors, enhancing overall energy system efficiency. P2P energy sharing provides options for prosumers to trade energy within the neighborhood through local buying and selling, allowing local funds to remain within the local economy.

Numerous studies have been conducted on P2P energy trading to reduce the electricity cost of the end-users prioritizing their preferences. For instance, the P2P trading constraints for a group of

[1] This chapter has significant materials from the following paper published by the PhD candidate:
Hussain, S., Azim, M. I., Lai, C., & Eicker, U. (2023). New coordination framework for smart home peer-to-peer trading to reduce the impact on distribution transformer. Energy, 129297.

households are modeled using the MILP in [196] to reduce operational expenses. An assessment is carried out in [197] to demonstrate the suitability of P2P trading in residential sectors under various tariff structures. A bi-level control is proposed for the batteries that have been controlled for P2P trading [158]. In [198], different types of prosumers in the distribution system are permitted to trade energy via P2P to minimize energy costs. For the same purpose, the authors designed a P2P EMS for a group of prosumers in [199]. Further, a token-based automated P2P trading scheme on the blockchain platform is formulated in [200]. A shared storage-dominated P2P trading strategy is reported in [201]. A privacy-preserving P2P trading mechanism is also modeled in [202] by taking the uncertainties of DERs into consideration.

Moreover, Paterakis et al. [203] propose a coordination strategy for the smart neighborhoods with transformer limit. However, this does not consider the thermal model of the transformer and pricing mechanism of P2P energy trading. Existing studies also analyze the impacts of solar PV systems with batteries [204] and EVs [8] on transformer lifespan to better understand the effects of these technologies. In [205], the authors present an incentive-ensured P2P transaction method that promotes active/reactive regulation through EVs, reducing voltage drop and network congestion. Similarly, in [206], the author proposes a P2P algorithm with a shared ESS to benefit the community. However, both studies only consider the EVs and ESS, respectively, and do not consider other DERs, for instance, but are not limited to EWH, ESS, PV, etc. From the above discussion, it can be concluded that these studies do not consider the impact on the distribution transformer while arranging P2P trading.

Distribution transformers have a crucial role in P2P energy trading systems, as they facilitate the delivery of electricity from its source to its destination. A valid P2P transaction should consider its implication for the distribution transformer and distribution network. For this reason, some literature has also focused on analyzing the impacts of P2P transactions on the distribution system. In particular, in [207], the authors studied power losses in distribution networks caused by P2P trading. Park et al. [208] have proposed P2P energy trading based on the flexibility to maintain the stability of the distribution network. The authors in [209] have formulated a local market for P2P energy trading in the presence of solar PV with batteries to reduce voltage fluctuation and power losses. From the above literature, we can conclude that, to the best of our knowledge, none of

the work has investigated the impact of HEMS-integrated P2P trading, with flexibility limit, on the distribution/pole-top transformer.

5.2 Motivation

The P2P energy trading approach provides a coordination and control methodology that effectively balances energy supply and demand across the grid, enabling increased integration of clean energy sources. Additionally, P2P energy trading is designed to enhance energy system efficiency so the power grid becomes more resilient and can meet more needs with its existing infrastructure. P2P trading is a next-generation energy management technique that economically benefits proactive consumers (prosumers) who are transacting their energy as goods and services. At the same time, P2P energy trading is also expected to help the grid by reducing peak demand, lowering reserve requirements, and curtailing network loss.

5.3 Objective

The successful implementation of the P2P energy trading mechanism still meets many risks and challenges. P2P energy trading consists of both financial and physical activities.

- Financial activities should properly coordinate the conflicting interests of various participants while providing secure and reliable transaction information. The energy traded in economic activities should be transmitted via the physical network.
- Consequently, the physical factors, including the distribution network constraints, operational constraints of the transformer, power transmission loss, unchecked power injection, etc., should be considered.

At present, researchers are directed either to the virtual layer or to the physical layer. However, for a successful deployment of P2P trading within the network, the requirements of both layers must be addressed. Hence, there is a need for a unified model that could capture both the virtual layer (pricing mechanism, market mechanism, and energy management system) and the physical layer (transformer limit and other physical constraints of the power system). Consumer-centricity of P2P

trading has been well-established in recent literature. However, the benefit of P2P energy trading to the distribution grid must also be demonstrated.

5.4 Methodology

The work presents a detailed analysis of a pole-top distribution transformer serving a smart community comprising multiple households as depicted in figure 5.1. The point of common connection (PCC) is where the transformer unit and all smart homes are located. The schematic diagram depicts a two-way power flow between the PCC and households and between the PCC and the grid via the transformer unit.

Power can be obtained from the grid or produced locally. Also, it can be sold to other end-users or the grid. EVs, batteries, PVs, and EWH are only a few examples of the various assets and technological capabilities that the system can accept. Depending on their needs, prosumers can make use of the vehicle-to-grid (EV,G), vehicle-to-home (EV,H), battery-to-grid (bat,G), battery-to-home (bat, H), PV-to-grid (PV,G), and PV-to-home (PV,H) features.

A dynamic demand response strategy determines the energy price that each house injects into the PCC. Under this strategy, buying energy costs ToU, and selling energy is FiT. By encouraging prosumers to produce excess energy and sell it back to the grid, the FiT strategy promotes the adoption of RESs and lowers total energy prices. Moreover, transformer load monitoring equipment is installed on the distribution transformer that serves the neighborhood. This device enables the management of excessive loading, which has the potential to accelerate the process of aging the transformer unit. The transformer load monitoring device allows the system to run effectively and sustainably.

5.4.1 HEMS Model

For the HEMS, we use the same model as discussed in chapter 3 section 3.2.1. The equations used for HEMS are from (3.1) to (3.24).

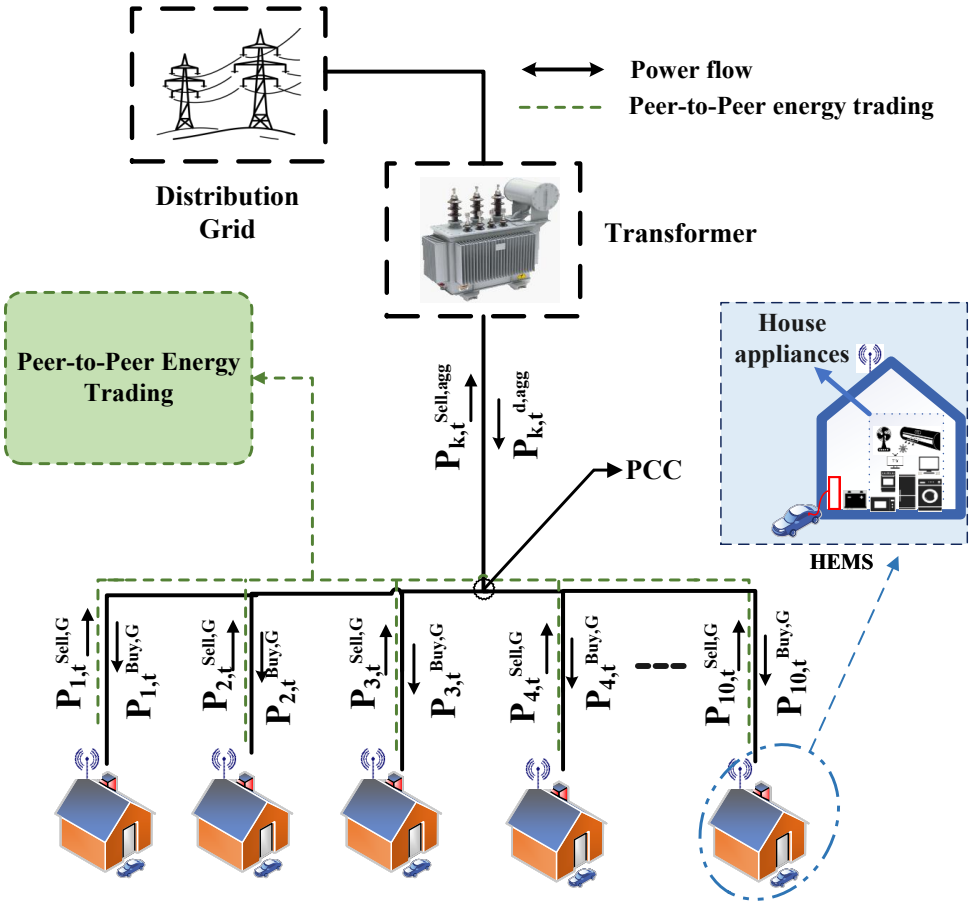

Figure 5.1: Conceptual diagram of HEMS- integrated P2P trading in the presence of a pole-top distribution transformer.

5.4.2 Smart Transformer

We assume that the smart transformer works as an aggregator. Its primary function is to optimize the lifespan of the transformer by reducing loss. It performs flexibility management as an aggregator, as discussed in Chapter 3, Section 3.2.2, by calculating the adaptive power limit for each prosumer. Additionally, it monitors and facilitates P2P energy trading.

Exceeding the designated capacity of transformers can lead to a rise in temperature, causing the insulation to deteriorate prematurely and reducing the transformer's lifespan. The thermal impact is primarily determined by the amount of load and the ambient temperature [210]. The IEEE standard C57.91 [211] provides a model for estimating the hottest-spot temperature and the decrease in lifespan of the transformer.

5.4.3 Transformer as Aggregator

The aggregated power demand of houses connected to a specific transformer is calculated as in equation (3.25). The aggregated power includes the base load, the power demand of EWH, the charging and discharging of EVs, and the battery. Similarly, equation (3.26) calculates the aggregated selling power, which includes excess generated power from PV to the DSO and discharging of EV and battery to the grid through a transformer.

$$TX^{load}_{HEMS_t} = P^{d_{agg}}_{k,t} + P^{sell_{agg}}_{k,t} \tag{5.1}$$

Flexibility limit through Transformer

The total bi-directional power flowing through the transformer is $P^{d_{agg}}_{k,t}$ and $P^{sell_{agg}}_{k,t}$ as in equation (5.1). The transformer in the proposed method provides a flexibility management service as in section 3.2.2. The transformer calculates the flexibility available to the grid from each household using equation (3.27) to (3.33).

The Transformer also calculates the maximum power limit of each house based on their flexibility as follows:

$$P^{max}_{h_k,t} = (P^{dem}_{h_k,t})_{C_1} - \alpha_{h_k,t} \cdot TX^{\text{rating}}, \qquad \forall t \in \mathcal{T}; \forall h_k \in \mathcal{H}; \forall j \in \mathcal{N} \tag{5.2}$$

The house rescheduled their appliance based on the limit provided by the transformer, which is within the flexibility bound of the household as below:

$$P^{Dem,G}_{h_k,t} \leq P^{max}_{h_k,t}, \qquad \forall t \in \mathcal{T}; \forall h_k \in \mathcal{H} \tag{5.3}$$

5.4.4 Thermal model of Transformer

The following equation calculates the transformer windings' hot spot temperature (HST).

$$\theta^{\text{HST}}_t = \theta^{\text{A}}_t + \Delta\theta^{\text{TO}}_t + \Delta\theta^{\text{HST}}_t \quad \forall t \in T \tag{5.4}$$

In equation (5.4), the temperature at the hottest spot of the winding denoted by θ_t^{HST}, is determined for each time instance t within the time horizon T. Additionally, the ambient temperature, θ_t^{A}, and the top-oil temperature increase over ambient temperature, denoted by θ_t^{TO}, as well as the winding HST rise over top oil temperature, represented by θ_t^{HST}, are also calculated for each time instance. The value for $\Delta\theta_t^{\mathrm{TO}}$ can be calculated using equation (5.5).

$$\Delta\theta_t^{\mathrm{TO}} = \left(\Delta\theta_t^{\mathrm{TO,U}} - \Delta\theta_{t-1}^{\mathrm{TO}}\right)\left(1 - e^{\frac{-\Delta t}{\tau^{\mathrm{TO}}}}\right) + \Delta\theta_{t-1}^{\mathrm{TO}} \quad \forall t \in T \tag{5.5}$$

In the equation (5.5), the term $\Delta\theta_t^{\mathrm{TO,U}}$ represents ultimate top-oil rise over the ambient temperature, with t being the time interval and τ^{TO} is the top-oil time constant. As expressed in equation (5.5), $\Delta\theta_t^{\mathrm{TO}}$ depends on the state in the previous time step.

$$\Delta\theta_t^{\mathrm{HST}} = \left(\Delta\theta_t^{\mathrm{HST,U}} - \Delta\theta_{t-1}^{\mathrm{HST}}\right)\left(1 - e^{\frac{-\Delta t}{\tau^{\mathrm{W}}}}\right) + \Delta\theta_{t-1}^{\mathrm{HST}} \forall t \in T \tag{5.6}$$

The calculation of $\Delta\theta_t^{\mathrm{HST}}$ in equation (5.4) is done using equation (5.6), where $\Delta\theta_t^{\mathrm{HST,U}}$ is the ultimate rise of the top-oil temperature above the ambient temperature and τ^w is the constant time for windings. It is important to note that, similar to equation (5.5), $\Delta\theta_t^{\mathrm{HST}}$ is also dependent on its previous state. The $\Delta\theta_t^{\mathrm{TO,U}}$ and $\Delta\theta_t^{\mathrm{HST,U}}$ are calculated as below:

$$\Delta\theta_t^{\mathrm{TO,U}} = \Delta\theta^{\mathrm{TO,R}} \cdot \left(\frac{k_t^2 \cdot T_R + 1}{T_R + 1}\right)^n \quad \forall t \in T \tag{5.7}$$

$$\Delta\theta_t^{\mathrm{HST,U}} = \Delta\theta^{\mathrm{HST,R}} \cdot k_t^{2\cdot \mathrm{m}} \quad \forall t \in T \tag{5.8}$$

Where k_t is the ratio of the transformer's load to nameplate rating, T_R is the ratio of losses at rated load to losses at no load, m and n are the transformer's cooling parameters, and $\Delta\theta^{\mathrm{HST,R}}$ and $\Delta\theta^{\mathrm{TO,R}}$ are top-oil rise over ambient and hottest-spot rise over top-oil at rated load, respectively. The definition of the ratio k_t is:

$$k_t = \frac{TX_{HEMS_t}^{load}}{TX^{\text{rating}}} \quad \forall t \in T \tag{5.9}$$

Where TX_t^{rating} is the nameplate rating and $T_{HEMS_t}^{load}$ is the load on the transformer after home

energy management performed by the houses connected to that transformer. This k_t can be changed according to different scenarios. For instance, the unmet load and extra export power from P2P will be fed into the transformer. These different scenarios will be discussed in detail in 5.7. Equations (5.4) to (5.8) show that the transformer temperatures change as the load ratio k_t rises (5.9).

5.4.5 Transformer Aging

Equation (5.10) correlates the winding hottest-spot temperature θ_t^{HST} to the accelerated ageing factor F_t^{AA}.

$$F_t^{\mathrm{AA}} = \exp\left(\frac{15000}{\theta_{t,ref}^{\mathrm{HST}} + 273} - \frac{15000}{\theta_t^{\mathrm{HST}} + 273}\right) \quad \forall t \in T \tag{5.10}$$

The accelerated ageing factor at a specific temperature θ_t^{HST} is referred to as F_t^{AA} [211]. As stated in reference [211], the standard temperature at which normal aging occurs is 110°C, considered the hottest spot. Transformer aging is accelerating if F_t^{AA} is greater than 1.

$$F_{EQA} = \frac{\sum_t^T F_{AA,t}\Delta t}{\sum_t^T \Delta t}. \tag{5.11}$$

Equation (5.12) below illustrates how to use this factor to calculate the transformer's loss of life (LoL):

$$LoL_t = \frac{F_{EQA} \cdot \Delta t}{\beta} \quad \forall t \in T \tag{5.12}$$

where β represents the transformer's typical insulating life. An average transformer must meet the IEEE standard's requirement for a normal insulating life β of at least 180,000 hours (20.5 years) [211]. Equations (5.4) to (5.12) can be used to calculate the transformer's aging while considering temperature, loads, and characteristic factors of the transformer.

The objective function (5.13) minimizes the loss of life of the transformer subjective to the equations (5.4) to (5.10).

$$J_{5k} = \min_p \sum_{t \in T} LoL_t \tag{5.13}$$

5.5 Peer-to-Peer Energy Trading

5.5.1 Mid-Market Rate

According to the concept of the mid-market rate, the price per unit of energy for energy trading is determined based on three different scenarios: 1) when generation is equal to demand, 2) when generation is greater than demand, and 3) when generation is lower than demand [47]. However, in all cases, energy trading between participants occurs at a P2P price λ_t^{P2P} equal to the mid-value between the buying and selling prices set by the grid for its trading with end-users.

$$\lambda_t^{P2P} = \frac{\lambda_t^{TOU} + \lambda_t^{FiT}}{2} \tag{5.14}$$

Case 1 (Power Export is Equal to Power Demand):

When the energy production of all prosumers in the network equals their energy demand, the net energy demand and production is zero. In this case, the surplus energy the sellers produce in the set H_s is sold to the buyers in the set H_b. The selling price λ_t^{FiT} and buying price λ_t^{TOU} of each participant, $h_s \in H_s$ and $h_b \in H_b$ respectively, are set equal and determined by the expression given in (5.14).

$$\lambda_{t,b}^{P2P} = \lambda_{t,s}^{P2P} = \lambda_t^{P2P} = \frac{\lambda_t^{TOU} + \lambda_t^{FiT}}{2} \tag{5.15}$$

Case 2 (Power Export is Greater Then Power Demand):

In this case, the net energy production is non-zero, and therefore, the sellers can sell the total surplus energy to the grid at a price λ_t^{FiT} after meeting the demand of prosumers with energy deficiency in the network. Clearly, the buying price $\lambda_{t,b}^{P2P}$ of each buyer is given below:

$$\lambda_{t,b}^{P2P} = \lambda_t^{P2P} = \frac{\lambda_t^{TOU} + \lambda_t^{FiT}}{2} \tag{5.16}$$

In this case, the price at which energy is sold by prosumers to the grid, $\lambda_{t,s}^{P2P}$, is determined based on the total energy generated, total demand of prosumers, and the buying and selling prices set by the grid. Specifically, $\lambda_{t,s}^{P2P}$ can be calculated as a function of the total energy generated

by prosumers, the total demand of prosumers, the mid-market rate, and the price at which surplus energy is sold to the grid, $\lambda_{t,s}^{FiT}$.

$$\lambda_{t,s}^{P2P} = \frac{\sum_{h_b}^{H_b} P_{h_b,t}^{Dem,G} \cdot \lambda_t^{P2P} + (\sum_{h_s}^{H_s} P_{h_s,t}^{Expt,G} - \sum_{h_b}^{H_b} P_{h_b,t}^{Dem,G}) \cdot \lambda_t^{FiT}}{\sum_{h_s}^{H_s} P_{h_s,t}^{Expt,G}} \tag{5.17}$$

The expression in Equation (5.17) calculates the overall revenue that the sellers can obtain in the network by selling their excess energy. The first term of the numerator, which is represented by the summation over all the buyers in H_b, denotes the revenue generated by selling energy to them at a price of λ_t^{P2P}, where $P_{h_b,t}^{Dem,G}$ represents the total energy demand of the respective buyer. The second term represents the extra energy sold to the grid by price λ_t^{FiT}.

Case 3 (Power Export is Less Then Power Demand):

In this scenario, the energy demand in the network is greater than the energy export, leading to a net energy demand. Consequently, the buyers in H_b need to fulfill their excess energy requirements, $(\sum_{h_b}^{H_b} P_{h_b,t}^{Dem,G} - \sum_{h_s}^{H_s} P_{h_s,t}^{Expt,G})$, by purchasing energy from the grid. The buying price $\lambda_{t,b}^{P2P}$ will be influenced by several factors, including the total available surplus energy $\sum_{h_s}^{H_s} P_{h_s,t}^{Expt,G}$, total energy demand $\sum_{h_b}^{H_b} P_{h_b,t}^{Dem,G}$, and the prices $\lambda_{t,b}^{P2P}$ and λ_t^{TOU}. Mathematically, this can be expressed as:

$$\lambda_{t,b}^{P2P} = \frac{\sum_{h_s}^{H_s} P_{h_s,t}^{Expt,G} \cdot \lambda_t^{P2P} + (\sum_{h_b}^{H_b} P_{h_b,t}^{Dem,G} - \sum_{h_s}^{H_s} P_{h_s,t}^{Expt,G}) \cdot \lambda_t^{TOU}}{\sum_{h_b}^{H_b} P_{h_b,t}^{Dem,G}} \tag{5.18}$$

As in Case 1, the selling price $\lambda_{t,s}^{P2P}$ charged by each seller $h_s \in H_s$ to the buyers for selling their surplus energy is determined as:

$$\lambda_{t,s}^{P2P} = \lambda_t^{P2P} = \frac{\lambda_t^{TOU} + \lambda_t^{FiT}}{2} \tag{5.19}$$

It should be noted that in the proposed P2P energy trading scheme, the values of $\lambda_{t,s}^{P2P}$ and $\lambda_{t,b}^{P2P}$ are determined based on the values of $\sum_{h_b}^{H_b} P_{h_b,t}^{Dem,G}$, $\sum_{h_s}^{H_s} P_{h_s,t}^{Expt,G}$, λ_t^{TOU}, and λ_t^{FiT}. These values are fixed for each time slot t, regardless of whether the prosumers involved in the energy trading decide to collaborate in a large group (grand coalition) or remain separated into smaller groups (disjoint coalition). This means that once a prosumer decides to participate in P2P energy trading, they need

to buy and sell using $\lambda_{t,b}^{P2P}$ and $\lambda_{t,s}^{P2P}$, which are set for that specific time slot t. The regulatory charges are not considered in the pricing scheme in this work, but the P2P platform provider may charge the prosumers a fee included in the trading price [212] and pay a subscription fee to the distribution system operator for using its infrastructure for P2P trading [139]. The proof that mid-market price is beneficial for both seller and buyer is provided in appendix C.

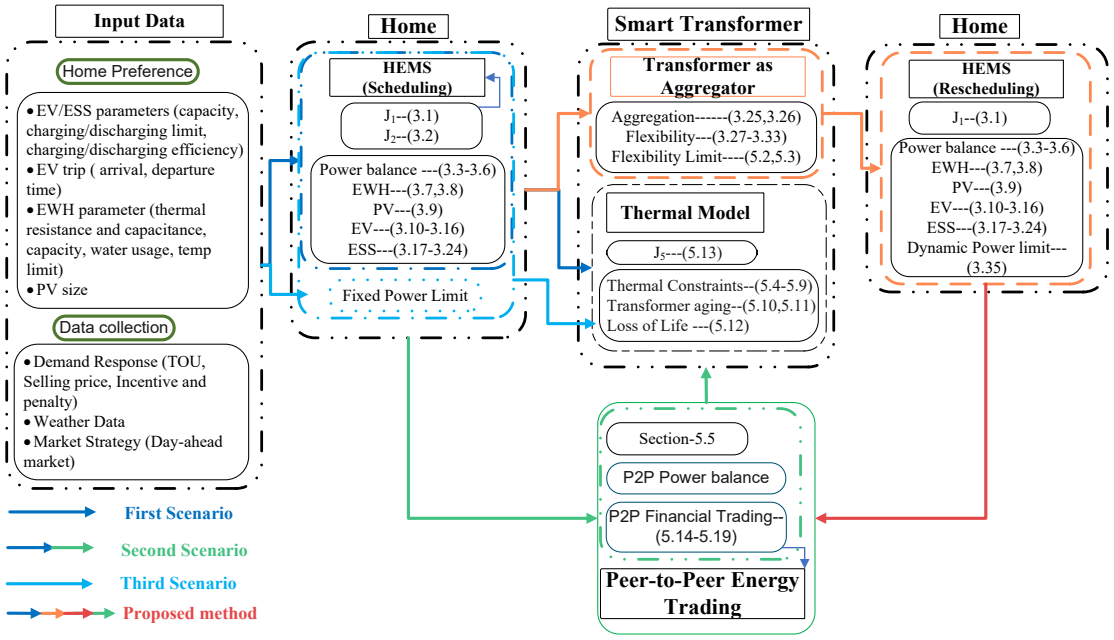

Figure 5.2: Proposed integrated framework.

5.6 Proposed Coordination Framework

The proposed strategy of HEMS-integrated P2P trading with flexibility provisioning consists of multiple prosumers, as shown in figure 5.1. In the proposed coordination framework, each prosumer has HEMS that receives input updates regarding customer preferences, as shown in 5.2. The desired upper/lower limit of the hot water temperature, arrival/departure time of the EV, and initial/final energy level of the battery at the beginning and end of the day. The information regarding parameters of the appliances used in the house is also provided to HEMS, such as type and built-in characteristic of the EV, battery, and EWH in table 3.1 and 3.2, respectively. Some information comes from the grid operator, for instance, demand response information (ToU, FiT), as shown in table 5.1.

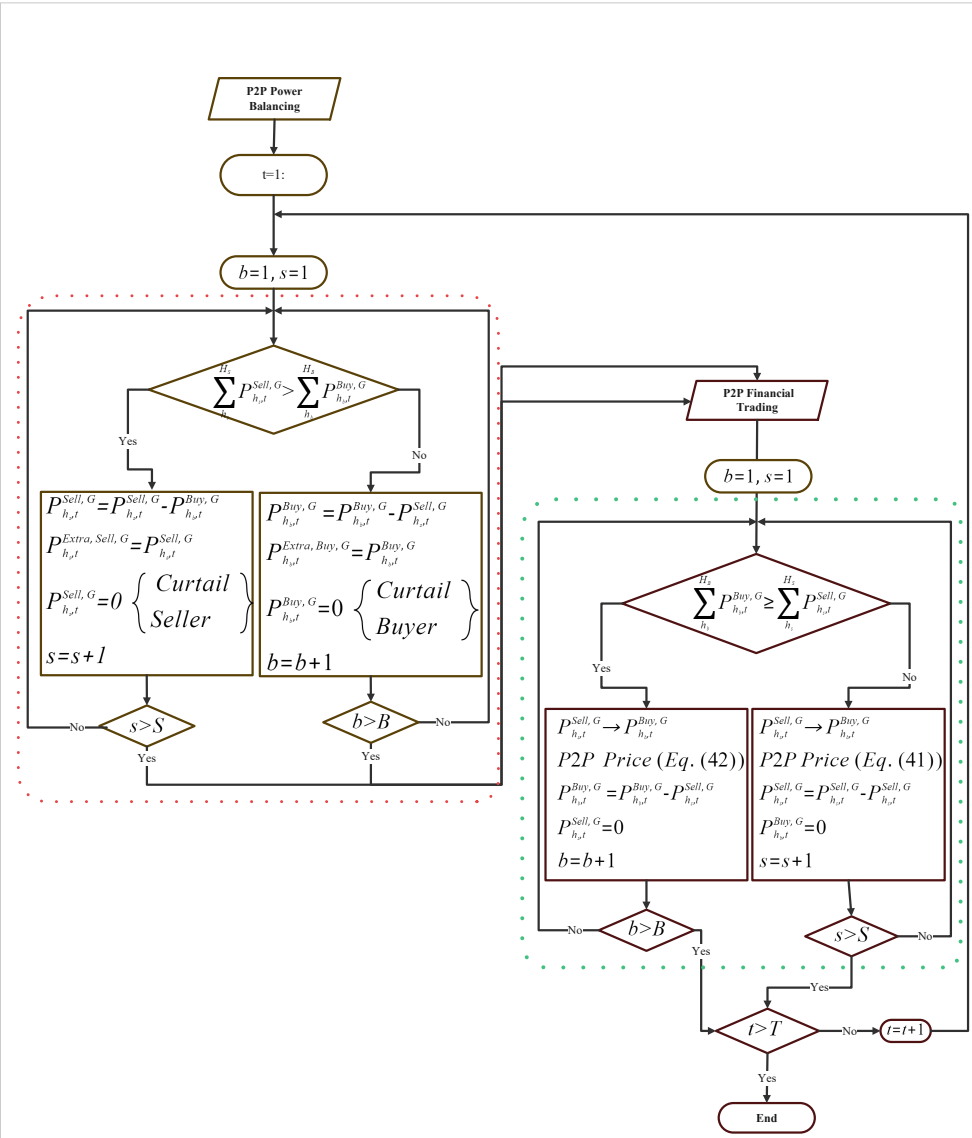

Figure 5.3: A flowchart demonstrating P2P energy trading process.

The HEMS schedules the house appliances based on the prosumer's energy-saving and subsequent cost-saving objectives as in (3.1) and (3.2), respectively. Prosumers become flexible energy resources with the presence of DERs when a HEMS is incorporated into them. The optimal load demand is determined at the house level and collectively sent to the transformer operator. To protect the privacy of prosumers, they only provide aggregated power profiles as shown in equations (3.25)-(5.3). The households also export to the grid.

The smart transformer acts as an aggregator, an intermediary between multiple houses, and a power grid. The aggregator exchanges information, the decision variables, from one level (home level) to another (grid). The information flow from the end-users to the aggregator is $P^{Buy,G}_{h_k,t}$, $P^{Sell,G}_{h_k,t}$,

Table 5.1: ToU Tariff of PG&E [5, 6] and FiT [7]

Tariff	Time of Day	Price ($/kWh)
Off-Peak	11:00 PM-8:00 AM	0.15
Shoulder	8:00 AM-2:00 PM and 9:00 PM-11:00 PM	0.22
Peak	2:00 PM-9:00 PM	0.42
FiT	All day	0.08

Table 5.2: Transformer Thermal data [8]

$\Delta\theta_t^{\mathrm{TO,R}}(^\circ C)$	$\Delta\theta_t^{\mathrm{HST,R}}(^\circ C)$	m	n	$\tau^{\mathrm{TO}}(min)$	$\tau^{\mathrm{W}}(min)$	$\theta_{t,ref}^{\mathrm{HST}}(^\circ C)$	T_R	Type	Voltage
56	80	0.8	0.9	90	7	110	6	ONAF	2.4kV/120V

$(P_{h_k,t}^{con})_{C_1}$, and $(P_{h_k,t}^{con})_{C_2}$. The information goes from the aggregator to the end-users are $P_{h_k,t}^{max}$, and $\alpha_{h_k,t}$. The transformer exchange information with grid are $P_{k,t}^{dem_{agg}}$, $P_{k,t}^{sell_{agg}}$, $P_{k,t}^{flex_{agg}^{up}}$, $P_{k,t}^{flex_{agg}^{dwon}}$, and TX^{rating}. The transformer operator performs several tasks as follows:

- Adds up the power demand (optimal) of prosumers while reducing electricity costs and energy, as (3.25) and (3.26).
- Calculates the flexibility of each prosumer as in (3.27)-(3.33) and (5.3).
- Aggregates the flexibility of all the prosumers as in (3.32).
- Calculates the flexibility index of the prosumer as in (3.35).
- On the other hand, the transformer operator also performs optimization using the thermal constraints of the transformer.
- The optimization model of the transformer operator minimizes the LoL of the transformer.

In this study, the transformer operator monitors the P2P energy trading, which is done before the transformer at PCC. After the P2P energy trading, the transformer operator checks whether it is technically feasible or not. In the P2P energy trading first, the power balance of buyers and sellers is done as shown in the first part (red highlighted) of the figure 5.3. Afterward, financial trading starts. The financial trading, as mentioned in the second part (green highlighted) in figure 5.3, is done using the mid-market rate as discussed in subsection 5.5.1. The relationship between HEMS,

Table 5.3: Controllable appliances used in houses

Appliance	Pr^{a}-1	Pr-2	Pr-3	Pr-4	Pr-5,10	Pr-6	Pr-7	Pr-8	Pr-9
EV	✓	✓	✓	✓	✗	✓	✓	✓	✗
Battery	✓	✓	✓	✗	✗	✓	✗	✓	✓
PV	✗	✓	✓	✓	✗	✓	✓	✓	✓
EWH	✓	✓	✓	✓	✓	✓	✓	✓	✓
Arrival time of EV	37 (6:00pm)	41 (7:00pm)	37 (6:00 PM)	33 (5:00 PM)	-	29 (4:00 PM)	39 (6:30 PM)	35 (5:30 PM)	-
Departure time of EV	92 (7:45AM)	95 (8:30 AM)	92 (7:45 AM)	88 (6:45 AM)	-	84 (5:45 AM)	94 (8:15 AM)	90 (7:15 AM)	-
Arrival SOC of EV	40 %	20 %	40 %	50 %	-	45 %	40 %	35 %	-
Departure SOC of EV	80 %	80 %	80 %	80 %	-	80 %	80 %	80 %	-

P2P, and transformer operator is presented in detail in figure 5.2. In this figure, we consider four different scenarios to examine the effectiveness of the proposed method.

- Scenario-1: HEMS connected directly with transformer [213, 8].
- Scenario-2: HEMS with integration of P2P with consideration of transformer [214, 215].
- Scenario-3: HEMS with fixed power limit by the transformer [203].
- Proposed Scenario: HEMS with dynamic power limit based on flexibility by transformer and integration of P2P.

5.7 Result and Discussion

5.7.1 Case Study

The proposed technique is tested on a 75 kVA pole-mount transformer, which provides power to 10 residential customers. The thermal model parameters are presented in Table 5.2 shows the thermal model parameters. The consumption patterns of customers are taken from a real-world (from California region) PECAN Street data set, as outlined in [216]. We consider different types of appliances for different prosumers, as shown in Table 5.3. Also, arrival times of EVs are different for each prosumer, as depicted in Table 5.3. Multiple varieties of EVs and solar PV batteries are presently available in the market. A suitable EV [4] and battery [3] are selected to satisfy the needs of the studied houses, as shown in Table 3.1. Similarly, the specification of EWH used in the houses is shown in Table 3.2. The pricing tariff is the ToU pricing scheme of Pacific gas and electricity [5, 6], and the FiT rate is set as 0.08 $/kWh [7] as shown in Table 5.1.

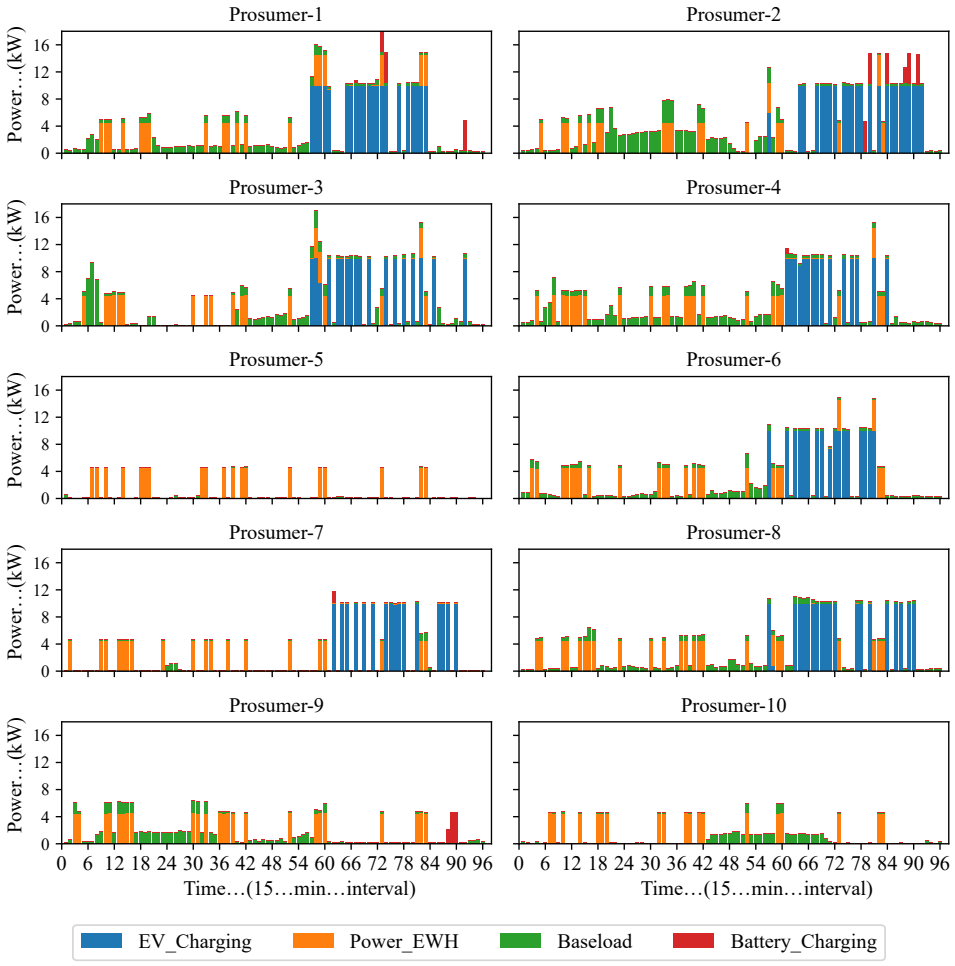

Figure 5.4: Power demand of ten studied houses.

The mathematical model presented earlier was implemented on the Python platform using the PYOMO package [184]. The model was run on a computer with an Intel(R) Core(TM) i7-10850H CPU @ 2.70GHz processor, 32.0 GB RAM, and Windows 11 Pro 64-bit operating system. The HEMS optimization is a MILP-based problem that was solved using the CPLEX solver [185], while the transformer model is a non-linear programming problem that was solved using the IPOPT solver [186].

5.7.2 HEMS Results

At the residential level, we consider each house equipped with HEMS. In this study, we consider different types of prosumers. Each prosumer has various controllable appliances in their houses. For

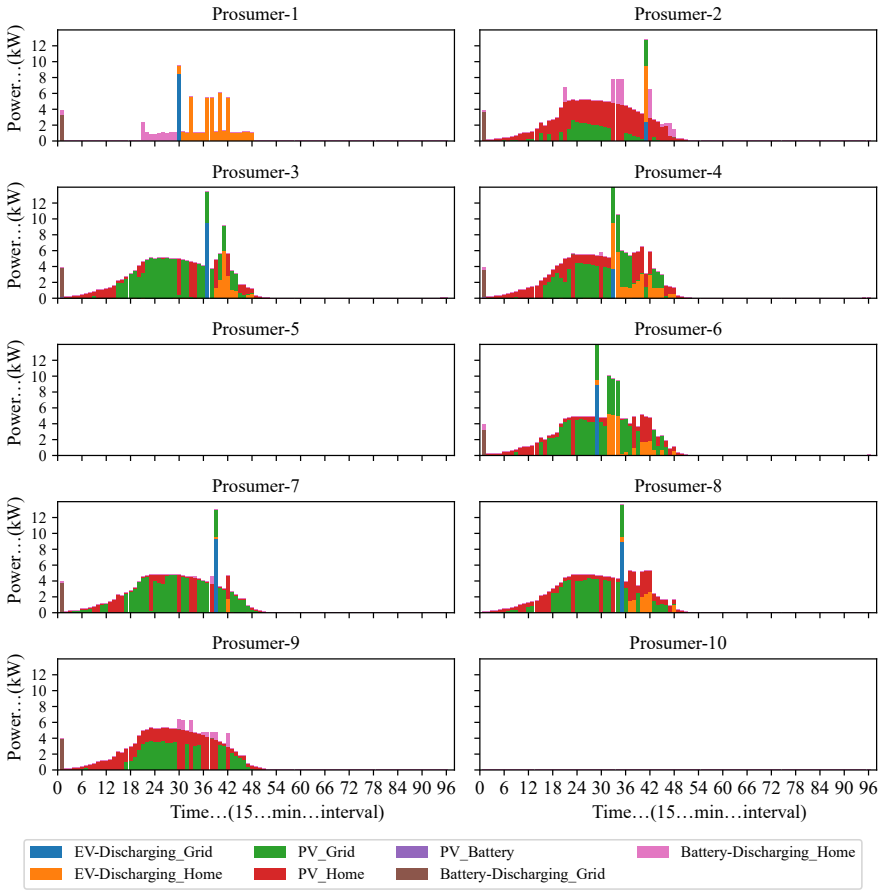

Figure 5.5: Power Export to the power Grid by ten houses.

instance, prosumer-1 has an EV, battery, and EWH but not PV. Similarly, house-5 and house-10 do not have EVs, batteries, and PVs. The details for all the prosumers are presented in table 5.3. The arrival and departure times of EVs are also different, as shown in table 5.3. Similarly, the state-of-charge (SoC) of each EV upon arrival is different, as illustrated in table 5.3. In this work, we consider only one type of battery, EWH, and EV for all the houses as displayed in table 3.1 and 3.2.

The HEMS optimizes the flexible home appliance as shown in figure 5.4, and 5.5 serve by one transformer at location k. Figure 5.4 presents the optimal load profiles of all the appliances for the studied ten prosumers. These households have HEMSs, which can schedule their home appliances such as batteries, EVs, and EWHs. When the grid operator provides a ToU signal, the prosumer schedules the controllable appliances to charge at a time interval when the price is low and discharge at a high pricing time to reduce the electricity cost. Consequently, another peak often

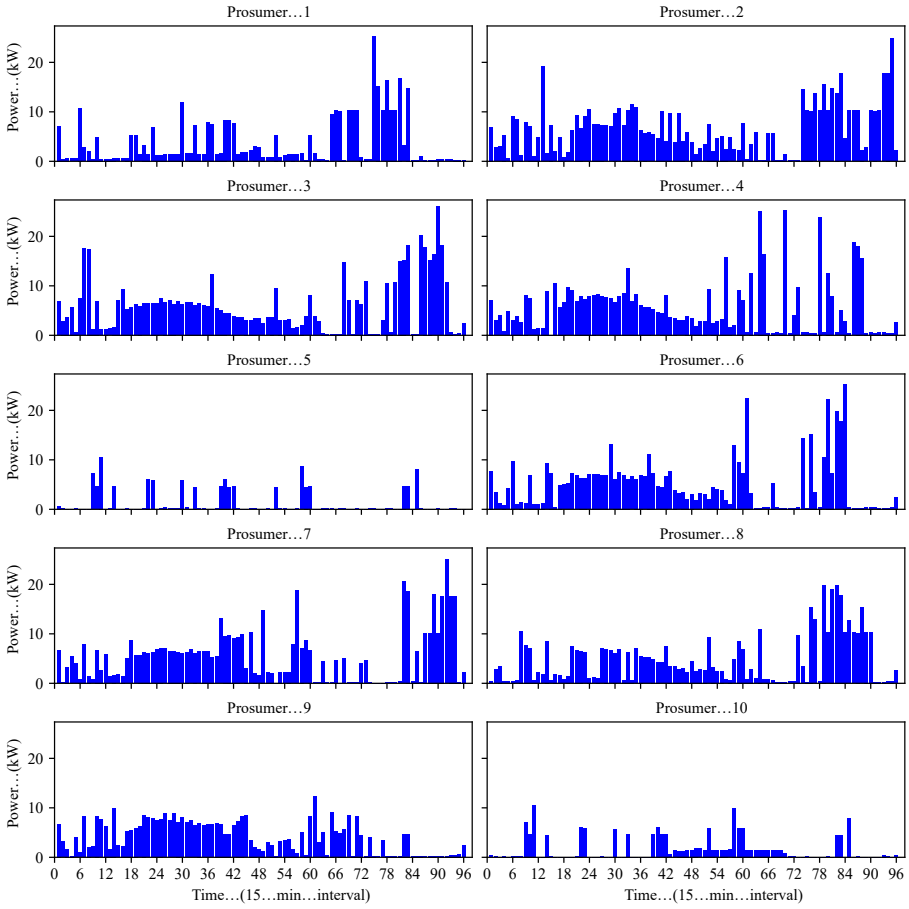

Figure 5.6: Dynamic power limit based on the flexibility of the prosumers.

appears at low price hours, known as a "rebound peak". The prosumer exports excess power to the grid at the FiT price as shown in 5.5. From figure 5.5, we can see that prosumer-1 does not have PV generation and export less power to the grid. Similarly, prosumer-5 and prosumer-10 do not have EV, ESS, or PV and can not export power to the grid.

Using the proposed method, we limit the prosumer based on the flexibility and power rating of the transformer, as discussed in section 5.4.3. The proposed method provides a dynamic power limit for each prosumer, as shown in figure 5.6.

5.7.3 P2P Results

As mentioned earlier, house-5 and house-10 are consumers. They do not have PV, battery, and EV. Consequently, they cannot sell power to their peers and can only buy power from their

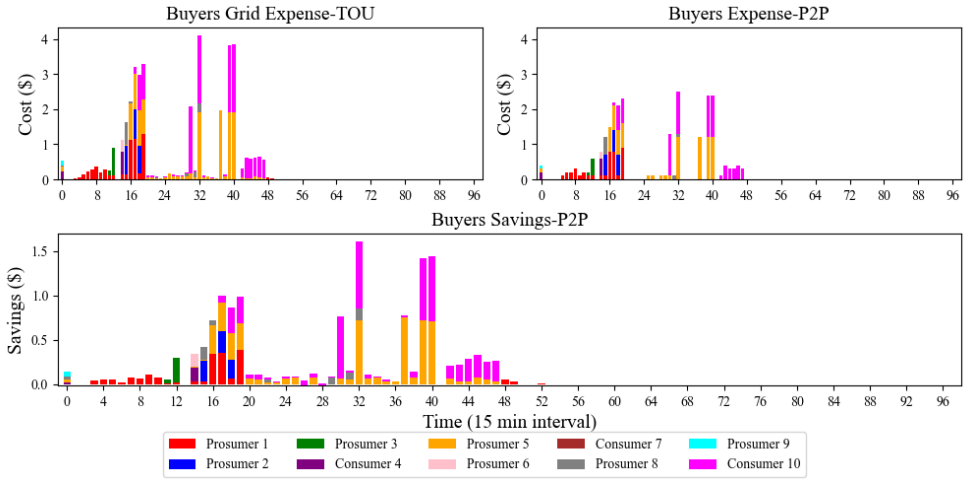

Figure 5.7: Buyer data for P2P trading in Scenario-2.

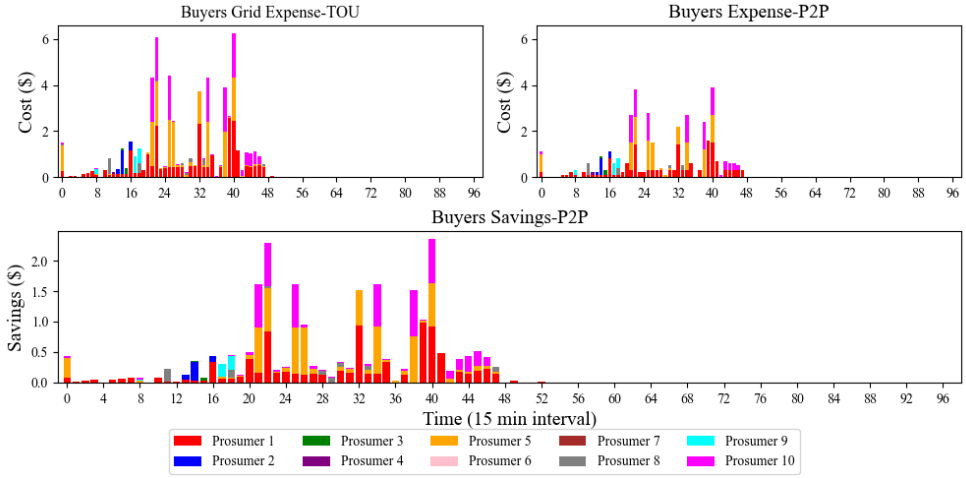

Figure 5.8: Buyer data for P2P trading in the Proposed Scenario.

neighbors. Figure 5.7 shows buyer expense from the grid through TOU and buyer expense if energy amounts are purchased through the P2P trading. From figure 5.7, it can be noticed that the buyer's cost is higher if buying from the grid than buying via P2P trading. The prosumers save money if they trade in P2P, as shown in figure 5.7. If we use our proposed method, which considers the flexibility limit on each house, then the P2P energy trading saves even more compared to scenario-2 as depicted in figure 5.8. The flexibility limit of the transformer forces the prosumer to self-consumption and shift their power to other time intervals, which in turn helps the prosumer to do P2P energy trading. From 5.8, it can be observed that overall, the prosumers save two times more than in scenario-2.

Figure 5.9 indicates seller earnings who export power to the grid at the FiT price and prosumer

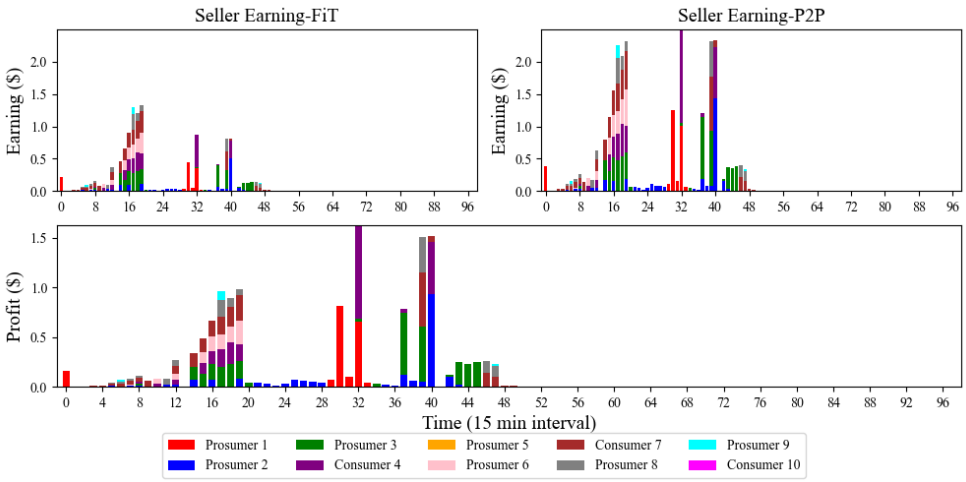

Figure 5.9: Seller data for P2P trading in Scenario-2.

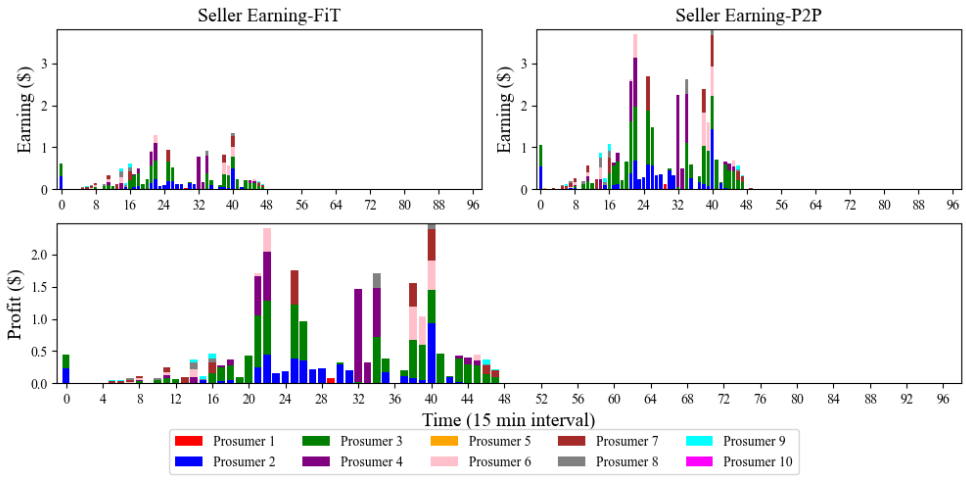

Figure 5.10: Seller data for P2P trading in the Proposed Scenario.

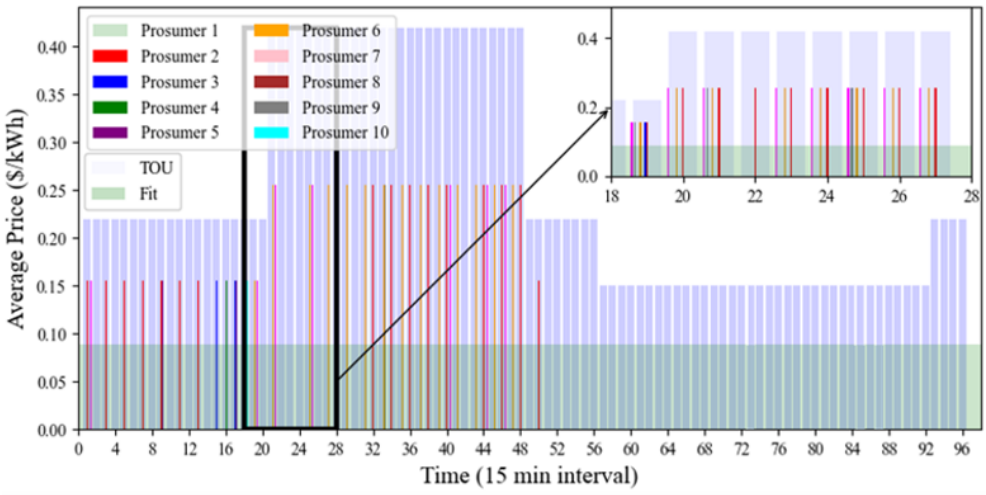

Figure 5.11: Average P2P prices of prosumers compared to TOU and FiT prices.

earnings when trading extra energy in a P2P market. The bottom figure in 5.9 presents the profit of prosumers when trading in the P2P market compared to the FiT. Similarly, figure 5.10 depicted the prosumers selling energy using the proposed method, But here, the overall profile of prosumers using proposed method is more than scenario-2 as shown in figure 5.10. From figures 5.8 and 5.10, it can be concluded using the proposed method, the buyers can save more, and sellers can profit more than the grid's TOU and scenario-2.

The average P2P prices of prosumers are illustrated in figure 5.11. It can be shown that, during trading times, the P2P prices (average) are higher than the flat FiT rate. As a result, sellers will experience a monetary benefit. In contrast, purchasers' average P2P prices are lower than the ToU grid costs, suggesting that buyers can also save some money.

5.7.4 Transformer Results

The HEMS of each household is optimized to have the lowest cost possible if the transformer power limit is not enforced. However, every home tries to allocate as much of the load associated with EV charging operations and controllable appliances during comparatively low price periods. The distribution transformer, therefore, can be overburdened during these periods at scenario-1 and scenario-2, as shown in figure 5.12. The red dashed line represents the maximum capacity of the transformed. When the flexibility limit is applied from the transformer on each house. The overall

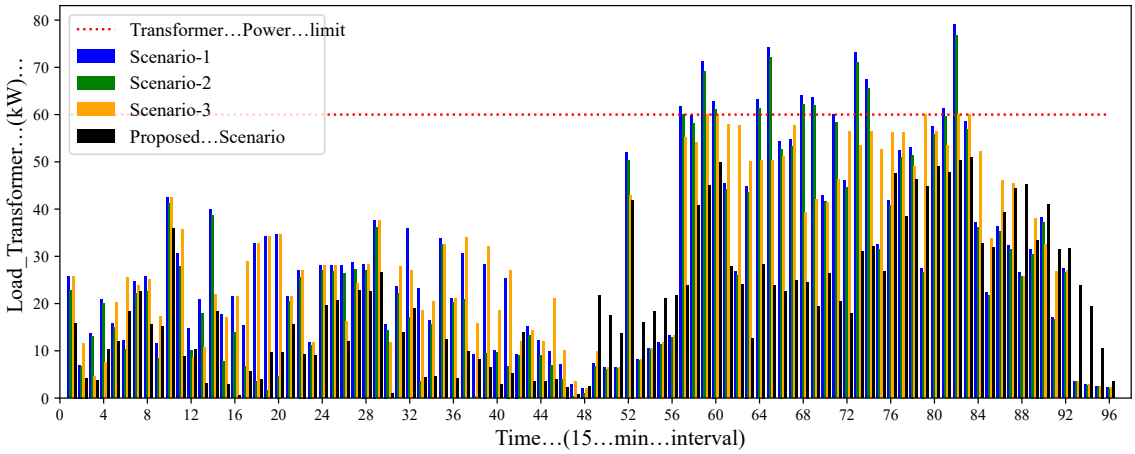

Figure 5.12: Load on the transformer.

load on the transformer is within the capacity limit of the transformer, as demonstrated in scenario-3 and the proposed method (see figure 5.12). The proposed method, thus, flattens the load profile of the transformer.

The temperature (hot spot) of the transformer winding is analyzed in figure 5.13. Figure 5.13 shows that the proposed method temperature is lower than the other scenarios. Such behavior can help to maintain/increase the lifetime of the transformer.

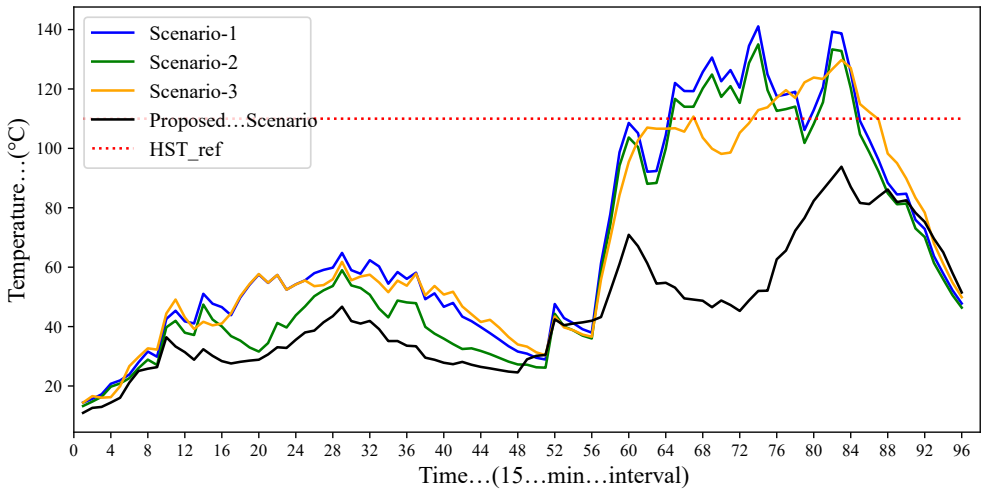

Figure 5.13: Hot Spot Temperature of transformer winding.

Figure 5.14 presents the impact of different scenarios on the accelerating aging factor of the transformer. The transformer does not experience accelerating aging using the proposed method, unlike the other scenarios. In Scenario-1 and Scenario-2, the accelerating aging is higher than the

reference (ref=1), which indicates that these scenarios can cause degradation before the recommended date of the manufacturer. The proposed method does not affect the accelerating aging of the studied transformer.

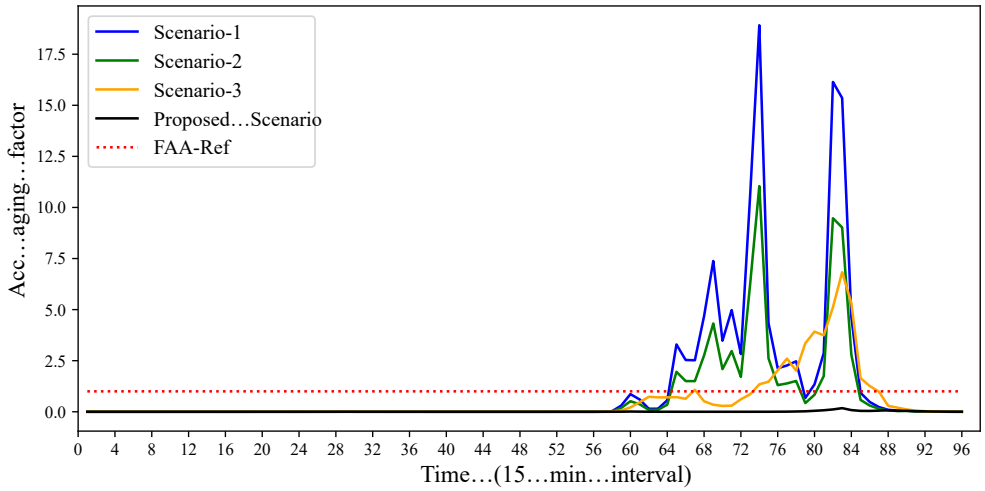

Figure 5.14: Accelerating Aging Effect.

Moreover, the costs of prosumers per day for four scenarios are shown in figure 5.15. From figure 5.15, it can be noticed that the proposed method offers low electricity costs per day compared to the other three scenarios. Thus, it is beneficial for the prosumers. Table 5.4 presents the life expectancy of the transformer. Using the proposed method, the transformer's lifetime also improves compared to other scenarios.

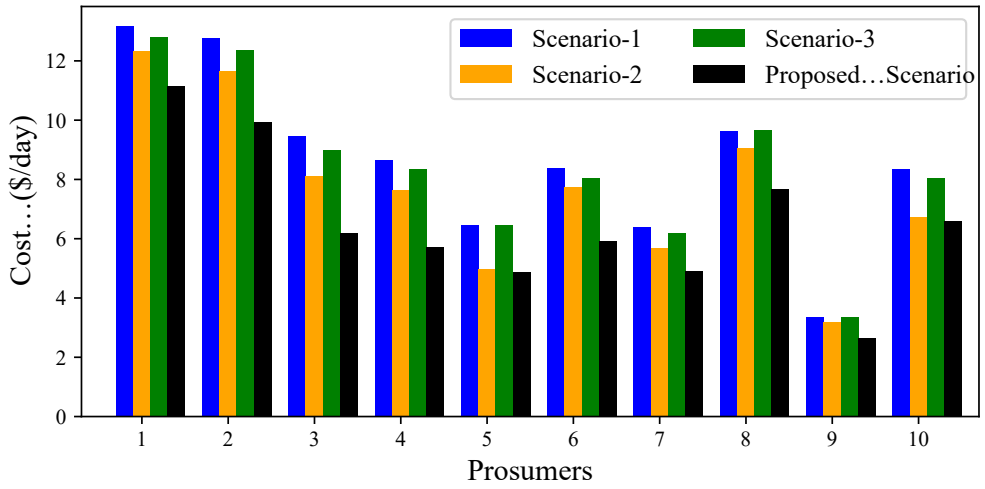

Figure 5.15: Cost Comparison.

Table 5.4: Transformer life expectancy

	Scenario-1	Scenario-2	Scenario-3	Proposed Method
Transformer life expectancy (year)	0.17	0.29	0.40	21.3

5.8 Summary

The coordination framework proposed in this chapter offers a comprehensive solution for optimizing HEMS-integrated P2P trading while considering its impact on a distribution transformer. With the increasing adoption of distributed energy resources, this framework provides a promising approach to managing energy flows locally, promoting a more sustainable, reliable, and efficient energy system. The proposed HEMS has been designed to minimize individual electricity costs under a dynamic pricing scheme. A detailed study of the proposed framework has been demonstrated in this work, including simulation results and comparison with existing methods, to articulate its effectiveness and potential for practical implementation. The electricity costs of the participating prosumers in the proposed method have been confirmed to be lower than those of other cases, ensuring the financial viability of the developed model. The proposed method prevents the distribution transformer from overloading, as seen in different scenarios. Besides, the accelerating aging of the distribution transformer is lower than that of the other three scenarios. As such, the temperature (hottest spot) of the distribution transformer in the proposed method has been below the recommended temperature of the transformer. The proposed method ensures that the transformer's life expectancy remains unaffected (21.3 years), with the loss of operational life found to be negligible compared to other techniques.

However, this work does not consider the operational constraints of the distribution network, e.g., loss minimization using optimal power flow, which will be incorporated in the future to extend the proposed framework. Furthermore, an advanced optimization process can be adopted to model P2P energy trading in a large-scale distribution system. These improvements are made in the chapter 6

Chapter 6

Smart Home P2P Energy Trading Considering Three-Phase Unbalanced Distribution Network Optimization

NOMENCLATURE

Indices, Sets and Functions

$P_{k,p,t}^{Expt}$	Aggregated active power export; kW
$P_{k,p,t}^{Impt}$	Aggregated active power imported; kW
$Q_{k,p,t}^{Expt}$	Aggregated reactive power export; kW
$Q_{k,p,t}^{Impt}$	Aggregated reactive power imported; kW
G_{kj}^{sp}	Conductance between bus k and k ; $p.u$
M	Very large number
$P_{h_k,t}^{\boldsymbol{BL}}$	Base load; kW
$P_{k,p,t}^{Impt}$, $P_{k,p,t}^{Expt}$	Aggregated imported/exported active power from/to DSO; $p.u$
$Q_{k,p,t}^{Impt}$, $Q_{k,p,t}^{Expt}$	Aggregated imported/exported reactive power from/to DSO; $p.u$

τ	Time step; $15min$
$\beta_t^{\textbf{Buy}}$, $\beta_t^{\textbf{Sell}}$	Buying, selling price; $\$/kWh$
$\beta_t^{\textbf{P2P}}$	Mid market price; $\$/kWh$
$\beta_t^{\textbf{P2P}}$	P2P price; $\$/kWh$
$\beta_{t,b}^{\textbf{LEM}}$	Buyer LEM price; $\$/kWh$
$\beta_{t,s}^{\textbf{LEM}}$	Seller LEM price; $\$/kWh$
$V_{\min_k}, V_{\max_k}$	Maximum and minimum voltage at bus k
$P_{g_{k,p,t}}^{max}, P_{g_{k,p,t}}^{min}$	Maximum and minimum active power generation at bus k of phase p
$Q_{g_{k,p,t}}^{max}, Q_{g_{k,p,t}}^{min}$	Maximum and minimum reactive power generation at bus k of phase p
$I_{l_{\max}}$	Maximum current injection; A
$P_{h_k,t}^{\textbf{Dem,DSO}}$	Buying power of household from DSO; kW
$P_{h_k,t}^{\textbf{Expt,DSO}}$	Selling power of household to DSO; kW
$P_{C_{h_k,t}}^{\textbf{EV}}$, $P_{C_{h_k,t}}^{\textbf{ESD}}$	Charging power of EV, ESD; kW
$P_{D_{h_k,t}}^{\textbf{EV,H}}$,$P_{D_{h_k,t}}^{\textbf{EV,DSO}}$	Discharging power of EV to home, G; kW
$P_{D_{h_k,t}}^{\textbf{ESD,H}}$,$P_{h_k,t}^{\textbf{ESD,DSO}}$	Discharging power of ESD to home, grid; kW
$P_{D_{h_k,t}}^{\textbf{EV}}$,$P_{D_{h_k,t}}^{\textbf{ESD}}$	Total discharging power of EV, ESD; kW
$P_{D_{h_k,t}}^{\textbf{PV,ESD}}$	Power of PV supply to ESD; kW
$P_{D_{h_k,t}}^{\textbf{PV,H}}$,$P_{D_{h_k,t}}^{\textbf{PV,DSO}}$	Power of PV supply to home, DSO; kW
$P_{h_k,t}^{\textbf{EWH}}$	Power demand of electric water heater; kW
$U_{h_k,t}^{\textbf{b,DSO}}$	Status of buying power; ON/OFF
$U_{h_k,t}^{\textbf{s,DSO}}$	Status of selling power; ON/OFF
$V_{k,p,t}^{rel}$	Real part of voltage at bus k of phase p
$V_{k,p,t}^{rel}$	Imaginary part of voltage at bus k of phase p
$I_{sp_k,p,t}^{rel}$	Real part of specific current injection at bus k of phase p
$I_{sp_k,p,t}^{Img}$	Imaginary part of specific current injection at bus k of phase p

6.1 Background

This chapter focuses on designing four-stage (HEMS, P2P, transformer, and OPF) optimization for ML-EMS (home, transformer/aggregator, and distribution level). [1] Despite the advantages that DERs can offer to the energy system [217], utilities are confronted with several technological problems due to their widespread integration. The primary focus of these challenges is to avoid the potential violations of operational constraints of distribution networks, which include breach of voltage limits and network congestion caused by overloading distribution assets. Voltage limit violations occur in distribution networks that accommodate DERs because reverse power injections of the DERs increase nodal voltage magnitudes [218]. A paper by Nizami et al. [219] presents a system for managing energy in a group of buildings. The system is broken down into two consecutive stages. The former stage involves creating a scheduling model by adopting MILP to minimize energy costs while user comfort is maintained in each building. The later stage involves all buildings participating in a transactive market for profit maximization. It is important to note that all buildings have solar PV and batteries, and during the former stage, no energy has been sold to the distribution network operator or transacted with other homes.

Researchers have explored various methods to enhance smart house coordination in neighborhoods. One such method is utilizing a decentralized online algorithm called the Lyapunov-based cost reduction technique to achieve coordination [220]. Similarly, to meet the same objective, [221] suggested a bi-level decentralized local energy management strategy. Researchers have also investigated and examined real-time pricing schemes and incentive-based peak load reduction strategies to minimize stress on the distribution transformer during peak hours [222, 223]. However, the methodologies used in [222, 223] significantly rely on end-user choices and do not ensure that the constraints imposed by distribution networks and their assets are considered.

Nevertheless, prosumers have an opportunity to maximize power exchange to their advantage in the context of an LEM, outperforming the advantages provided by the FiT program [224]. These prosumers consequently can establish energy communities that are anticipated to be valuable in

[1] This chapter has significant materials from the following paper Submitted by the Ph.D. candidate:
Hussain, S., Azim, M. I., Lai, C., & Eicker, U. (2023). Multi-stage Optimization for Energy Management and Trading for Smart Homes Considering Operational Constraints of a Distribution Network. Energy and Buildings (Submitted first revision).

determining the future of the energy landscape [107]. Community members can trade substantial amounts of locally generated energy among themselves using P2P exchanges. In contrast, all the energy that is not traded is sent through the traditional power grid [107]. Constraint optimization algorithms [156], game theory [225], auction theory [226], blockchain solutions [227], and other optimization models have all been utilized to analyze P2P trading among prosumers. Furthermore, designing energy market structures for prosumers under the control of regulated utilities has received a lot of attention [228]. In decentralized energy markets, prosumers who satisfy in-the-moment demand from customers or other prosumers are immediately compensated [229].

P2P trading has been the subject of numerous studies as an approach to reducing end-user electricity bills. For instance, to save operational costs, Elkazaz et al. [196] have used MILP to model P2P trading constraints for a group of homes. The paired houses exchange energy, but the import/export tariff is not considered. This is not lucrative to prosumers, implying that they are selling power without receiving any financial return. For batteries used in the P2P trade, Long et al. [158] have presented a bi-level control strategy. Javadi et al. [198] have allowed prosumers in the residential, industrial, and commercial sectors to exchange energy over P2P and reduce costs. Garcia et al. [199] have addressed P2P energy management for prosumers and proposed a P2P EMS to reduce electricity expenses.

Some other studies, like the one in [203], have focused on smart communities with transformer constraints. However, they have neglected to consider the transformer's thermal model, distribution network operational constraints, and the pricing scheme for P2P energy trading. Although existing research has examined the effect of EVs and solar PV systems with batteries on transformer lifespan, they have not considered the consequences of P2P trading on distribution networks and transformers [8, 204]. In [230], the authors have developed a model for distributing energy that can be used in a community environment. In this situation, a DER, such as a Renewable Energy Source or an ESD, has been installed in each building. To reduce energy expenditures independently of energy sharing, the first phase has optimized the DERs and controlled loads within each building. The energy-sharing profile for each building was then determined, along with appropriate payment mechanisms, using a non-cooperative sharing game.

Considering the insights presented above, it becomes apparent that a comprehensive approach

involving integrating a four-stage energy management system (home, aggregator encompassing P2P and transformer stages, and DSO) is imperative. The complexity of the energy landscape necessitates a holistic understanding and coordination across these stages to ensure optimal outcomes for all stakeholders. More research is needed to explore the complex interactions between these stages properly to create a win-win situation for the stakeholders involved.

6.2 Contribution

In this study, a four-stage optimization methodology is introduced and implemented within a three-level framework. A novel coordination structure encompassing households and an aggregator is established. This framework addresses transformer loss of life optimization using thermal constraints of the transformer, P2P energy trading facilitated by LEM, and optimal power flow for a three-phase unbalanced distribution network. In this chapter, our objective is to compare the implications of HEMS with MILP-based P2P energy trading on the distribution transformer and the three-phase unbalanced distribution network. The effects are assessed comprehensively, including a comparison with OpenDSS (a distribution system simulator) as a reference, where power flow analysis is executed. This analysis aims to provide valuable insights into the benefits and drawbacks of both HEMS and MILP-based P2P energy trading in terms of their impacts on the transformer's performance and the overall stability of the distribution network. Our study seeks to clarify the best strategy for optimizing energy usage and trade while guaranteeing the secure and dependable functioning of the distribution network.

6.3 Methodology

6.3.1 Energy Management Structure

The primary goal of the EMS is to decrease the overall energy traded between the local community and the DSO. This can boost local energy usage and reduce the operational expenses of each home. The proposed approach contains three levels illustrated in figure 6.1.

- ***Stage-1:*** Each house has a HEMS installed, allowing users to track their energy usage and

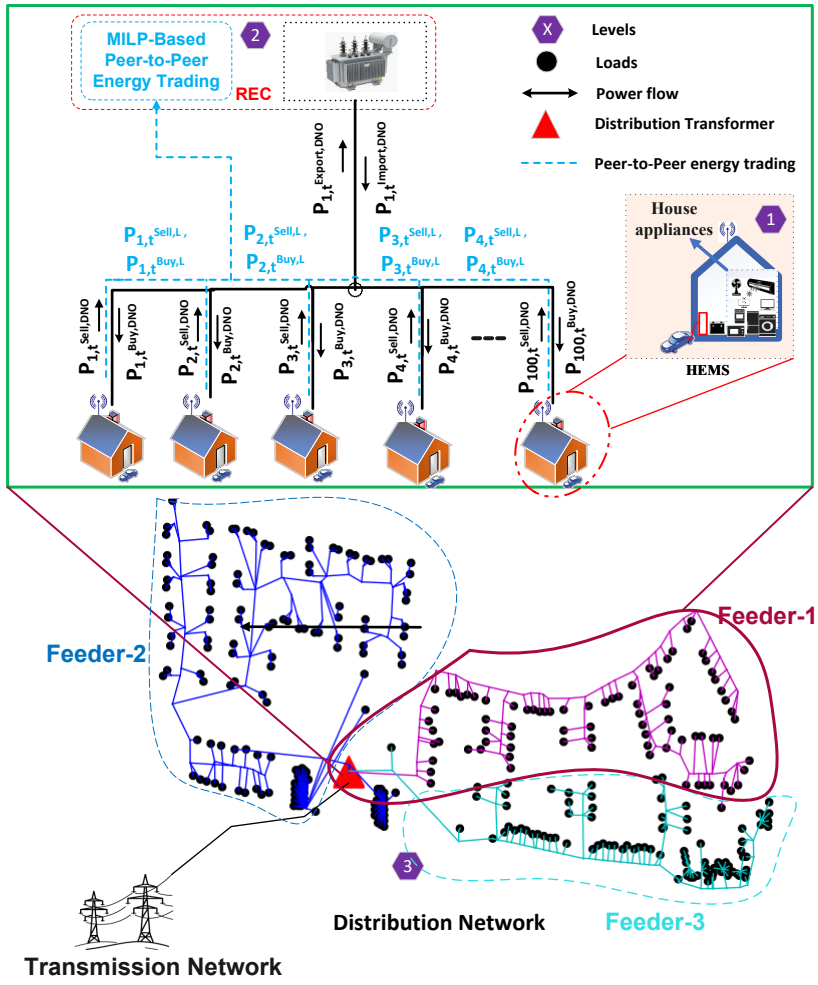

Figure 6.1: Conceptual diagram of multi-stage Optimization framework.

production. During this first stage, energy exchanges with the DSO are reduced for each home without sharing extra energy within the local community. HEMS results are uploaded to the central controller, as shown in Figure 6.1.

- ***Stage-2:*** In this chapter, the transformer is considered the residential energy coordinator (REC). At this stage, P2P energy trading, based on MILP, is utilized to streamline the sequential operation of every house by using information that the central controller has access to. In this second (proposed scenario) scenario, prosumers can reduce their electricity costs by buying and selling energy from the local community and the grid.

- ***Stage-3:*** The thermal model of the transformer is optimized to reduce loss of life (increase

duration a transformer is expected to operate efficiently) in accordance with the thermal constraint of the transformer. At this stage, the transformer is taking the power demand coming from Stage 1 and Stage 2.

- ***Stage-4:*** In this stage, the whole low-voltage distribution network optimization is performed using optimal power flow, as shown in figure 6.1. In this work, the studied distribution network has three phases and is unbalanced to make it as close to the real system as possible.

6.3.2 HEMS Model

For the HEMS, we use the same model as discussed in chapter 3 section 3.2.1. The equations used for HEMS are from (3.1) to (3.24).

6.3.3 Local Energy Market (LEM) Mechanism

Neighborhood Power Exchange Constraints:

To begin, each home's power usage from the PCC has two parts: $P^{Buy,L}_{h_j,t}$ and $P^{Buy,DSO}_{h_j,t}$. The first represents power from other homes, while the second is from the DSO via transformer. Similarly, when a home sells power back to the PCC, it has two components: $P^{Sell,L}_{h_j,t}$ and $P^{Sell,DSO}_{h_j,t}$. The first is used by other homes without going through the transformer, while the second flows to the DSO through the transformer. Additionally, the power exported into the neighborhood should match the power aggregated from local DERs at every instant, as stated in (6.3).

$$P^{Buy,DSO}_{h_j,t} + P^{Buy,L}_{h_j,t} = P^{BL}_{h_j,t} + P^{EWH}_{h_j,t} + (P^{EV}_{C_{h_j,t}} - P^{EV,H}_{D_{h_j,t}}) + (P^{ESS}_{C_{h_j,t}} - P^{ESS,H}_{D_{h_j,t}}) - P^{PV,H}_{D_{h_j,t}}, \quad \forall t \in \mathcal{T}; \forall h_j \in \mathcal{H} \quad (6.1)$$

$$P^{Sell,DSO}_{h_j,t} + P^{Sell,L}_{h_j,t} = P^{EV,DSO}_{D_{h_j,t}} + P^{ESS,DSO}_{D_{h_j,t}} + P^{PV,DSO}_{D_{h_j,t}}, \qquad \forall t \in \mathcal{T}; \forall h_j \in \mathcal{H} \qquad (6.2)$$

$$\sum_{h} P_{h,t}^{buy,L} = \sum_{h} P_{h,t}^{sell,L}, \qquad \forall t \in \mathcal{T}; \forall h_j \in \mathcal{H} \tag{6.3}$$

$$0 \leqslant P_{h_k,t}^{buy,DSO} \leqslant M \cdot U_{h_k,t}^{b,DSO}, \qquad \forall t \in \mathcal{T}; \forall h_k \in \mathcal{H} \tag{6.4}$$

$$0 \leqslant P_{h_k,t}^{sell,DSO} \leqslant M \cdot U_{h_k,t}^{s,DSO}, \qquad \forall t \in \mathcal{T}; \forall h_k \in \mathcal{H} \tag{6.5}$$

$$0 \leqslant P_{h_k,t}^{buy,L} \leqslant M \cdot U_{h_k,t}^{b,L}, \qquad \forall t \in \mathcal{T}; \forall h_k \in \mathcal{H} \tag{6.6}$$

$$0 \leqslant P_{h_k,t}^{sell,L} \leqslant M \cdot U_{h_k,t}^{s,L}, \qquad \forall t \in \mathcal{T}; \forall h_k \in \mathcal{H} \tag{6.7}$$

$$\beta_t^{Sell} \leqslant \beta_{t,b}^{LEM}, \beta_{t,s}^{LEM} \leqslant \beta_t^{Buy} \qquad \forall t \in \mathcal{T} \tag{6.8}$$

$$EWH \quad and \quad PV \quad Operational \quad Constraints \quad (3.7) - (3.9) \tag{6.9}$$

$$EV \quad Operational \quad Constraints \quad (3.10) - (3.14) \tag{6.10}$$

$$ESD \quad Operational \quad Constraints \quad (3.17) - (3.24) \tag{6.11}$$

Where $P_{h_j,t}^{Buy,DSO}$ is the power buy from the grid with β_t^{Buy} price, $P_{h_j,t}^{Buy,L}$ is the power buy from the neighborhood prosumer with price of $\beta_{t,b}^{P2P}$. Similarly, the prosumer sells energy to the neighborhood and the grid at $P_{h_j,t}^{Sell,L}$ and $P_{h_j,t}^{Sell,DSO}$ by price β_t^{Sell}.

Trading Price Constraints

In this section, a new way for homes in a community to trade energy locally is presented. This trading function is run after the HEMS is run, and each home already knows the buying or selling action at each time slot of the day. As illustrated in figure 6.1, the residents of the homes first trade energy with others in the community using the local buying and selling prices instead of trading

directly with the DSO. After trading together within the community, if the community requires more energy or has surplus energy to sell, it trades directly with the DSO. To encourage energy trading among the homes of the community, the local buying/selling prices that are proposed by the local trading manager of the central operation unit should be smaller/larger than the buying/ selling prices that the DSO proposes.

Case 1 (Power Export is Equal to Power Import):

When the energy production of prosumers in the network equals their energy demand, the net network demand is zero. In this case, prosumers in set h with a surplus of energy sell to those in set H. The selling and buying prices (β_t^{FiT} and β_t^{TOU} respectively) for each participant ($h \in h$ and $H \in H$) are determined by (6.12).

$$\beta_{t,b}^{LEM} = \beta_{t,s}^{LEM} = \beta_t^{P2P} \tag{6.12}$$

Case 2 (Power Export is Greater than Power Import):

Since there is a net energy output in this situation that is not zero, the sellers can satisfy prosumers' demand with an energy shortage in the network before selling the entire surplus of energy to the grid at a β_t^{FiT}. The following clearly indicates each buyer's purchase price $\beta_{t,b}^{P2P}$:

$$\beta_{t,b}^{LEM} = \beta_t^{P2P} \tag{6.13}$$

In this case, the cost at which energy is sold by prosumers to the grid, $\beta_{t,s}^{LEM}$, is determined based on the total energy generated, the net power demand of prosumers, and the buying/selling expenses imposed by the grid. Specifically, $\beta_{t,s}^{LEM}$ can be calculated as a function of the total energy generated by prosumers, the total power demand of prosumers, the mid-market rate, and the price at which surplus energy is sold to the grid, $\beta_{t,s}^{FiT}$.

$$\beta_{t,s}^{LEM} = \frac{\sum_h^H P_{h,t}^L \cdot \beta_t^{P2P} + \sum_h^H (P_{h,t}^{gen} - P_{h,t}^L) \cdot \beta_t^{FiT}}{\sum_h^H P_{h,t}^{gen}} \tag{6.14}$$

The expression in Equation (6.14) calculates the overall revenue that the sellers can obtain in

the network. The first term of the numerator, which is represented by the summation over all the buyers in H, denotes the revenue generated by selling energy to them at a price of β_t^{P2P}, where $P_{h,t}^{L}$ represents the total energy demand of the respective buyer. The second term represents the extra energy that is sold to the grid at a price β_t^{FiT}.

Case 3 (Power Export is Less than Power Import):

In this scenario, the energy export by the prosumers is less than the power demand, leading to net energy demand. Consequently, the buyers in H need to fulfill their excess energy requirements, $(\sum_H^H P_{h,t}^{L} - \sum_h^h P_{h,t}^{gen})$, by buying energy from the grid. The buying price $\beta_{t,b}^{LEM}$ will be influenced by several factors, including the total available surplus energy $\sum_h^H P_{h,t}^{gen}$, total energy demand $\sum_h^H P_{h,t}^{L}$, and the prices $\beta_{t,b}^{P2P}$ and β_t^{TOU}. Mathematically, this can be expressed as:

$$\beta_{t,b}^{LEM} = \frac{\sum_h^H P_{h,t}^{gen} \cdot \beta_t^{P2P} + \sum_h^H (P_{h,t}^{L} - P_{h,t}^{gen}) \cdot \beta_t^{TOU}}{\sum_h^H P_{h,t}^{L}} \tag{6.15}$$

Similar to Case 1, the selling price $\beta_{t,s}^{P2P}$ each seller $h \in h$ will charge the buyer for purchasing their extra energy will be calculated as follows:

$$\beta_{t,s}^{LEM} = \beta_t^{P2P} \tag{6.16}$$

It should be mentioned that in the proposed P2P energy trading scheme, the values of $\beta_{t,s}^{P2P}$ and $\beta_{t,b}^{P2P}$ are determined based on the values of $\sum_H^H P_{h,t}^{L}$, $\sum_h^h P_{h,t}^{gen}$, β_t^{TOU}, and β_t^{FiT}. These values are fixed for each time slot t, regardless of whether the prosumers involved in the energy trading decide to collaborate in a large group (grand coalition) or remain separated into smaller groups (disjoint coalition). This means that once a prosumer decides to take part in P2P energy trading, they need to buy and sell using $\beta_{t,b}^{P2P}$ and $\beta_{t,s}^{P2P}$, which are set for that specific time slot t. Regulatory charges are not considered when pricing is optimized in this work, which will be done in future work. P2P platform providers may charge prosumers a fee included in the trading cost [231] and pay a subscription expenditure to the distribution network operator for operating their infrastructure for trading [232].

The objective function is the same as that of HEMS to minimize the household's electricity consumption and reduce the electricity cost.

$$J_{6,h_j} = \sum_{t \in T} (P^{Buy,DSO}_{h_j,t} \cdot \beta^{Buy}_{t} + P^{Buy,L}_{h_j,t} \cdot \beta^{LEM}_{t,b} - P^{Sell,DSO}_{h_j,t} \cdot \beta^{Sell}_{t} - P^{Sell,L}_{h_j,t} \cdot \beta^{LEM}_{t,s})\tau \quad (6.17)$$

6.3.4 Transformer Model

Thermal model of Transformer

The mathematical modeling of the thermal model of the transformer is the same as discussed in the chapter 5 section 5.4.4 from equations (5.4) to (5.13).

6.3.5 Three Phase Unbalance Distribution Network

The model formulation for a three-phase distribution network, with the unbalanced structure, is significant in achieving optimal power/voltage control [233]. The formulation adopts the current mismatch method, as presented in [234]. Unlike transmission systems, which often assume balanced conditions, distribution networks exhibit unbalanced characteristics. The primary objective is to minimize distribution network losses, although the model can be tailored to explore various objective functions, accommodate DERs, and facilitate decentralized solutions.

The power balance equation of the distribution system is one of the operational constraints for the distribution system operation.

$$P_{g_{k,p,t}} + P^{Expt}_{k,p,t} - P^{Impt}_{k,p,t} = (V^{rel}_{k,p,t})(I^{rel}_{sp_k,p,t}) + (V^{img}_{k,p,t})(I^{img}_{sp_{k,p,t}}), \quad \forall t \in \mathcal{T}; \forall k \in \mathcal{B}; \forall p \in \mathcal{P} \quad (6.18)$$

$$Q_{g_{k,p,t}} + Q^{Expt}_{k,p,t} - Q^{Impt}_{k,p,t} = (V^{img}_{k,p,t})(I^{rel}_{sp_k,p,t}) - (V^{rel}_{k,p,t})(I^{img}_{sp_{k,p,t}}), \quad \forall t \in \mathcal{T}; \forall k \in \mathcal{B}; \forall p \in \mathcal{P} \quad (6.19)$$

Power balance equations (6.18) and (6.19) have three parts on the left-hand side. The first part represents the active and reactive power generated by the distribution substation, respectively. The second part in both equations indicates the total exported power to the DSO. The third part, $P^{Impt}_{k,p,t}$ and $Q^{Impt}_{k,p,t}$ in (6.18) and (6.19), represent the combined active power and reactive power demand of homes located at bus k. The right-hand side represents active and reactive power losses through the lines involving that bus, respectively. The reactive power is determined using a constant power factor of the load, e.g., 0.85 [101].

The current mismatch equations define the relationship between nodal voltages and power export from each supply in the distribution network. These equations are mathematically expressed in operational constraints (6.20)-(6.22). Incorporating unbalanced three-phase operational considerations in the model enables a more accurate representation of real-world distribution networks. It supports the development of efficient and effective optimization strategies for improved grid performance.

$$I^{rel}_{\text{cal}_{k,p,t}} = \sum_{j\in\Omega}\sum_{p\in\sigma_p}(G^{sp}_{kj}(V^{rel}_{j,p,t}) - B^{sp}_{kj}(V^{img}_{j,p,t})), \quad \forall t \in \mathcal{T}; \forall k,j \in \mathcal{B}; \forall s,p \in \mathcal{P} \tag{6.20}$$

$$I^{img}_{cal_{k,p,t}} = \sum_{j\in\Omega}\sum_{p\in\sigma_p}(G^{sp}_{kj}(V^{img}_{j,p,t}) + B^{sp}_{kj}(V^{rel}_{j,p,t})), \quad \forall t \in \mathcal{T}; \forall k,j \in \mathcal{B}; \forall s,p \in \mathcal{P} \tag{6.21}$$

$$\Delta I_{k,p,t} = I_{calc_{k,p,t}} - I_{sp_{k,p,t}}, \quad \forall t \in \mathcal{T}; \forall k \in \mathcal{B}; \forall p \in \mathcal{P} \tag{6.22}$$

Where in (6.20), (6.21) the real/imaginary calculated current injection $I^{rel}_{\text{cal}_{k,p,t}}$, $I^{img}_{cal_{k,p,t}}$. The magnitude of the steady-state voltage at each node must comply with the voltage limits defined in (6.23), where the upper and lower voltage limits for nodes are those of the corresponding distribution code. In addition to the above constraints, the active/reactive power drawn from the grid is limited by upper and lower bounds, as in equation (6.24) and (6.25).

$$V_{\min_k} \leq V_k^p \leq V_{\max_k}, \quad \forall t \in \mathcal{T}; \forall k \in \mathcal{B}; \forall p \in \mathcal{P} \tag{6.23}$$

$$P_{g_{k,p,t}}^{min} \leq P_{g_{k,p,t}} \leq P_{g_{k,p,t}}^{max}, \quad \forall t \in \mathcal{T}; \forall k = s; \forall p \in \mathcal{P} \tag{6.24}$$

$$Q_{g_{k,p,t}}^{min} \leq Q_{g_{k,p,t}} \leq Q_{g_{k,p,t}}^{max}, \quad \forall t \in \mathcal{T}; \forall k = s; \forall p \in \mathcal{P} \tag{6.25}$$

Objective Function

The DSO performs a system-level optimal power flow analysis. The objective of the DSO has been defined as the minimization of total system losses. The objective of the DSO optimization is shown in the equation below:

$$J_7 = \sum_{t \in \mathcal{T}} \left(\sum_{j=1}^{N} \sum_{k=1}^{N} G_{j,k} \Big((V_{j,t}^{rel} - V_{k,t}^{rel})^2 + (V_{j,t}^{img} - V_{k,t}^{img})^2 \Big) \right) \tag{6.26}$$

6.4 Four-Stage Coordination Framework

The proposed strategy of four-stage optimization consists of multiple houses having HEMS that can sell and buy energy to/from the DSO.

In the proposed coordination framework, each prosumer has a HEMS that receives input updates regarding customer preferences, as shown in figure 6.2. The desired upper and lower limits of the hot water temperature for EWH, arrival and departure times of the EVs, and initial and final energy levels of the ESD at the beginning and end of the day. The PV power for each house is also fed into the HEMS. The information regarding parameters of the DERs used in the house is also provided to HEMS, such as the type and built-in characteristics of the EV, ESD, and EWH in table 3.1 and 3.2, respectively. Some information comes from the DSOs, for instance, demand response information (ToU, FiT) and market strategies, as shown in table 5.1. Figure 6.2 illustrates the detailed flow of the first scenario and the proposed method. The arrows depict the connection between different stages and demonstrate the flow of the algorithm.

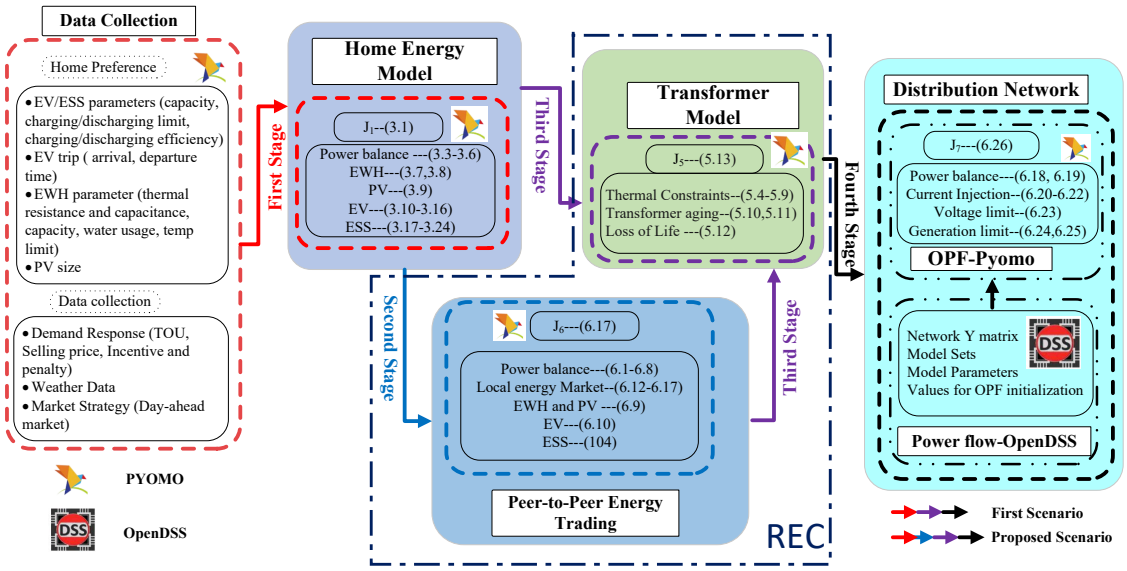

Figure 6.2: Block diagram of the four-stage Optimization.

In the first stage, the HEMS schedules the house appliances based on the minimization of the electricity cost objective, as in (3.1). Prosumers become flexible energy resources with the presence of DERs when a HEMS is incorporated into them. The optimal load demand is determined at the house level and collectively sent to the transformer operator. The aggregated optimal power imported and exported is provided to the distribution transformer.

The second level acts as residential energy coordinator (REC), which includes the transformer thermal model and MILP-based P2P optimization model. P2P energy trading is done at the second stage of the coordination framework. At this stage, the neighborhood can buy and sell energy in the locality using the LEM. The household can trade with each other in the local energy market. The prosumer can sell and buy energy from the local community using the local energy market price for selling and buying using (6.1)-(6.9). If prosumers still have surplus energy, they can trade with DSO through the grid price mechanism. Similarly, they can buy unmet energy from the grid using the FiT as equation (6.12)-(6.16). The optimal power demand of P2P energy trading is provided to the transformer.

The smart distribution transformer serves as an intermediary between multiple homes and a distribution network. In the third stage, the transformer thermal model is optimized based on the optimal power demand from HEMS and P2P energy trading, leading to an extended lifespan. The

flow of information from end-users to the aggregator is represented by $P_{h_k,t}^{Buy,DSO}$ and $P_{h_k,t}^{Sell,DSO}$. During this stage, the impact of HEMS and P2P energy trading on the transformer is analyzed using the thermal constraint, as outlined in equations (5.4) through (5.13).

During the fourth stage, the optimization of unbalanced three-phase power is conducted through optimal power flow after optimizing the transformer's lifespan. The necessary data for optimal power flow is obtained from the distribution network simulation in OpenDSS. The power flow is executed in OpenDSS, while the PYOMO abstract model is utilized to calculate optimal power, as demonstrated in equations (6.18)-(6.26). In this work, the effects of HEMS and P2P energy trading on the three-phase unbalanced distribution network are assessed by integrating an OPF formulation.

6.5 Result and Discussion

6.5.1 Case Study

The implementation of the proposed four-stage EMS optimization model's coordination framework was carried out using the Python platform and the PYOMO software package [184]. The computational setup utilized for this implementation featured an Intel(R) Core(TM) i7-10850H CPU @ 2.70GHz 2.71 GHz processor, accompanied by 62.0 GB RAM.

To address the MILP problems in the first and second stages, the CPLEX solver was employed [185]. Subsequently, for the non-linear programming problems in the third and fourth stages, the IPOPT solver [186] was utilized. MILP is chosen because it offers global optimal solutions for complex problems, especially in large-scale energy systems. MILP effectively manages real-world trade-offs and objectives. Additionally, it benefits from efficient mathematical solvers like CPLEX, enhancing computational performance and relaxing the constraints to solve the problem within a reasonable amount of time. However, this work does not consider a comprehensive evaluation of open and commercial solvers such as CPLEX, BARON, and GUROBI as a prospect for future investigations.

The time step selected for the optimization is 15 min. The time horizon for the optimization is one day. Hence, the number of intervals within the optimization is 96. The thermal model parameters are presented in Table 6.2. The consumption patterns of customers are taken from a

real-world (from the California region) PECAN Street data set, as outlined in [216]. Table 6.1 shows the action times, i.e., arrival and departure, of EVs, which are different for each prosumer. Similarly, the state of charge (SOC) of each prosumer is different, as shown in table 6.1. Multiple varieties of EVs and solar PV batteries are presently available on the market. A suitable EV [4] and battery [3] are selected to satisfy the needs of the studied houses, as shown in Table 3.1. Similarly, the specification of EWH used in the houses is shown in Table 3.2. The pricing tariff is the ToU pricing scheme of Pacific gas and electricity [5, 6], and the FiT rate is set at 0.08 $/kWh [7] as shown in Table 5.1. This study undertakes a comparison of two distinct scenarios. The first scenario entails households equipped solely with HEMS. The analysis of their influence on transformers and distribution systems aligns with prior research [203, 235, 215]. Subsequently, the study presents a second (proposed) scenario: residences equipped with HEMS in conjunction with P2P energy trading facilitated through LEMs. The following analysis examines the impact of this configuration on transformers and one of the three feeders (feeder-1) of the radial distribution network [233].

Table 6.1: EV's SOC and time of arrival/departure.

Appliance	House-1	House-2	House-3	House-4	House-5	House-7	.....	House-100
EV's arrival	37 (6:00pm)	41 (7:00pm)	37 (6:00 PM)	33 (5:00 PM)	29 (4:00 PM)	39 (6:30 PM)	.....	35 (5:30 PM)
EV's departure	92 (7:45AM)	95 (8:30 AM)	92 (7:45 AM)	88 (6:45 AM)	84 (5:45 AM)	94 (8:15 AM)	.....	90 (7:15 AM)
EV's arrival SOC	40 %	20 %	40 %	50 %	45 %	40 %	.....	35 %
EV's departure SOC	80 %	80 %	80 %	80 %	80 %	80 %	.....	80 %

Table 6.2: Distribution transformer Thermal data [9]

$\Delta\theta_t^{\mathrm{TO,R}}(^\circ C)$	$\Delta\theta_t^{\mathrm{HST,R}}(^\circ C)$	m	n	$\tau^{\mathrm{TO}}(min)$	$\tau^{\mathrm{W}}(min)$	$\theta_{t,ref}^{\mathrm{HST}}(^\circ C)$	T_R	Type
55	80	0.8	0.8	155	5	110	8	ONAN

6.5.2 HEMS (First Stage)

At the residential level, each house is assumed to be equipped with HEMS. The action times of various EVs are considered distinct, as illustrated in table 5.3. Similarly, the state-of-charge (SOC) of each EV upon arrival is different, as illustrated in table 5.3. In this work, three types of EV, one type of ESD and EWH, are used for all the prosumers, as shown in Tables 3.1 and 3.2, respectively.

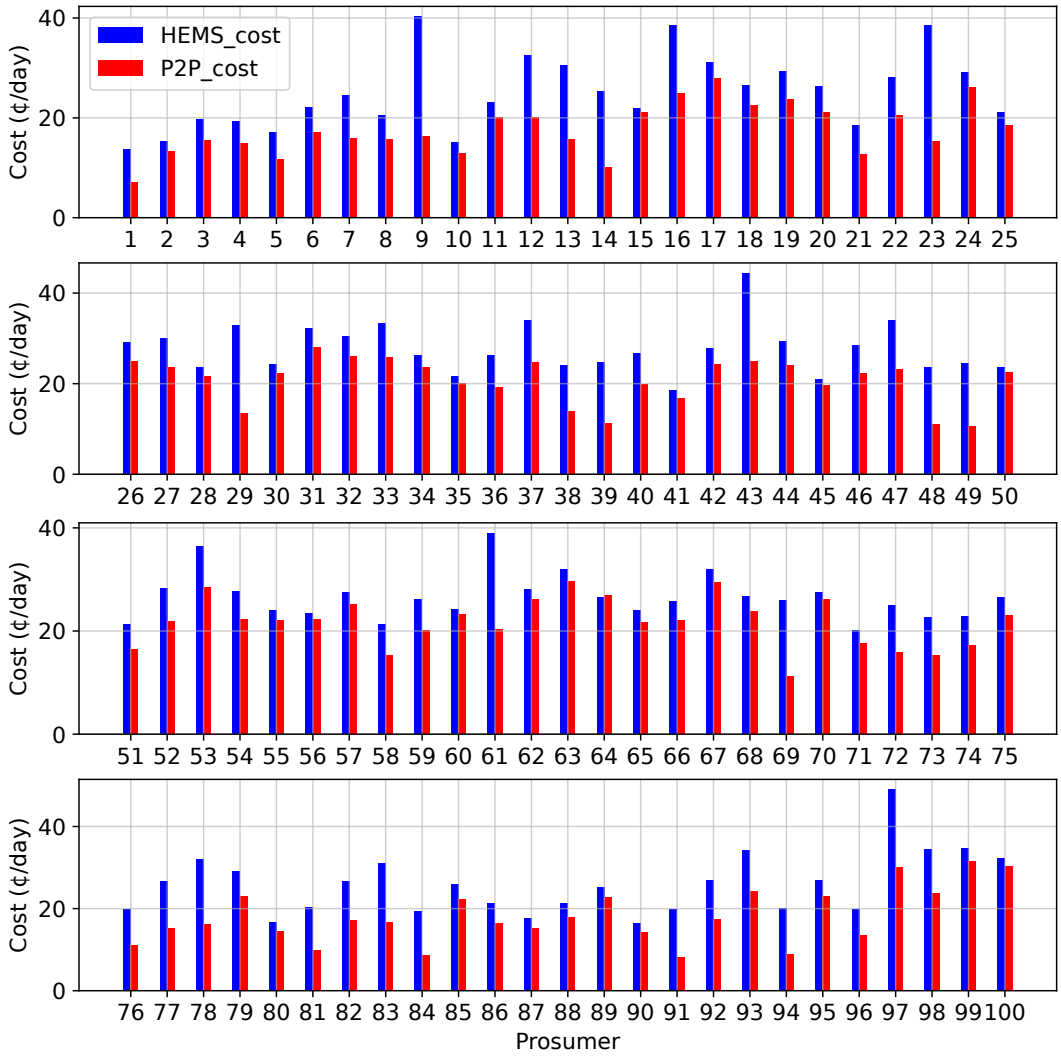

Figure 6.3: Cost of electricity consumption of Prosumers.

The sum of optimal power demand from HEMS and P2P energy for all the prosumers is displayed in figure 6.4. According to Figure 6.4, while using HEMS, there is a peak (1579 kW) at low price time from time steps 72 to 92. It shows that using the P2P energy trading mechanism, the power profile reduces the peak to 956 kW because the prosumers buy/sell energy in the neighborhood.

Moreover, the costs of prosumers per day for four scenarios are shown in figure 6.3. From figure 6.3, it can be noticed that the proposed P2P method offers low electricity costs per day compared to the HEMS.

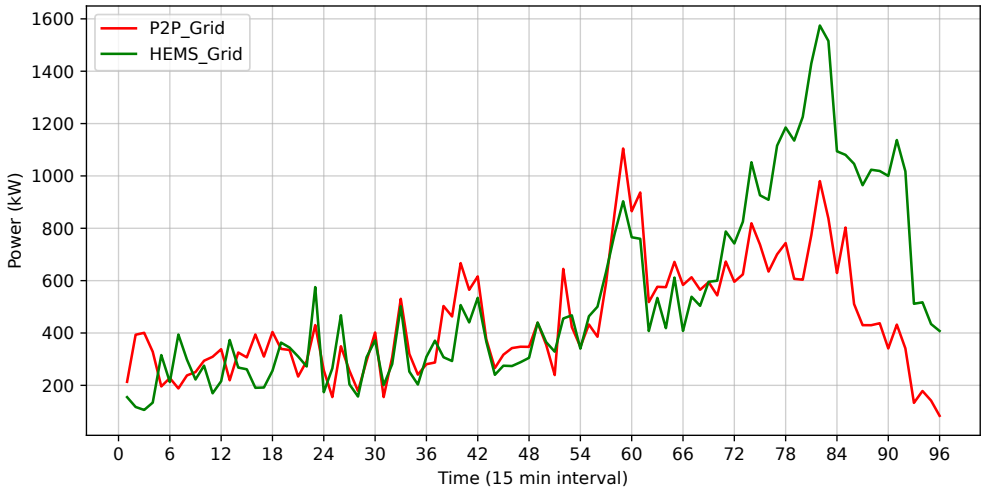

Figure 6.4: Sum of the optimal power demand of HEMS (green) and P2P (red).

6.5.3 P2P energy trading (Second Stage)

The MILP-based P2P energy trading outcome is an optimal LEM buy and sell price. The LEM sells and buys in between the ToU and FiT tariffs, as shown in figure 6.5. This means that buyers can buy energy at a lower price than ToU, and sellers can sell their energy at a higher rate than FiT. This makes the buyer more profitable, and the seller earns more money. Therefore, the consumer prefers to fulfill their energy required using LEM compared to the DSO electricity market. Similarly, the seller will prefer to sell their energy in the neighborhood. Such preference will have a positive impact on the transformer, such as less overloading during peak hours and improving the lifetime of the transformer. Also, there will be less power losses and lower congestion in the distribution network.

6.5.4 Distribution Transformer (third Stage)

In this work, the assumption is made that the transformer is connected to a household equipped with HEMS. The household schedules its appliances in accordance with the DSO tariff (TOU and FiT). In another case, the home can trade its energy in the local community and optimize its appearance according to the LEM price.

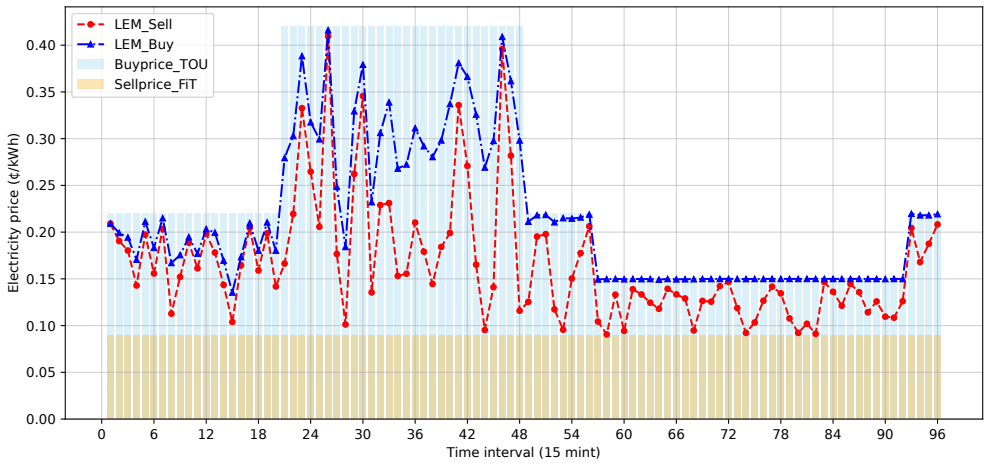

Figure 6.5: LEM, TOU, and FiT price for buyer and seller.

Home (has HEMS) connected to Transformer

The HEMS of each house is optimized to have the lowest electricity expense. However, every home tries to allocate as much of the load associated with EV charging operations and controllable appliances during comparatively low price periods (for ToU). The distribution transformer can be overloaded during these periods when the price of the electricity is low when using HEMS, as shown in figure 6.6a. Because each house tends to reduce electricity cost and does not care about the transformer or distribution network operation. So, there is a peak at the time of low price, as shown in the top subplot of figure 6.6a. The red dashed line represents the maximum power limit of the distribution transformer. Using equation 6.27, the transformer having HEMS in the neighborhood is overloaded by approximately 145.31%.

$$\text{Percentage Overload } = \left(\frac{\text{Peak Power-Transformer Capacity}}{\text{Transformer Capacity}} \right) \times 100\% \qquad (6.27)$$

The HST of the distribution transformer winding is analyzed in the second subplot of figure 6.6a. This figure shows that with overloading the transformer, the HST of the transformer increases from the recommended HST temperature, which is 110 $^{\circ}C$. Because of a rise in the HST temperature compared to the preferred temperature, the accelerating aging effect increases, as shown in the bottom figure in 6.6a. The accelerating aging effect is higher than the reference (ref=1). Such

behavior decreases the lifetime of the transformer. The loss of life of the transformer is 0.62% per day when having HEMS in the neighborhood. Please note that in this case study, we only consider one feeder of the three feeders as a case study. If we include the other two feeders with the same transformer, it will affect the LoL of the transformer.

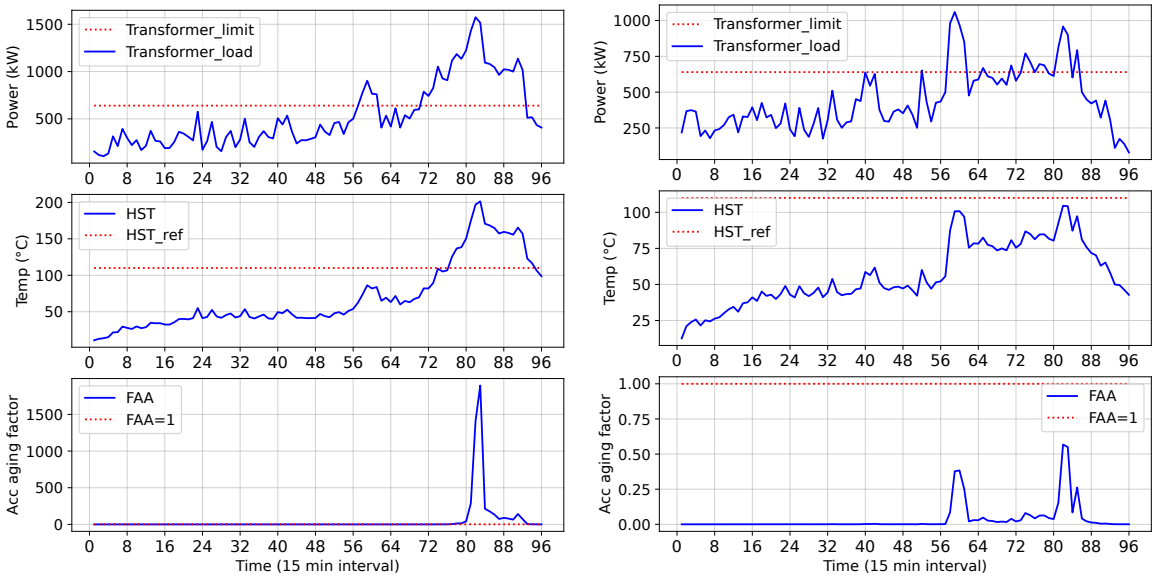

(a) Effect on the transformer with HEMS neighborhood.

(b) Effect on the transformer with P2P energy trading neighborhood.

Figure 6.6: Comparison of Transformer having HEMS and P2P in neighborhood.

Home (can take part in LEM) connected to Transformer

As mentioned earlier, in this study, homes can trade with each other through LEM mechanisms. Every home tries to sell its energy to the neighborhood and buy from the local community. Thus, less power is required from the grid via the distribution transformer. Thus, reduce the load on the transformer as shown at the top figure in 6.6b. The prosumers take part in LEM, causing less overload on the transformer as in the HEMS scenario. Thus, the HST of the transformer winding is analyzed in figure 6.6b, and does not increase from the reference (preferred) temperature (110 C°). Due to the preferred temperature, the accelerating aging effect did not increase the reference (ref=1), as shown in the bottom figure in 6.6b. Such behavior does not decrease the lifetime of the transformer. In such a system, the loss of life of the transformer having HEMS and P2P energy trading in the neighborhood is 0.6% and 0.00059% per day, respectively.

6.5.5 Distribution Network Operator (Fourth Stage)

Results from the modeled OPF simulation are exhibited in figure 6.7 to figure 6.12. The solid lines in the figures 6.9 - 6.12 show the result using OPF, while the dashed line represents the power flow results in OpenDSS.

In Figure 6.7, the temporal progression of current magnitudes across all nodes, corresponding to the 3 phases of a bus over the time horizon T, is illustrated. Notably, the currents are monitored under different operational setups: HEMS alone and HEMS constraint combined with P2P energy sharing.

Figure 6.7a showcases the current profile when utilizing HEMS within a household. In this study, it is observed that the current occasionally surpasses prescribed voltage (PU) thresholds. This occurrence can be attributed to each household's strategy of optimizing appliance scheduling to curtail electricity costs.

In comparison, Figure 6.7b illustrates the current profile when P2P energy sharing is integrated. Remarkably, the current magnitude remains within acceptable limits, as opposed to the scenario depicted in Figure 6.7a. This outcome affirms the efficacy of P2P energy sharing in maintaining a more regulated and efficient energy consumption pattern, thus alleviating concerns about current spikes beyond PU thresholds.

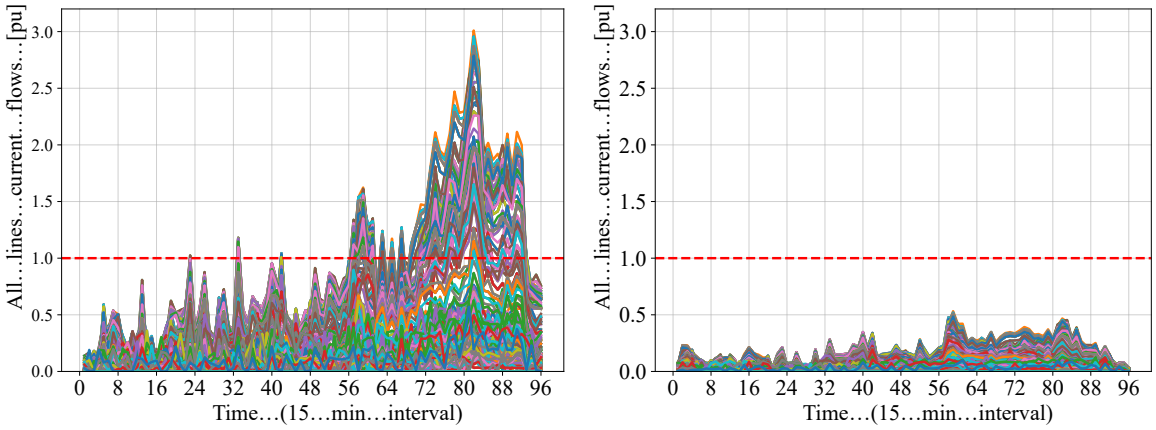

(a) All line Current using HEMS.

(b) All line Current using P2P.

Figure 6.7: Comparison of All line Current using HEMS and P2P.

In Figure 6.8, an investigation into voltage dynamics within a European low-voltage distribution

network is presented. The analysis delves into the influence of HEMS deployment and integration of P2P energy trading. Figure 6.8a illustrates the impact of HEMS on voltage profiles. The application

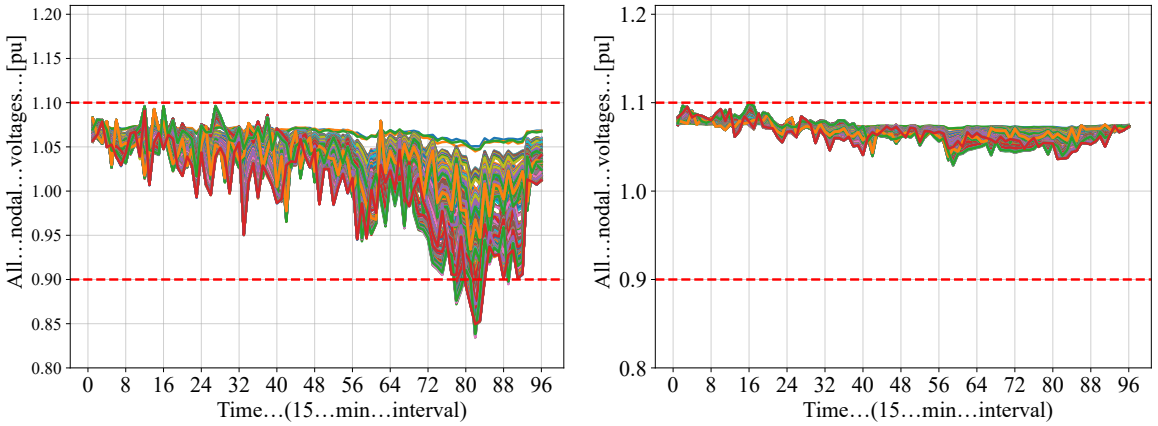

(a) All nodal voltage after HEMS.

(b) All nodal voltage after P2P.

Figure 6.8: Comparison of All voltage using HEMS and P2P.

of HEMS, driven by localized optimization strategies to curtail individual electricity expenses, inadvertently results in a degradation of voltage profiles across nodes, potentially jeopardizing network stability.

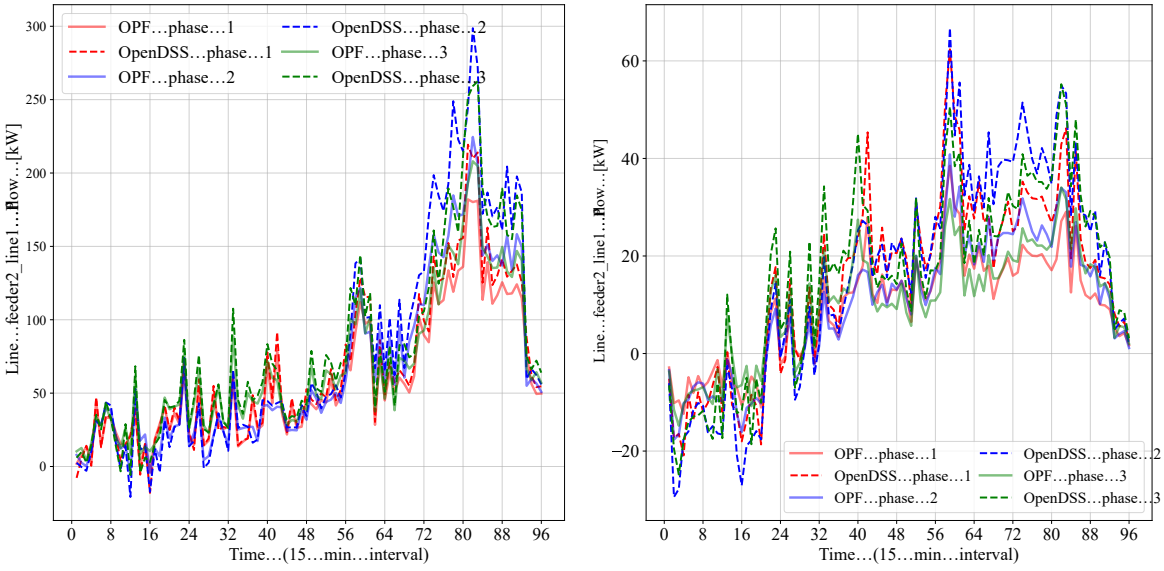

(a) Active power flow using HEMS.

(b) Active power flow using P2P.

Figure 6.9: Comparison of active power using HEMS and P2P.

In contrast, Figure 6.8b portrays voltage profiles under the framework of P2P energy trading.

Notably, the voltage levels observed across nodes are consistently maintained within the prescribed operational bounds. This observation underscores the efficacy of P2P energy exchange in upholding stable voltage profiles, ensuring the network operates reliably and adheres to stipulated voltage limits. This stands as a compelling solution, mitigating concerns regarding voltage degradation commonly associated with HEMS-centric approaches.

The result from 6.9 to 6.12 represents the line current, power, and voltage profiles of a specific line and feeder. In this work, "*line1*" of "*feeder-2*" of the European low-voltage distribution network is used as an example for showing the result. The active power and reactive power of the line "*line1 feeder2*" is shown in figures 6.9 and 6.10. Notably, these figures underscore a noteworthy disparity in power requirements between HEMS users and prosumers engaging in P2P energy trading. HEMS users exhibit substantially higher active and reactive power demands than their counterparts utilizing P2P mechanisms.

Furthermore, the line current of the prosumer using P2P is lower than that of the prosumer having HEMS, as shown in figure 6.11. This behavior causes degradation in the voltage profile having HEMS. In contrast, prosumers accessing LEM have improved voltage profiles, as shown in figures 6.12a and 6.12b, respectively.

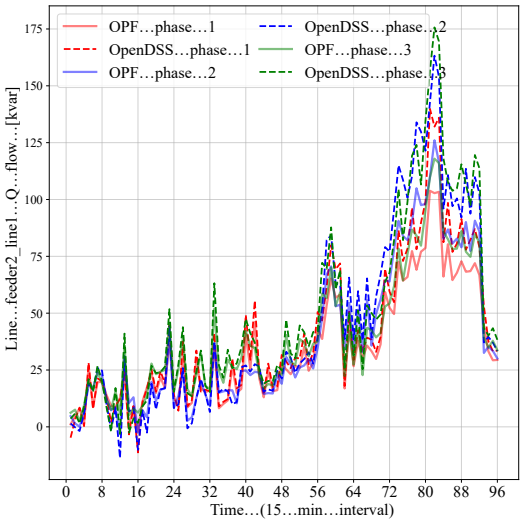

(a) Reactive power flow using HEMS.

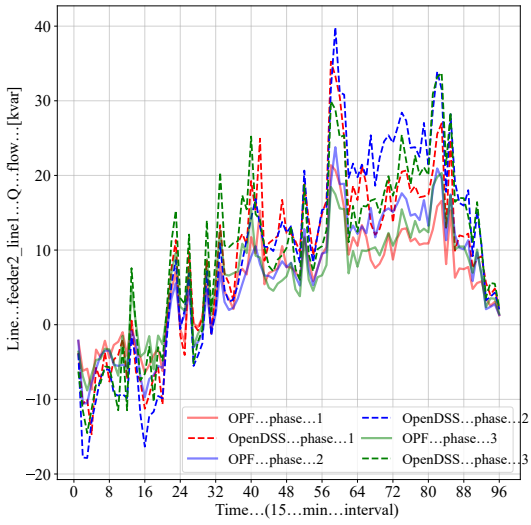

(b) Reactive power flow using P2P.

Figure 6.10: Comparison of reactive power using HEMS and P2P.

6.5.6 Compare results with OpenDSS

In this work, a comparison was conducted between the results obtained from OPF using Python and power flow computations driven by OpenDSS. Figure 6.9 to 6.12 visually depicts this comparison, where dashed lines represent OpenDSS results and solid lines signify OPF results using PYOMO.

The results indicate that employing OPF yields a marked improvement in voltage profiles, contributing to a more stable network. Additionally, OPF leads to notable reductions in line currents, enhancing system efficiency. Moreover, applying OPF effectively minimizes peak power demands, a critical factor in efficient load management, which positively impacts grid resilience and reliability. Overall, this comparison highlights the advantages of utilizing OPF, facilitated by PYOMO, in power system analysis, emphasizing improved voltage profiles, reduced line currents, and efficient peak power demand management.

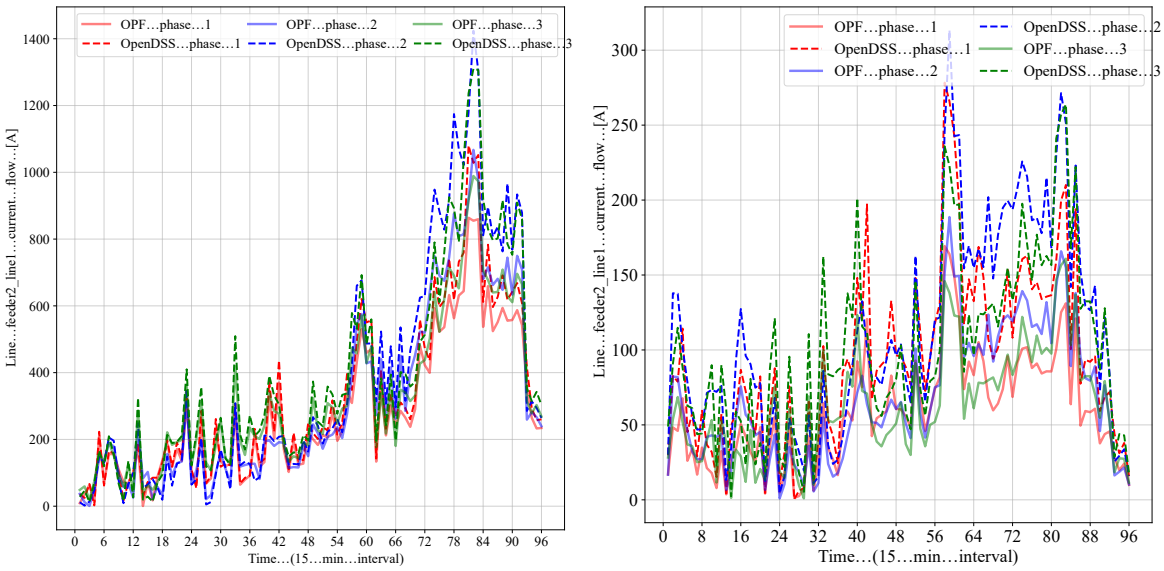

(a) Line current flow using HEMS.

(b) Line current flow using P2P.

Figure 6.11: Comparison of line current using HEMS and P2P.

After analyzing the result, it is clear that households utilizing only HEMS have a notable influence on the transformer. This influence leads to transformer overload, increased HST temperatures,

and decreased lifetime. Furthermore, such neighborhoods negatively impact the distribution network, resulting in voltage reduction. However, by implementing the proposed approach, the transformer's lifespan can be extended by reducing the load and hence reducing the HST temperatures. Additionally, this strategy has the potential to enhance the voltage profile and reduce the electricity cost of the end-user.

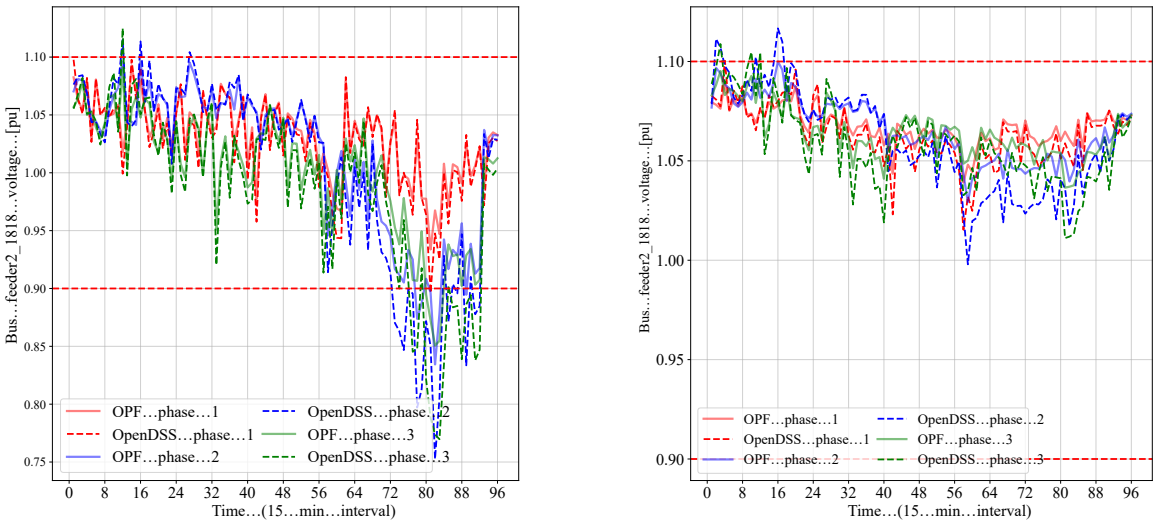

(a) Feeder voltage using HEMS.

(b) Feeder voltage using P2P.

Figure 6.12: Comparison of feeder voltage using HEMS and P2P.

The results indicate that employing OPF yields a marked improvement in voltage profiles, contributing to a more stable network. Additionally, OPF leads to notable reductions in line currents, enhancing system efficiency. Moreover, applying OPF effectively minimizes peak power demands, a critical factor in efficient load management, positively impacting grid resilience and reliability. Overall, this comparison highlights the advantages of utilizing OPF, facilitated by PYOMO, in power system analysis, emphasizing improved voltage profiles, reduced line currents, and efficient peak power demand management.

After analyzing the result, it is clear that households utilizing HEMS have a notable influence on the transformer. This influence leads to transformer overload, increased HST temperatures, and decreased lifetime. Furthermore, such neighborhoods negatively impact the distribution network, reducing voltage. However, by implementing the proposed approach, the transformer's lifespan can be extended by reducing the load and hence reducing the HST temperatures. Additionally,

this strategy has the potential to enhance the voltage profile and reduce the electricity cost of the end-user.

6.6 Summary

This chapter illustrates a four-stage coordination model, facilitating P2P energy trading among numerous homes, aggregator, and the DSO. The coordination framework proposed in this work offers a comprehensive solution for optimizing HEMS and MILP-based P2P trading while considering its impact on a distribution network. With the increasing adoption of DERs, this framework has provided a promising approach to managing energy flows in the local energy community using LEM and, hence, promoting a sustainable, reliable, and efficient energy management system. The proposed HEMS and MILP-based P2P trading framework has been designed to minimize individual electricity costs under a DSO's tariff structure. This work has also demonstrated a detailed study of the proposed framework, including simulation results, comparison with HEMS, and implications on the distribution network to articulate its effectiveness and potential for practical implementation. The electricity costs of the 100 prosumers participating in P2P energy trading in the proposed method have been confirmed to be lower than the HEMS scenario, ensuring the financial viability of the proposed model. By comparing the optimal power demand of all prosumers, the proposed method effectively reduces peak power by 38.85%.

Using the proposed method, the hot spot temperature of the distribution transformer is lower than the other scenarios and the recommended temperature (110 $^{\circ}C$). Similarly, the accelerated aging of the distribution transformer in a P2P neighborhood has been lower than in a neighborhood with HEMS and the reference (ref=1). The loss of life of the transformer per day is negligible using the proposed method (0.00059 %) compared to another scenario (0.69 %).

Furthermore, the effects of HEMS and P2P on the three-phase unbalanced distribution network have been analyzed. The energy community with P2P energy trading and LEM has been found to abide by the voltage and current limits, while the community with HEMS may violate these constraints.

Chapter 7

Conclusion

The final chapter presents concluding remarks and future research directions for extending the conducted research.

7.1 Summary

This thesis primarily focuses on developing a robust coordination framework that helps all stakeholders, such as consumers, prosumers, aggregators, distribution system operators, and the grid. In this thesis, we develop two main coordination frameworks one is grid-centric, and the other is prosumer-centric. In grid-centric, the DSO requests peak reduction using prosumers' flexibility. In prosumer-centric, the prosumers use P2P energy trading to utilize the local energy market and reduce the power imported from the grid during peak hours. This work is divided into different portions.

In **Chapter 1**, the motivation and problem statement were presented, along with the main research objectives and the overall layout of the thesis.

Chapter 2 provides a literature review relevant to the work presented in subsequent chapters. In this chapter, we discuss the control architecture used in the multi-level framework, focusing on the flexibility and demand-side flexibility, along with the associated flexibility services and resources. We also explore the demand response program and the electricity market that is utilized to ensure flexibility. The chapter concludes by summarizing recent research on P2P trading, including its

types, benefits, market structures, and operational layers.

In **Chapter-3**, a brief overview of the background topic related to the research objective of the chapter was presented. The concept of HEMS and the mathematical model of multi-level EMS, in which various ESS, EVs, and EWH technologies were discussed, along with their applications in smart grids. To satisfy the techno-economic objective of the complete network, energy management becomes a multi-level optimization problem with many objectives and constraints on each level separately or many combined levels. The proposed novel three-level framework is used to tackle the contradictory nature of the objectives of end-users and DSOs by upward and downward flexibility provision. At the first stage (HEMS), each house optimizes its appliance operation to minimize the electricity cost. The aggregator collects the flexibility of each household, and the cohort flexibility is conveyed to the DSO. The DSO performs optimal power flow to minimize system losses and sends the optimal flexibility reduction request to the aggregator. The aggregator then disaggregates the flexibility requests to each participant as a peak limit on each house's consumption. The proposed architecture reduces peak demand, distribution system losses, and generation cost by 11.96%, 33.6%, and 1.8%, respectively. However, the electricity cost of the end-users is high after the flexibility provision due to the adaptive power limit on the prosumer. We develop a novel incentive program to motivate the prosumer to participate in this coordination framework.

In **Chapter 4**, a novel incentive program is developed based on the flexibility provided to the DSO or aggregator. This chapter used the ML-EMS flexibility coordination framework for an adaptive incentive program. The results show that our proposed strategy has increased the monetary benefits for prosumers for their flexibility services provided to the DSO compared to other scenarios. Upon considering a use-case of 100% penetration of EVs, ESSs, and PVs at the first stage, the proposed approach was able to reduce the power losses, peak load, and average load of the overall system by 24.6%, 20.8%, and 3.7%, respectively compared to the base case (scenario-1). Furthermore, it increases the minimum load by 42%, thus flattening the load profile of the distribution network.

In chapter-5, a rule-based P2P energy trading is designed where the prosumer can trade with each other through P2P energy trading. The monetary benefits of the proposed P2P kW trading

strategy have been determined and compared with the FiT scheme to demonstrate its superior performance. The designed P2P trading model has also been implemented on a transformer model to determine the physical network issues associated with the mechanism. In this chapter, a smart transformer model is developed for the ML-EMSs. Previously, it was considered a passive element that only delivered electricity to the end-user by changing the voltage level. The smart transformer provides the trading hub for the transaction energy between different connected homes. Also, it gives additional EMS to reduce the maintenance cost of these expensive assets. The electricity costs of the participating prosumers in the proposed method have been confirmed to be lower than those of other cases, ensuring the financial viability of the developed model. As seen in different scenarios, the proposed method prevents the distribution transformer from overloading. Besides, the accelerating aging of the distribution transformer is lower than that of the other three scenarios. As such, the distribution transformer's temperature (hottest spot) in the proposed method has been below the recommended temperature of the transformer. If this behavior occurs throughout the years, the life expectancy of transformers using the proposed method compared to other scenarios is 21.3, 0.17, 0.29, and 0.40, respectively. The proposed method ensures that the transformer's life expectancy remains unaffected (21.3 years), with the loss of operational life found to be negligible compared to other techniques.

In Chapter 6, a MILP-based framework is developed for decentralized P2P energy trading, allowing prosumers to trade at their preferred rates in the local energy market. A four-stage coordination framework enabling P2P energy trading between multiple households, aggregators, and DSOs. The coordination framework proposed in this chapter offers a comprehensive solution for optimizing HEMS- and MILP-based P2P trading while considering its impact on a distribution network. The electricity costs of the 100 prosumers participating in P2P energy trading in the proposed method have been confirmed to be lower than the HEMS scenario, ensuring the financial viability of the proposed model. By comparing the optimal power demand of all prosumers, the proposed method effectively reduces peak power by 38.85%. Using the proposed method, the hot spot temperature of the distribution transformer is lower than the other scenarios and the recommended temperature (110 $^{\circ}C$). Similarly, the accelerated aging of the distribution transformer in a P2P neighborhood has been lower than in a neighborhood with HEMS and the reference (ref=1). Using

the proposed method, the loss of life of the transformer having HEMS and P2P energy trading in the neighborhood is 0.6 % and 0.00059 % per day, respectively. Furthermore, the effects of HEMS and P2P on the three-phase unbalanced distribution network (OPF using PYOMO and power flow using OpenDSS) have been analyzed. The energy community with P2P energy trading and LEM has been found to abide by the voltage and current limits, while the community with HEMS may violate these constraints.

7.2 Limitations and Recommendation for Future Research

This thesis is the starting point for thoroughly examining the EMS and P2P energy trading coordination framework. We must continue our research efforts and strive toward a more sustainable and efficient energy environment. The following sections will illuminate potential avenues of exploration and progress, laying the foundation for a more cohesive and efficient energy future.

Chapter 3 presents the ML-EMS modeling for flexibility provision. However, the HEMS model can be enhanced to incorporate comprehensive models for uninterruptible loads like dishwashers, dryers, washing machines, and other smart appliances. We use an RC model for one of the real buildings for HEMS. However, it should be appropriately incorporated in ML-EMS. Thermal Modeling of the building can be added to the ML-EMS with a thermal energy storage system like heat pumps and thermal storage tanks. This work can be further extended by flexibility assessment based on the appliances. In the cost objective function, it's more practical to consider the degradation cost of the battery and EV from the charging and discharging to the home or DSO. To gain a comprehensive understanding of the proposed method's effectiveness, it is imperative that we evaluate it under varying weather conditions, including hot, cold, sunny, partly sunny, and cloudy days, instead of solely relying on results from a single day.

In **Chapter 4**, a novel incentive program was developed, but this work can be extended by assessing the economic model for revenue generation of aggregators and the fairness and financial sustainability of the incentive programs between end-users and different stakeholders. Also, create a framework to incentivize prosumers based on their appliance flexibility, contributing to a more responsive energy system.

In **Chapter 5**, advanced P2P trading strategies beyond the rule and a MILP-based approach can be investigated. Explore machine learning and AI-driven strategies to optimize P2P energy trading and improve cost-effectiveness in ML-EMS. Similarly, AI-based prediction for transformer performance will help the different types of electricity market for flexibility (day-ahead, intra-day, or balancing power market). As power electronics are evolving, using a digital transformer as a smart hub could be the next step to implementing these algorithms on the smart transformer. Develop the solid-state transformer model as a smart hub for energy transactions. Integrate features to enhance trading efficiency and reduce maintenance costs of these critical assets. The digital transformer is based on power electronics circuits and converters, in which the power utility can regulate the active and reactive power flow by controlling the phase angles of the converters. This technology will improve the stability of the network and increase its efficiency. Therefore, it is suggested to be the case study of future works.

In **Chapter 6**, future work could explore the electrical and thermal limits of the transformer by leveraging the flexibility of the prosumer. This can further improve the performance of the transformer in three-phase unbalanced distribution networks.

The proposed ML-EMS can be tested on a real-test system, and the proposed method can be validated. However, such a system must first be coupled with a simulation environment. Interaction between the optimization and the simulation environment is necessary to validate the proposed ML-EMS using day-ahead optimization. A framework needs to be designed in which the day-ahead optimization gives the optimal set points to the simulation, and the simulation gives its set point back to the intra-day optimization to reduce the mismatch and give the result back to the simulation. Such a platform will make the model more realistic for the real-time implementation.

Appendix A

Objectives and Constraints in Multi-level

Table A.1: Multi-Level EMS and Objectives

Reference	EMS Type	Objectives
[37]	HEMS	Minimize electricity costs.
	Aggregator	Minimize total load deviation and rescheduling costs of customers.
[38]	Local HEMS	Minimize electricity costs and consumer discomfort.
	Global HEMS	Optimize electricity costs for each household after ESS operation and power trading.
[41]	HEMS	Minimize total energy costs.
	Aggregator	Reschedule user power profiles and provide incentives in return.
[8]	HEMS	Minimize electricity costs.
	Aggregator/Transformer	Minimize temperature damage costs and electricity costs.
[39]	HEMS	Three objective functions are used: 1). Minimize energy consumption. 2). Minimize electricity costs. 3). Maximize comfort level.
	GEMS	Minimize total system losses and utilize total flexibility in local distribution networks.
[40]	Home	Minimize electricity costs.
	Aggregator	Minimize total active power loss and rescheduling deviation in low voltage distribution.
	GEMS	Minimize total active power loss and rescheduling deviation of HEMS aggregators in medium voltage distribution.
[18]	Transformer	Minimize electricity costs at home with energy and power soft constraints on transformers.
[9]	Transformer	Reduce transformer hottest-spot temperature with minimal load shifting.

Table A.2: Constraints at Different Levels

	Constraints	
HEMS	**Power/Energy at Home**	
	Ensure balanced net energy/power consumption in households.	[236]
	Prevent violation of power limits in the household.	[41]
	Limit buying and selling power from/to the grid.	[40]
	Electric Vehicle (EV)	
	Determine State of Charge (SoC) of EV. Maintain total energy of EV battery at the start and end of the day. Enforce SoC within specified range. Limit charging/discharging power based on EV availability.	[8]
	Electric Water Heater (EWH)	
	Monitor water temperature and EWH state. Control temperature in the EWH tank. Ensure water temperature remains within set limits. Update room temperature and maintain within bounds.	[41]
	Non-interruptible Loads:	
	Define non-interruptible appliance operation time range. Prevent interruption once appliance operation has begun. Align controllable appliance cycle time.	[41]
	Ensure Power delivered to home and grid by PV	[40]
	Reactive power constraints for PV and ESS	[236]
Aggregator	Ensure energy from only controllable appliances can be sold to grid and neighbors	[41]
	Manage absorption and injection of reactive power	[41]
	Assign a single demand profile for each consumer by the aggregator	[40]
	Enforce current and voltage limits	[41]
	Balance active and reactive power	[40]
	Ensure HEMS aggregator power aligns with schedules by VVO	[40]
	Prevent overlapping buying and selling power processes with the grid	[40]
	Restrict Household Switching Temperature (HST) below transformer limit	[40]
	Power and energy-based soft constraint: Aggregated home power ¡ transformer critical power	[8]
	Enforce constraints for prosumer selling power and predicted PV generation	[18]
Distribution System	Manage active and reactive power of each feeder line phase	[40]
	Enforce three-phase line voltage limits	[40]
	Constrain node square voltage magnitude within allowed range	[40]
	Regulate reactive power supported by Circuit breaker at node	[40]
	Control voltage and OLTC tap changes	[40]
	Limit sold electricity to avoid excessive grid injection	[9]
	Active and reactive power generation limit	[2]
	Flexibility limit	[2]

Appendix B

Results of three objectives use in Varennes Library

Figure B.1 power profiles of the imported power from the grid using three objectives compared with measure value. From these profiles, it can be seen that power consumption is reduced when the peak price occurs using objectives 1 and 2, while the power imported from the grid is higher using the objective of maximizing power export.

Objective 1 is to minimize the energy cost, and Objective 2 is to minimize the energy consumption of the building or maximize the local consumption. Figure B.2 shows that the heat pump, which is a shiftable load, reduces power consumption during high price intervals using the cost minimization objective. Figure B.2 also shows that using maximizing local energy consumption, the PV supply to the building is high, and heat pump power is high when there is local production. When there is no solar, the heat pump is kept as much as possible to reduce power consumption.

Figure B.3 shows the optimal indoor temperature of the building with measure indoor temperature. It can be seen that objective 1 is cost minimization, which reduces the heat consumption of the building, resulting in the reduction in indoor temperature at time interval peak hours. Similarly, using the objective of minimizing energy, the indoor temperature increases when solar power is there, and another interval is kept at a lower bound.

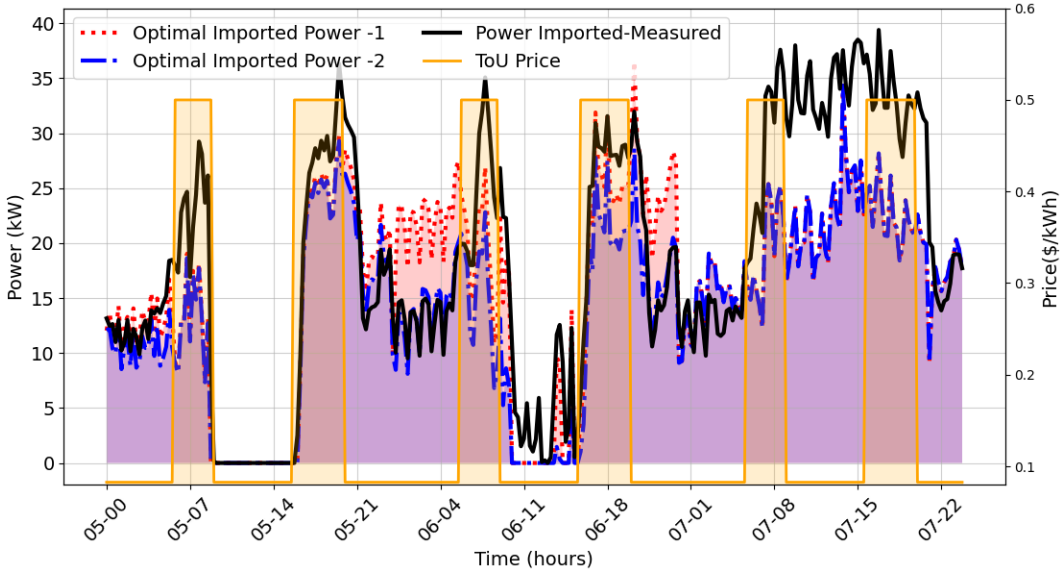

Figure B.1: Power imported from the grid using objectives 1 and 2..

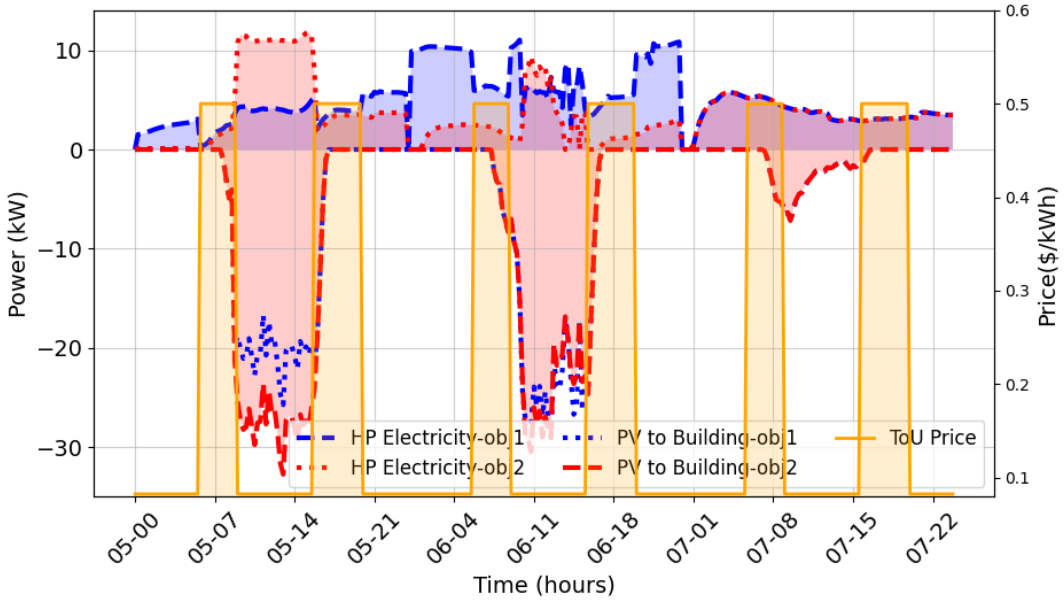

Figure B.2: Controllable load profile using objectives 1 and 2.

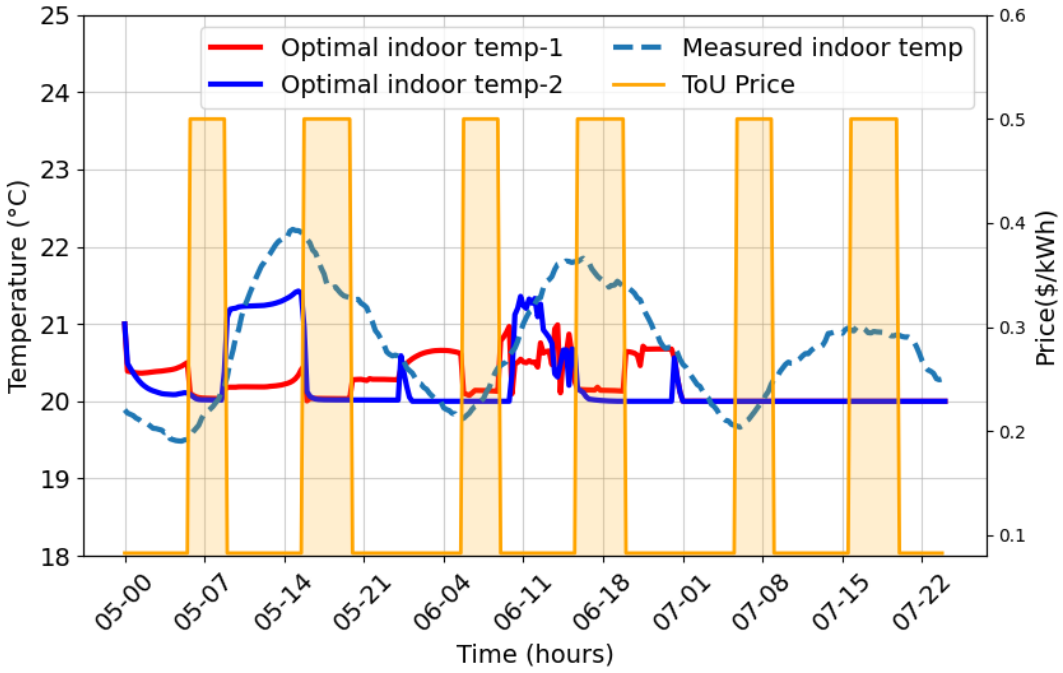

Figure B.3: Indoor temperature profile using objectives 1 and 2.

Appendix C

Proof that MMR Pricing Mechanism is Beneficial

Theorem-1:

For considering mid-market rate pricing schemes in Case-1, Case-2, and Case-3, a pricing mechanism of the proposed P2P trading to confirm the stability of the coalition as well as to guarantee the benefit to the prosumers for forming the social coalition.

Proof:

Case-1: In this scheme, the trading price (i.e., both the selling and buying prices, denoted as $\lambda_{t,b}^{P2P}$ and $\lambda_{t,s}^{P2P}$) must satisfy the condition $\lambda_t^{FiT} \leq \lambda_{t,b}^{P2P}$, $\lambda_{t,s}^{P2P} \leq \lambda_t^{TOU}$. We then consider the three cases outlined above and note that the trading prices in Case 1, the buying price in Case 2, and the selling price in Case 3 all satisfy this condition.

Case-2: Let's start by assuming that the sum of the power demand of the buyers and the sum of all exported power is equal to a constant y as below :

$$y = \frac{\sum_{h_b}^{H_b} P_{h_b,t}^{Dem,G}}{\sum_{h_s}^{H_s} P_{h_s,t}^{Expt,G}} \tag{C.1}$$

We note that for Case 2, y is less than one since the total surplus of the suppliers exceeds the

total power demand. Based on this assumption, we can rewrite equation (5.17) as:

$$\begin{aligned} \lambda_{t,s}^{P2P} &= y \cdot \lambda_t^{P2P} + (1-y)\lambda_t^{FiT} \\ &= (y \cdot \lambda_t^{P2P} + \lambda_t^{FiT}) - y \cdot \lambda_t^{FiT} \end{aligned} \tag{C.2}$$

We then use equation (5.14) to establish that $\lambda_t^{P2P} > \lambda_t^{FiT}$ since $\lambda_t^{TOU} > \lambda_t^{FiT}$. This enables us to confirm that $\lambda_{t,s}^{P2P} \geq \lambda_t^{FiT}$ using equation (C.2).

Now to prove that $\lambda_{t,s}^{P2P} \leq \lambda_t^{TOU}$, we start by assuming the opposite, i.e., $\lambda_{t,s}^{P2P} > \lambda_t^{TOU}$. We then use equation (C.2) to obtain:

$$y \cdot \lambda_t^{P2P} + \lambda_t^{FiT} - y \cdot \lambda_t^{FiT} > \lambda_{t,b}^{P2P} \tag{C.3}$$

We can then substitute λ_t^{P2P} with $\frac{\lambda_t^{FiT}+\lambda_t^{TOU}}{2}$ from equation (5.14) and rearrange the terms to obtain:

$$\lambda_t^{FiT} - \frac{y}{2}\lambda_t^{FiT} > \lambda_t^{TOU} - \frac{y}{2}\lambda_t^{TOU}. \tag{C.4}$$

However, since $y < 1$ and $\lambda_t^{TOU} > \lambda_t^{FiT}$, this inequality cannot hold, which contradicts our initial assumption. Therefore, we can conclude that $\lambda_{t,s}^{P2P} \leq \lambda_{t,b}^{P2P}$, and hence $\lambda_{t,s}^{P2P}$ satisfies the condition $\lambda_t^{FiT} \leq \lambda_{t,s}^{P2P} \leq \lambda_t^{TOU}$.

Case-3: Now to prove that $\lambda_{t,b}^{P2P}$ in equation (5.18) satisfies the condition $\lambda_t^{FiT} \leq \lambda_{t,b}^{P2P} \leq \lambda_t^{TOU}$. We assume that the sum of the exported power of the seller and the power demand of all buyers is equal to a constant y^* in equation (5.18) as below :

$$y^* = \frac{\sum_{h_s}^{H_s} P_{h_s,t}^{Expt,G}}{\sum_{h_b}^{H_b} P_{h_b,t}^{Dem,G}} \tag{C.5}$$

We note that for Case 3, y^* is less than one since the total power demand of the buyer is greater than the total power exported. Based on this assumption, we can rewrite equation (5.18) as:

$$\begin{aligned} \lambda_{t,b}^{P2P} &= y^* \cdot \lambda_t^{P2P} + (1-y^*)\lambda_t^{TOU} \\ &= (y^* \cdot \lambda_t^{P2P} + \lambda_t^{TOU}) - y^* \cdot \lambda_t^{TOU} \end{aligned} \tag{C.6}$$

From (5.14) we can say that $\lambda_t^{P2P} < \lambda_t^{TOU}$ since $\lambda_t^{TOU} > \lambda_t^{FiT}$. This enables us to confirm that $\lambda_{t,b}^{P2P} \leq \lambda_t^{TOU}$ using equation (C.5).

Now to prove that $\lambda_{t,b}^{P2P} \geq \lambda_t^{FiT}$, we assume that $\lambda_{t,b}^{P2P} < \lambda_t^{FiT}$. We then use equation (C.5) to obtain:

$$(y^* \cdot \lambda_t^{P2P} + \lambda_t^{TOU}) - y^* \cdot \lambda_t^{TOU} < \lambda_t^{FiT} \tag{C.7}$$

We can then substitute λ_t^{P2P} with $\frac{\lambda_t^{FiT}+\lambda_t^{TOU}}{2}$ from equation (5.14) and rearrange the terms to obtain:

$$\lambda_t^{TOU} - \frac{y^*}{2}\lambda_t^{TOU} < \lambda_t^{FiT} - \frac{y^*}{2}\lambda_t^{FiT}. \tag{C.8}$$

However, since $y^* < 1$ and $\lambda_t^{TOU} > \lambda_t^{FiT}$, this inequality cannot hold, which contradicts our initial assumption. Therefore, we can conclude that $\lambda_{t,b}^{P2P} \geq \lambda_t^{FiT}$, and hence $\lambda_{t,b}^{P2P}$ satisfies the condition $\lambda_t^{FiT} \leq \lambda_{t,s}^{P2P} \leq \lambda_t^{TOU}$.

Therefore, by showing that both $\lambda_{t,s}^{P2P}$ and $\lambda_{t,b}^{P2P}$ satisfy the required conditions. Therefore, to complete the proof of Theorem 1, we need to demonstrate that both equations (5.17) and (5.18) also satisfy the conditions $\lambda_t^{FiT} \leq \lambda_{t,s}^{P2P} \leq \lambda_t^{TOU}$ and $\lambda_t^{FiT} \leq \lambda_{t,b}^{P2P} \leq \lambda_t^{TOU}$, respectively. Once we establish these conditions, we can conclude that the grand coalition is stable.

Bibliography

[1] S. Hussain, C. Z. El-Bayeh, C. Lai, and U. Eicker, "Multi-Level Energy Management Systems Toward a Smarter Grid: A Review," *IEEE Access*, vol. 9, pp. 71994–72016, 2021.

[2] S. Hussain, C. Lai, and U. Eicker, "Flexibility: Literature review on concepts, modeling, and provision method in smart grid," *Sustainable Energy, Grids and Networks*, p. 101113, 2023.

[3] M. A. Fotouhi Ghazvini, J. Soares, O. Abrishambaf, R. Castro, and Z. Vale, "Demand response implementation in smart households," *Energy Build.*, vol. 143, pp. 129–148, may 2017.

[4] X. Wu, X. Hu, S. Moura, X. Yin, and V. Pickert, "Stochastic control of smart home energy management with plug-in electric vehicle battery energy storage and photovoltaic array," *Journal of Power Sources*, vol. 333, pp. 203–212, 2016.

[5] "Pacific gas and electric company; 2015. tech. rep," 2023.

[6] X. Wu, X. Hu, X. Yin, C. Zhang, and S. Qian, "Optimal battery sizing of smart home via convex programming," *Energy*, vol. 140, pp. 444–453, 2017.

[7] "Feed-in tariffs (fits) in america," 2023.

[8] M. R. Sarker, D. J. Olsen, and M. A. Ortega-Vazquez, "Co-optimization of distribution transformer aging and energy arbitrage using electric vehicles," *IEEE Transactions on Smart Grid*, vol. 8, no. 6, pp. 2712–2722, 2016.

[9] M. Humayun, M. Z. Degefa, A. Safdarian, and M. Lehtonen, "Utilization improvement of transformers using demand response," *IEEE transactions on power delivery*, vol. 30, no. 1, pp. 202–210, 2014.

[10] "Global EV Outlook 2020," *Glob. EV Outlook 2020*, 2020.

[11] H. Farhangi, "The path of the smart grid," *IEEE Power Energy Mag.*, vol. 8, pp. 18–28, jan 2010.

[12] K. Mahmud, B. Khan, J. Ravishankar, A. Ahmadi, and P. Siano, "An internet of energy framework with distributed energy resources, prosumers and small-scale virtual power plants: An overview," *Renew. Sustain. Energy Rev.*, vol. 127, p. 109840, jul 2020.

[13] M. E. Peck and D. Wagman, "Energy trading for fun and profit buy your neighbor's rooftop solar power or sell your own-it'll all be on a blockchain," *IEEE Spectrum*, vol. 54, no. 10, pp. 56–61, 2017.

[14] S. Braithwait, "Behavior modification," *IEEE Power and Energy Magazine*, vol. 8, no. 3, pp. 36–45, 2010.

[15] N. Ruiz, I. Cobelo, and J. Oyarzabal, "A direct load control model for virtual power plant management," *IEEE Transactions on Power Systems*, vol. 24, no. 2, pp. 959–966, 2009.

[16] "Overview of Hydro-Québec's Energy Resources Setting new sights with our clean energy," 2019.

[17] S. G. F. Mohamed, *Control and optimization of energy storage in AC and DC power grids*. PhD thesis, Florida International University, 2019.

[18] C. Z. El-Bayeh, I. Mougharbel, M. Saad, A. Chandra, D. Asber, L. Lenoir, and S. Lefebvre, "Novel soft-constrained distributed strategy to meet high penetration trend of pevs at homes," *Energy and Buildings*, vol. 178, pp. 331–346, 2018.

[19] P. Siano, G. De Marco, A. Rolán, and V. Loia, "A survey and evaluation of the potentials of distributed ledger technology for peer-to-peer transactive energy exchanges in local energy markets," *IEEE Systems Journal*, vol. 13, no. 3, pp. 3454–3466, 2019.

[20] S. Schey, D. Scoffield, and J. Smart, "A first look at the impact of electric vehicle charging on the electric grid in the ev project," *World Electric Vehicle Journal*, vol. 5, no. 3, pp. 667–678, 2012.

[21] K. McKenna and A. Keane, "Residential load modeling of price-based demand response for network impact studies," *IEEE Transactions on Smart Grid*, vol. 7, no. 5, pp. 2285–2294, 2015.

[22] I. Azim, "Peer-to-peer energy trading in low-voltage distribution networks," 2022.

[23] K. Zhang, S. Troitzsch, S. Hanif, and T. Hamacher, "Coordinated market design for peer-to-peer energy trade and ancillary services in distribution grids," *IEEE transactions on smart grid*, vol. 11, no. 4, pp. 2929–2941, 2020.

[24] J. Kim and Y. Dvorkin, "A p2p-dominant distribution system architecture," *IEEE Transactions on Power Systems*, vol. 35, no. 4, pp. 2716–2725, 2019.

[25] "Rate Flex D — Hydro-Québec."

[26] "Hourly ontario energy price (hoep)."

[27] F. Elghitani and W. Zhuang, "Aggregating a large number of residential appliances for demand response applications," *IEEE Transactions on Smart Grid*, vol. 9, no. 5, pp. 5092–5100, 2017.

[28] U. F. E. R. Commission *et al.*, "Assessment of demand response and advanced metering," tech. rep., Staff Report. http://tinyurl. com/38ze3p (or www. ferc. gov/legal/staff . . . , 2007.

[29] N. Sadeghianpourhamami, M. Strobbe, and C. Develder, "Real-world user flexibility of energy consumption: Two-stage generative model construction," in *Proceedings of the 31st Annual ACM Symposium on Applied Computing*, pp. 2148–2153, 2016.

[30] L. Yao, W. H. Lim, and T. S. Tsai, "A real-time charging scheme for demand response in electric vehicle parking station," *IEEE Transactions on Smart Grid*, vol. 8, no. 1, pp. 52–62, 2016.

[31] R. Wang, G. Xiao, and P. Wang, "Hybrid centralized-decentralized (hcd) charging control of electric vehicles," *IEEE Transactions on Vehicular Technology*, vol. 66, no. 8, pp. 6728–6741, 2017.

[32] D. K. Molzahn, F. Dörfler, H. Sandberg, S. H. Low, S. Chakrabarti, R. Baldick, and J. Lavaei, "A survey of distributed optimization and control algorithms for electric power systems," *IEEE Transactions on Smart Grid*, vol. 8, no. 6, pp. 2941–2962, 2017.

[33] S. Nigam, "Reliability assessment of a distribution network with a microgrid," in *2017 North American Power Symposium (NAPS)*, pp. 1–6, IEEE, 2017.

[34] H. Pourbabak, T. Chen, and W. Su, "Centralized, decentralized, and distributed control for energy internet," in *The Energy Internet*, pp. 3–19, Elsevier, 2019.

[35] S. Althaher, P. Mancarella, and J. Mutale, "Automated demand response from home energy management system under dynamic pricing and power and comfort constraints," *IEEE Transactions on Smart Grid*, vol. 6, no. 4, pp. 1874–1883, 2015.

[36] Z. Xu, W. Su, Z. Hu, Y. Song, and H. Zhang, "A hierarchical framework for coordinated charging of plug-in electric vehicles in china," *IEEE Transactions on Smart Grid*, vol. 7, no. 1, pp. 428–438, 2015.

[37] M. Rastegar, M. Fotuhi-Firuzabad, and M. Moeini-Aghtai, "Developing a two-level framework for residential energy management," *IEEE Transactions on Smart Grid*, vol. 9, no. 3, pp. 1707–1717, 2016.

[38] I.-Y. Joo and D.-H. Choi, "Distributed optimization framework for energy management of multiple smart homes with distributed energy resources," *Ieee Access*, vol. 5, pp. 15551–15560, 2017.

[39] O. Alrumayh and K. Bhattacharya, "Flexibility of residential loads for demand response provisions in smart grid," *IEEE Transactions on Smart Grid*, vol. 10, no. 6, pp. 6284–6297, 2019.

[40] D. Mak and D.-H. Choi, "Optimization framework for coordinated operation of home energy management system and volt-var optimization in unbalanced active distribution networks considering uncertainties," *Applied Energy*, vol. 276, p. 115495, 2020.

[41] M. R. Sarker, M. A. Ortega-Vazquez, and D. S. Kirschen, "Optimal coordination and scheduling of demand response via monetary incentives," *IEEE Transactions on Smart Grid*, vol. 6, no. 3, pp. 1341–1352, 2014.

[42] H. Kikusato, K. Mori, S. Yoshizawa, Y. Fujimoto, H. Asano, Y. Hayashi, A. Kawashima, S. Inagaki, and T. Suzuki, "Electric vehicle charge–discharge management for utilization of photovoltaic by coordination between home and grid energy management systems," *IEEE Transactions on Smart Grid*, vol. 10, no. 3, pp. 3186–3197, 2018.

[43] H. R. Gholinejad, A. Loni, J. Adabi, and M. Marzband, "A hierarchical energy management system for multiple home energy hubs in neighborhood grids," *Journal of Building Engineering*, vol. 28, p. 101028, 2020.

[44] D. Li, W.-Y. Chiu, H. Sun, and H. V. Poor, "Multiobjective optimization for demand side management program in smart grid," *IEEE Transactions on Industrial Informatics*, vol. 14, no. 4, pp. 1482–1490, 2017.

[45] Z. Kaheh, R. B. Kazemzadeh, and M. K. Sheikh-El-Eslami, "Simultaneous consideration of the balancing market and day-ahead market in stackelberg game for flexiramp procurement problem in the presence of the wind farms and a dr aggregator," *IET Generation, Transmission & Distribution*, vol. 13, no. 18, pp. 4099–4113, 2019.

[46] M. Alizadeh, M. P. Moghaddam, N. Amjady, P. Siano, and M. Sheikh-El-Eslami, "Flexibility in future power systems with high renewable penetration: A review," *Renewable and Sustainable Energy Reviews*, vol. 57, pp. 1186–1193, 2016.

[47] annex67, "annex67." `https://www.annex67.org/`, 2022. [Online; accessed 18-october-2022].

[48] J. Ma, V. Silva, R. Belhomme, D. S. Kirschen, and L. F. Ochoa, "Evaluating and planning flexibility in sustainable power systems," in *2013 IEEE power & energy society general meeting*, pp. 1–11, IEEE, 2013.

[49] F. Plaum, R. Ahmadiahangar, A. Rosin, and J. Kilter, "Aggregated demand-side energy flexibility: A comprehensive review on characterization, forecasting and market prospects," *Energy Reports*, vol. 8, pp. 9344–9362, 2022.

[50] G. Reynders, J. Diriken, and D. Saelens, "Generic characterization method for energy flexibility: Applied to structural thermal storage in residential buildings," *Applied energy*, vol. 198, pp. 192–202, 2017.

[51] R. De Coninck and L. Helsen, "Quantification of flexibility in buildings by cost curves–methodology and application," *Applied Energy*, vol. 162, pp. 653–665, 2016.

[52] A. Bampoulas, M. Saffari, F. Pallonetto, E. Mangina, and D. P. Finn, "A fundamental unified framework to quantify and characterise energy flexibility of residential buildings with multiple electrical and thermal energy systems," *Applied Energy*, vol. 282, p. 116096, 2021.

[53] C. Finck, R. Li, R. Kramer, and W. Zeiler, "Quantifying demand flexibility of power-to-heat and thermal energy storage in the control of building heating systems," *Applied Energy*, vol. 209, pp. 409–425, 2018.

[54] M. Zade, Z. You, B. Kumaran Nalini, P. Tzscheutschler, and U. Wagner, "Quantifying the flexibility of electric vehicles in germany and california—a case study," *Energies*, vol. 13, no. 21, p. 5617, 2020.

[55] Z. Yu, F. Lu, Y. Zou, and X. Yang, "Quantifying the flexibility of lighting systems by optimal control in commercial buildings: Insight from a case study," *Energy and Buildings*, vol. 225, p. 110310, 2020.

[56] L. Hurtado, J. Rhodes, P. Nguyen, I. Kamphuis, and M. Webber, "Quantifying demand flexibility based on structural thermal storage and comfort management of non-residential buildings: A comparison between hot and cold climate zones," *Applied energy*, vol. 195, pp. 1047–1054, 2017.

[57] M. Afzalan and F. Jazizadeh, "Residential loads flexibility potential for demand response using energy consumption patterns and user segments," *Applied Energy*, vol. 254, p. 113693, 2019.

[58] D. Fischer, T. Wolf, J. Wapler, R. Hollinger, and H. Madani, "Model-based flexibility assessment of a residential heat pump pool," *Energy*, vol. 118, pp. 853–864, 2017.

[59] J. de Jong, A. Hassel, J. Jansen, C. Egenhofer, and Z. Xu, "Improving the market for flexibility in the electricity sector," *Centre for European Policy Studies*, vol. 13093, 2017.

[60] "Strategic platform for innovation and research in intelligent power." `https://ipower-net.weebly.com/`, 2009. Accessed: 2022-10-29.

[61] B. Brandherm, J. Baus, and J. Frey, "Peer energy cloud–civil marketplace for trading renewable energies," in *2012 Eighth International Conference on Intelligent Environments*, pp. 375–378, IEEE, 2012.

[62] D. Gantenbein, C. Binding, B. Jansen, A. Mishra, and O. Sundström, "Ecogrid eu: An efficient ict approach for a sustainable power system," in *2012 Sustainable Internet and ICT for Sustainability (SustainIT)*, pp. 1–6, IEEE, 2012.

[63] "Open Utility. A glimpes into the future of Britain's energy economy," 2022.

[64] "Local electricity retail markets for prosumer smart grid power services. ," 2022.

[65] T. Sousa, T. Soares, P. Pinson, F. Moret, T. Baroche, and E. Sorin, "Peer-to-peer and community-based markets: A comprehensive review," *Renewable and Sustainable Energy Reviews*, vol. 104, pp. 367–378, 2019.

[66] E. A. Soto, L. B. Bosman, E. Wollega, and W. D. Leon-Salas, "Peer-to-peer energy trading: A review of the literature," *Applied Energy*, vol. 283, p. 116268, 2021.

[67] A. J. Satchwell, P. A. Cappers, J. Deason, S. P. Forrester, N. M. Frick, B. F. Gerke, and M. A. Piette, "A conceptual framework to describe energy efficiency and demand response interactions," *Energies*, vol. 13, no. 17, p. 4336, 2020.

[68] P. Munankarmi, J. Maguire, S. P. Balamurugan, M. Blonsky, D. Roberts, and X. Jin, "Community-scale interaction of energy efficiency and demand flexibility in residential buildings," *Applied Energy*, vol. 298, p. 117149, 2021.

[69] Y. Chen, P. Xu, J. Gu, F. Schmidt, and W. Li, "Measures to improve energy demand flexibility in buildings for demand response (dr): A review," *Energy and Buildings*, vol. 177, pp. 125–139, 2018.

[70] K. Aduda, T. Labeodan, W. Zeiler, G. Boxem, and Y. Zhao, "Demand side flexibility: Potentials and building performance implications," *Sustainable cities and society*, vol. 22, pp. 146–163, 2016.

[71] P. Palensky and D. Dietrich, "Demand side management: Demand response, intelligent energy systems, and smart loads," *IEEE transactions on industrial informatics*, vol. 7, no. 3, pp. 381–388, 2011.

[72] J. C. Vasquez, J. M. Guerrero, J. Miret, M. Castilla, and L. G. De Vicuna, "Hierarchical control of intelligent microgrids," *IEEE Industrial Electronics Magazine*, vol. 4, no. 4, pp. 23–29, 2010.

[73] V. Hamidi, F. Li, L. Yao, and M. Bazargan, "Domestic demand side management for increasing the value of wind," in *2008 China International Conference on Electricity Distribution*, pp. 1–10, IEEE, 2008.

[74] C. Eid, E. Koliou, M. Valles, J. Reneses, and R. Hakvoort, "Time-based pricing and electricity demand response: Existing barriers and next steps," *Utilities Policy*, vol. 40, pp. 15–25, 2016.

[75] J. Han and M. A. Piette, "Solutions for summer electric power shortages: Demand response and its applications in air conditioning and refrigerating systems," 2008.

[76] X. Yan, Y. Ozturk, Z. Hu, and Y. Song, "A review on price-driven residential demand response," *Renewable and Sustainable Energy Reviews*, vol. 96, pp. 411–419, 2018.

[77] W. W. Hogan, "Time-of-use rates and real-time prices," *John F. Kennedy School of Government, Harvard University*, 2014.

[78] M. H. Albadi and E. F. El-Saadany, "A summary of demand response in electricity markets," *Electric power systems research*, vol. 78, no. 11, pp. 1989–1996, 2008.

[79] H. Firoozi and H. Khajeh, "Optimal day-ahead scheduling of distributed generations and controllable appliances in microgrid," in *2016 Smart Grids Conference (SGC)*, pp. 1–6, IEEE, 2016.

[80] J. Ponoćko and J. V. Milanović, "Forecasting demand flexibility of aggregated residential load using smart meter data," *IEEE Transactions on Power Systems*, vol. 33, no. 5, pp. 5446–5455, 2018.

[81] K. Paridari and L. Nordström, "Flexibility prediction, scheduling and control of aggregated tcls," *Electric Power Systems Research*, vol. 178, p. 106004, 2020.

[82] F. Wang, B. Xiang, K. Li, X. Ge, H. Lu, J. Lai, and P. Dehghanian, "Smart households' aggregated capacity forecasting for load aggregators under incentive-based demand response programs," *IEEE Transactions on Industry Applications*, vol. 56, no. 2, pp. 1086–1097, 2020.

[83] R. Pinto, R. J. Bessa, and M. A. Matos, "Multi-period flexibility forecast for low voltage prosumers," *Energy*, vol. 141, pp. 2251–2263, 2017.

[84] B. Neupane, T. B. Pedersen, and B. Thiesson, "Utilizing device-level demand forecasting for flexibility markets," in *Proceedings of the Ninth International Conference on Future Energy Systems*, pp. 108–118, 2018.

[85] K. Wang, R. Yin, L. Yao, J. Yao, T. Yong, and N. Deforest, "A two-layer framework for quantifying demand response flexibility at bulk supply points," *IEEE Transactions on Smart Grid*, vol. 9, no. 4, pp. 3616–3627, 2016.

[86] G. De Zotti, S. A. Pourmousavi, J. M. Morales, H. Madsen, and N. K. Poulsen, "Consumers' flexibility estimation at the tso level for balancing services," *IEEE Transactions on Power Systems*, vol. 34, no. 3, pp. 1918–1930, 2018.

[87] K. Kouzelis, Z. H. Tan, B. Bak-Jensen, J. R. Pillai, and E. Ritchie, "Estimation of residential heat pump consumption for flexibility market applications," *IEEE Transactions on Smart Grid*, vol. 6, no. 4, pp. 1852–1864, 2015.

[88] M. Pertl, F. Carducci, M. Tabone, M. Marinelli, S. Kiliccote, and E. C. Kara, "An equivalent time-variant storage model to harness ev flexibility: Forecast and aggregation," *IEEE transactions on industrial informatics*, vol. 15, no. 4, pp. 1899–1910, 2018.

[89] E. C. Kara, M. D. Tabone, J. S. MacDonald, D. S. Callaway, and S. Kiliccote, "Quantifying flexibility of residential thermostatically controlled loads for demand response: a data-driven approach," in *Proceedings of the 1st ACM conference on embedded systems for energy-efficient buildings*, pp. 140–147, 2014.

[90] A. Wang, R. Li, and S. You, "Development of a data driven approach to explore the energy flexibility potential of building clusters," *Applied Energy*, vol. 232, pp. 89–100, 2018.

[91] M. Heleno, M. A. Matos, and J. P. Lopes, "Availability and flexibility of loads for the provision of reserve," *IEEE Transactions on Smart Grid*, vol. 6, no. 2, pp. 667–674, 2014.

[92] V. Rasouli, Á. Gomes, and C. H. Antunes, "Characterization of aggregated demand-side flexibility of small consumers," in *2020 International Conference on Smart Energy Systems and Technologies (SEST)*, pp. 1–6, IEEE, 2020.

[93] N. Ruiz, B. Claessens, J. Jimeno, J. A. López, and D. Six, "Residential load forecasting under a demand response program based on economic incentives," *International Transactions on Electrical Energy Systems*, vol. 25, no. 8, pp. 1436–1451, 2015.

[94] G. Kotsis, I. Moschos, C. Corchero, and M. Cruz-Zambrano, "Demand aggregator flexibility forecast: Price incentives sensitivity assessment," in *2015 12th International Conference on the European Energy Market (EEM)*, pp. 1–5, IEEE, 2015.

[95] C. Gorria, J. Jimeno, I. Laresgoiti, M. Lezaun, and N. Ruiz, "Forecasting flexibility in electricity demand with price/consumption volume signals," *Electric Power Systems Research*, vol. 95, pp. 200–205, 2013.

[96] O. Alrumayh and K. Bhattacharya, "Flexibility of Residential Loads for Demand Response Provisions in Smart Grid," *IEEE Trans. Smart Grid*, vol. 10, no. 6, pp. 6284–6297, 2019.

[97] C. Z. El-Bayeh, I. Mougharbel, M. Saad, A. Chandra, D. Asber, L. Lenoir, and S. Lefebvre, "Novel Soft-Constrained Distributed Strategy to meet high penetration trend of PEVs at homes," *Energy Build.*, vol. 178, pp. 331–346, nov 2018.

[98] F. L. Müller, B. Jansen, and O. Sundström, "Autonomous estimation of the energetic flexibility of buildings," in *2017 American Control Conference (ACC)*, pp. 2713–2718, IEEE, 2017.

[99] H. Khajeh, H. Firoozi, H. Laaksonen, and M. Shafie-khah, "A new local market structure for meeting customer-level flexibility needs," in *2020 International Conference on Smart Energy Systems and Technologies (SEST)*, pp. 1–6, IEEE, 2020.

[100] A. S. Gazafroudi, M. Khorasany, R. Razzaghi, H. Laaksonen, and M. Shafie-khah, "Hierarchical approach for coordinating energy and flexibility trading in local energy markets," *Applied Energy*, vol. 302, p. 117575, 2021.

[101] S. Hussain, O. Alrumayh, R. P. Menon, C. Lai, and U. Eicker, "Novel incentive-based multi-level framework for flexibility provision in smart grids," *IEEE Transactions on Smart Grid*, 2023.

[102] Z. Kaheh, R. B. Kazemzadeh, and M. K. Sheikh-El-Eslami, "Flexible ramping services in power systems: Background, challenges, and procurement methods," *Iranian Journal of Science and Technology, Transactions of Electrical Engineering*, vol. 45, no. 1, pp. 1–13, 2021.

[103] R. E. S. IRENA, "International renewable energy agency," *Renewable Energy Target Setting, Abu Dhabi, UAE*, 2015.

[104] K. Alvehag, "Measures to increase demand side flexibility in the Swedish electricity system Abbreviated version," 2020.

[105] S. S. Torbaghan, N. Blaauwbroek, D. Kuiken, M. Gibescu, M. Hajighasemi, P. Nguyen, G. J. Smit, M. Roggenkamp, and J. Hurink, "A market-based framework for demand side flexibility scheduling and dispatching," *Sustainable Energy, Grids and Networks*, vol. 14, pp. 47–61, 2018.

[106] D. Frieden, A. Tuerk, J. Roberts, S. D'Herbemont, A. F. Gubina, and B. Komel, "Overview of emerging regulatory frameworks on collective self-consumption and energy communities in europe," in *2019 16th International Conference on the European Energy Market (EEM)*, pp. 1–6, IEEE, 2019.

[107] R. Lazdins, A. Mutule, and D. Zalostiba, "Pv energy communities—challenges and barriers from a consumer perspective: A literature review," *Energies*, vol. 14, no. 16, p. 4873, 2021.

[108] W. Tushar, T. K. Saha, C. Yuen, D. Smith, and H. V. Poor, "Peer-to-peer trading in electricity networks: An overview," *IEEE Transactions on Smart Grid*, vol. 11, no. 4, pp. 3185–3200, 2020.

[109] O. Abrishambaf, F. Lezama, P. Faria, and Z. Vale, "Towards transactive energy systems: An analysis on current trends," *Energy Strategy Reviews*, vol. 26, p. 100418, 2019.

[110] F. Rahimi and A. Ipakchi, "Using a transactive energy framework: Providing grid services from smart buildings," *IEEE Electrification Magazine*, vol. 4, no. 4, pp. 23–29, 2016.

[111] J. Guerrero, D. Gebbran, S. Mhanna, A. C. Chapman, and G. Verbič, "Towards a transactive energy system for integration of distributed energy resources: Home energy management, distributed optimal power flow, and peer-to-peer energy trading," *Renewable and Sustainable Energy Reviews*, vol. 132, p. 110000, 2020.

[112] M. Khorasany, Y. Mishra, and G. Ledwich, "Market framework for local energy trading: A review of potential designs and market clearing approaches," *IET Generation, Transmission & Distribution*, vol. 12, no. 22, pp. 5899–5908, 2018.

[113] M. Khorasany, Y. Mishra, and G. Ledwich, "Hybrid trading scheme for peer-to-peer energy trading in transactive energy markets," *IET Generation, Transmission & Distribution*, vol. 14, no. 2, pp. 245–253, 2020.

[114] T. Sousa, T. Soares, P. Pinson, F. Moret, T. Baroche, and E. Sorin, "Peer-to-peer and community-based markets: A comprehensive review," *Renewable and Sustainable Energy Reviews*, vol. 104, pp. 367–378, 2019.

[115] M. J. Fell, "Social impacts of peer-to-peer energy trading: a rapid realist review protocol," *Centre for Research into Energy Demand Solutions (CREDS): Oxford, UK*, 2019.

[116] J. Kang, R. Yu, X. Huang, S. Maharjan, Y. Zhang, and E. Hossain, "Enabling localized peer-to-peer electricity trading among plug-in hybrid electric vehicles using consortium blockchains," *IEEE Transactions on Industrial Informatics*, vol. 13, no. 6, pp. 3154–3164, 2017.

[117] P. Baez-Gonzalez, E. Rodriguez-Diaz, J. C. Vasquez, and J. M. Guerrero, "Peer-to-peer energy market for community microgrids [technology leaders]," *IEEE Electrification Magazine*, vol. 6, no. 4, pp. 102–107, 2018.

[118] F. Moret and P. Pinson, "Energy collectives: A community and fairness based approach to future electricity markets," *IEEE Transactions on Power Systems*, vol. 34, no. 5, pp. 3994–4004, 2018.

[119] L. Wang, Y. Zhang, W. Song, and Q. Li, "Stochastic cooperative bidding strategy for multiple microgrids with peer-to-peer energy trading," *IEEE Transactions on Industrial Informatics*, vol. 18, no. 3, pp. 1447–1457, 2021.

[120] A. Paudel, K. Chaudhari, C. Long, and H. B. Gooi, "Peer-to-peer energy trading in a prosumer-based community microgrid: A game-theoretic model," *IEEE Transactions on Industrial electronics*, vol. 66, no. 8, pp. 6087–6097, 2018.

[121] L. He, Y. Liu, and J. Zhang, "Peer-to-peer energy sharing with battery storage: Energy pawn in the smart grid," *Applied Energy*, vol. 297, p. 117129, 2021.

[122] R. Jing, M. N. Xie, F. X. Wang, and L. X. Chen, "Fair p2p energy trading between residential and commercial multi-energy systems enabling integrated demand-side management," *Applied Energy*, vol. 262, p. 114551, 2020.

[123] Z. Wang, X. Yu, Y. Mu, and H. Jia, "A distributed peer-to-peer energy transaction method for diversified prosumers in urban community microgrid system," *Applied Energy*, vol. 260, p. 114327, 2020.

[124] N. K. Meena, J. Yang, and E. Zacharis, "Optimisation framework for the design and operation of open-market urban and remote community microgrids," *Applied Energy*, vol. 252, p. 113399, 2019.

[125] D. H. Nguyen, "Optimal solution analysis and decentralized mechanisms for peer-to-peer energy markets," *IEEE Transactions on Power Systems*, vol. 36, no. 2, pp. 1470–1481, 2020.

[126] M. Elkazaz, M. Sumner, and D. Thomas, "A hierarchical and decentralized energy management system for peer-to-peer energy trading," *Applied Energy*, vol. 291, p. 116766, 2021.

[127] A. Esmat, M. de Vos, Y. Ghiassi-Farrokhfal, P. Palensky, and D. Epema, "A novel decentralized platform for peer-to-peer energy trading market with blockchain technology," *Applied Energy*, vol. 282, p. 116123, 2021.

[128] C. Lyu, Y. Jia, and Z. Xu, "Fully decentralized peer-to-peer energy sharing framework for smart buildings with local battery system and aggregated electric vehicles," *Applied Energy*, vol. 299, p. 117243, 2021.

[129] C. Giotitsas, A. Pazaitis, and V. Kostakis, "A peer-to-peer approach to energy production," *Technology in Society*, vol. 42, pp. 28–38, 2015.

[130] N. Szabo, "Formalizing and securing relationships on public networks," *First monday*, 1997.

[131] M. Andoni, V. Robu, D. Flynn, S. Abram, D. Geach, D. Jenkins, P. McCallum, and A. Peacock, "Blockchain technology in the energy sector: A systematic review of challenges and opportunities," *Renewable and sustainable energy reviews*, vol. 100, pp. 143–174, 2019.

[132] E. Sorin, L. Bobo, and P. Pinson, "Consensus-based approach to peer-to-peer electricity markets with product differentiation," *IEEE Transactions on Power Systems*, vol. 34, no. 2, pp. 994–1004, 2018.

[133] E. Mengelkamp, J. Gärttner, K. Rock, S. Kessler, L. Orsini, and C. Weinhardt, "Designing microgrid energy markets: A case study: The brooklyn microgrid," *Applied Energy*, vol. 210, pp. 870–880, 2018.

[134] T. Morstyn, A. Teytelboym, and M. D. McCulloch, "Bilateral contract networks for peer-to-peer energy trading," *IEEE Transactions on Smart Grid*, vol. 10, no. 2, pp. 2026–2035, 2018.

[135] S. Chakraborty, T. Baarslag, and M. Kaisers, "Automated peer-to-peer negotiation for energy contract settlements in residential cooperatives," *Applied Energy*, vol. 259, p. 114173, 2020.

[136] Y. Zhou, J. Wu, and C. Long, "Evaluation of peer-to-peer energy sharing mechanisms based on a multiagent simulation framework," *Applied energy*, vol. 222, pp. 993–1022, 2018.

[137] C. Long, J. Wu, C. Zhang, M. Cheng, and A. Al-Wakeel, "Feasibility of peer-to-peer energy trading in low voltage electrical distribution networks," *Energy Procedia*, vol. 105, pp. 2227–2232, 2017.

[138] C. Long, J. Wu, C. Zhang, L. Thomas, M. Cheng, and N. Jenkins, "Peer-to-peer energy trading in a community microgrid," in *2017 IEEE power & energy society general meeting*, pp. 1–5, IEEE, 2017.

[139] W. Tushar, C. Yuen, H. Mohsenian-Rad, T. Saha, H. V. Poor, and K. L. Wood, "Transforming energy networks via peer-to-peer energy trading: The potential of game-theoretic approaches," *IEEE Signal Processing Magazine*, vol. 35, no. 4, pp. 90–111, 2018.

[140] W. Tushar, T. K. Saha, C. Yuen, M. I. Azim, T. Morstyn, H. V. Poor, D. Niyato, and R. Bean, "A coalition formation game framework for peer-to-peer energy trading," *Applied Energy*, vol. 261, p. 114436, 2020.

[141] M. L. Di Silvestre, P. Gallo, M. G. Ippolito, E. R. Sanseverino, and G. Zizzo, "A technical approach to the energy blockchain in microgrids," *IEEE Transactions on Industrial Informatics*, vol. 14, no. 11, pp. 4792–4803, 2018.

[142] W. Tushar, T. K. Saha, C. Yuen, T. Morstyn, H. V. Poor, R. Bean, *et al.*, "Grid influenced peer-to-peer energy trading," *IEEE Transactions on Smart Grid*, vol. 11, no. 2, pp. 1407–1418, 2019.

[143] A. Anees, T. Dillon, and Y.-P. P. Chen, "A novel decision strategy for a bilateral energy contract," *Applied Energy*, vol. 253, p. 113571, 2019.

[144] Y. Wang, K. Lai, F. Chen, Z. Li, and C. Hu, "Shadow price based co-ordination methods of microgrids and battery swapping stations," *Applied Energy*, vol. 253, p. 113510, 2019.

[145] Z. Li, J. Kang, R. Yu, D. Ye, Q. Deng, and Y. Zhang, "Consortium blockchain for secure energy trading in industrial internet of things," *IEEE transactions on industrial informatics*, vol. 14, no. 8, pp. 3690–3700, 2017.

[146] P. Chakraborty, E. Baeyens, and P. P. Khargonekar, "Distributed control of flexible demand using proportional allocation mechanism in a smart grid: Game theoretic interaction and price of anarchy," *Sustainable Energy, Grids and Networks*, vol. 12, pp. 30–39, 2017.

[147] K. A. Melendez, V. Subramanian, T. K. Das, and C. Kwon, "Empowering end-use consumers of electricity to aggregate for demand-side participation," *Applied Energy*, vol. 248, pp. 372–382, 2019.

[148] X. Yang, G. Wang, H. He, J. Lu, and Y. Zhang, "Automated demand response framework in elns: Decentralized scheduling and smart contract," *IEEE Transactions on Systems, Man, and Cybernetics: Systems*, vol. 50, no. 1, pp. 58–72, 2019.

[149] Y. Li, W. Yang, P. He, C. Chen, and X. Wang, "Design and management of a distributed hybrid energy system through smart contract and blockchain," *Applied Energy*, vol. 248, pp. 390–405, 2019.

[150] B. A. Bhatti and R. Broadwater, "Energy trading in the distribution system using a non-model based game theoretic approach," *Applied Energy*, vol. 253, p. 113532, 2019.

[151] S. Noor, W. Yang, M. Guo, K. H. van Dam, and X. Wang, "Energy demand side management within micro-grid networks enhanced by blockchain," *Applied energy*, vol. 228, pp. 1385–1398, 2018.

[152] J. Wang, H. Zhong, C. Wu, E. Du, Q. Xia, and C. Kang, "Incentivizing distributed energy resource aggregation in energy and capacity markets: An energy sharing scheme and mechanism design," *Applied Energy*, vol. 252, p. 113471, 2019.

[153] F. Luo, Z. Y. Dong, G. Liang, J. Murata, and Z. Xu, "A distributed electricity trading system in active distribution networks based on multi-agent coalition and blockchain," *IEEE Transactions on Power Systems*, vol. 34, no. 5, pp. 4097–4108, 2018.

[154] K. Chen, J. Lin, and Y. Song, "Trading strategy optimization for a prosumer in continuous double auction-based peer-to-peer market: A prediction-integration model," *Applied energy*, vol. 242, pp. 1121–1133, 2019.

[155] W. Liu, D. Qi, and F. Wen, "Intraday residential demand response scheme based on peer-to-peer energy trading," *IEEE Transactions on Industrial Informatics*, vol. 16, no. 3, pp. 1823–1835, 2019.

[156] A. Lüth, J. M. Zepter, P. C. del Granado, and R. Egging, "Local electricity market designs for peer-to-peer trading: The role of battery flexibility," *Applied energy*, vol. 229, pp. 1233–1243, 2018.

[157] S. Nguyen, W. Peng, P. Sokolowski, D. Alahakoon, and X. Yu, "Optimizing rooftop photovoltaic distributed generation with battery storage for peer-to-peer energy trading," *Applied Energy*, vol. 228, pp. 2567–2580, 2018.

[158] C. Long, J. Wu, Y. Zhou, and N. Jenkins, "Peer-to-peer energy sharing through a two-stage aggregated battery control in a community microgrid," *Applied energy*, vol. 226, pp. 261–276, 2018.

[159] F. Si, J. Wang, Y. Han, Q. Zhao, P. Han, and Y. Li, "Cost-efficient multi-energy management with flexible complementarity strategy for energy internet," *Applied Energy*, vol. 231, pp. 803–815, 2018.

[160] M. Khorasany, Y. Mishra, and G. Ledwich, "A decentralized bilateral energy trading system for peer-to-peer electricity markets," *IEEE Transactions on industrial Electronics*, vol. 67, no. 6, pp. 4646–4657, 2019.

[161] Z. Li, J. Kang, R. Yu, D. Ye, Q. Deng, and Y. Zhang, "Consortium blockchain for secure energy trading in industrial internet of things," *IEEE Transactions on Industrial Informatics*, vol. 14, no. 8, pp. 3690–3700, 2018.

[162] N. Z. Aitzhan and D. Svetinovic, "Security and privacy in decentralized energy trading through multi-signatures, blockchain and anonymous messaging streams," *IEEE Transactions on Dependable and Secure Computing*, vol. 15, no. 5, pp. 840–852, 2018.

[163] S. Wang, A. F. Taha, J. Wang, K. Kvaternik, and A. Hahn, "Energy crowdsourcing and peer-to-peer energy trading in blockchain-enabled smart grids," *IEEE Transactions on Systems, Man, and Cybernetics: Systems*, vol. 49, no. 8, pp. 1612–1623, 2019.

[164] C. Zhang, J. Wu, Y. Zhou, M. Cheng, and C. Long, "Peer-to-peer energy trading in a microgrid," *Applied Energy*, vol. 220, pp. 1–12, 2018.

[165] M. T. Devine and P. Cuffe, "Blockchain electricity trading under demurrage," *IEEE Transactions on Smart Grid*, vol. 10, no. 2, pp. 2323–2325, 2019.

[166] S. Noor, W. Yang, M. Guo, K. H. van Dam, and X. Wang, "Energy demand side management within micro-grid networks enhanced by blockchain," *Applied Energy*, vol. 228, pp. 1385–1398, 2018.

[167] X. Zhang, S. Zhu, J. He, B. Yang, and X. Guan, "Credit rating based real-time energy trading in microgrids," *Applied energy*, vol. 236, pp. 985–996, 2019.

[168] J. Guerrero, A. C. Chapman, and G. Verbič, "Decentralized p2p energy trading under network constraints in a low-voltage network," *IEEE Transactions on Smart Grid*, vol. 10, no. 5, pp. 5163–5173, 2018.

[169] T. Baroche, P. Pinson, R. L. G. Latimier, and H. B. Ahmed, "Exogenous cost allocation in peer-to-peer electricity markets," *IEEE Transactions on Power Systems*, vol. 34, no. 4, pp. 2553–2564, 2019.

[170] H. Almasalma, S. Claeys, and G. Deconinck, "Peer-to-peer-based integrated grid voltage support function for smart photovoltaic inverters," *Applied Energy*, vol. 239, pp. 1037–1048, 2019.

[171] Y. Xu, H. Sun, and W. Gu, "A novel discounted min-consensus algorithm for optimal electrical power trading in grid-connected dc microgrids," *IEEE Transactions on Industrial Electronics*, vol. 66, no. 11, pp. 8474–8484, 2019.

[172] M. Pilz and L. Al-Fagih, "Recent advances in local energy trading in the smart grid based on game-theoretic approaches," *IEEE Transactions on Smart Grid*, vol. 10, no. 2, pp. 1363–1371, 2017.

[173] W. Tushar, T. K. Saha, C. Yuen, T. Morstyn, M. D. McCulloch, H. V. Poor, and K. L. Wood, "A motivational game-theoretic approach for peer-to-peer energy trading in the smart grid," *Applied energy*, vol. 243, pp. 10–20, 2019.

[174] W. Saad, Z. Han, H. V. Poor, and T. Başar, "A noncooperative game for double auction-based energy trading between phevs and distribution grids," in *2011 IEEE international conference on smart grid communications (SmartGridComm)*, pp. 267–272, IEEE, 2011.

[175] S. Nakamoto and A. Bitcoin, "A peer-to-peer electronic cash system," *Bitcoin.–URL: https://bitcoin. org/bitcoin. pdf*, vol. 4, p. 2, 2008.

[176] K. Christidis and M. Devetsikiotis, "Blockchains and smart contracts for the internet of things," *Ieee Access*, vol. 4, pp. 2292–2303, 2016.

[177] M. Rastegar, M. Fotuhi-Firuzabad, H. Zareipour, and M. Moeini-Aghtaieh, "A probabilistic energy management scheme for renewable-based residential energy hubs," *IEEE Transactions on Smart Grid*, vol. 8, no. 5, pp. 2217–2227, 2016.

[178] M. Nistor and C. H. Antunes, "Integrated management of energy resources in residential buildings—a markovian approach," *IEEE Transactions on Smart Grid*, vol. 9, no. 1, pp. 240–251, 2016.

[179] K. Oikonomou and M. Parvania, "Optimal coordination of water distribution energy flexibility with power systems operation," *IEEE Transactions on Smart Grid*, vol. 10, no. 1, pp. 1101–1110, 2018.

[180] F. Lezama, J. Palominos, A. Y. Rodríguez-González, A. Farinelli, and E. Munoz de Cote, "Agent-based microgrid scheduling: An ict perspective," *Mobile Networks and Applications*, vol. 24, no. 5, pp. 1682–1698, 2019.

[181] T. Logenthiran, D. Srinivasan, and T. Z. Shun, "Demand side management in smart grid using heuristic optimization," *IEEE transactions on smart grid*, vol. 3, no. 3, pp. 1244–1252, 2012.

[182] U. S. E. Framework, "Usef: The framework explained," *Arnhem: USEF*, 2015.

[183] N. Paterakis, O. Erdinc, A. B. I. T. on ..., and undefined 2015, "Optimal household appliances scheduling under day-ahead pricing and load-shaping demand response strategies," *ieeexplore.ieee.org*.

[184] W. E. Hart, J.-P. Watson, and D. L. Woodruff, "Pyomo: modeling and solving mathematical programs in python," *Mathematical Programming Computation*, vol. 3, no. 3, pp. 219–260, 2011.

[185] IBM, "IBM ILOG CPLEX Optimization Studio," 2012.

[186] COIN—OR, "IPOPT," 2017.

[187] H. sadat, *Power system Analysis*. 1999.

[188] E. Jalilov, *Development of Heuristic Model-Based Predictive Control Strategies for an Institutional Net-Zero Energy Building*. PhD thesis, Concordia University, 2021.

[189] H. Hao, D. Wu, J. Lian, and T. Yang, "Optimal coordination of building loads and energy storage for power grid and end user services," *IEEE Transactions on Smart Grid*, vol. 9, no. 5, pp. 4335–4345, 2017.

[190] E. Yao, P. Samadi, V. W. Wong, and R. Schober, "Residential demand side management under high penetration of rooftop photovoltaic units," *IEEE Transactions on Smart Grid*, vol. 7, no. 3, pp. 1597–1608, 2015.

[191] S. Huang and Q. Wu, "Real-time congestion management in distribution networks by flexible demand swap," *IEEE Transactions on Smart Grid*, vol. 9, no. 5, pp. 4346–4355, 2017.

[192] S. Gottwalt, J. Gärttner, H. Schmeck, and C. Weinhardt, "Modeling and valuation of residential demand flexibility for renewable energy integration," *IEEE Transactions on Smart Grid*, vol. 8, no. 6, pp. 2565–2574, 2016.

[193] M. Rastegar, M. Fotuhi-Firuzabad, and M. Moeini-Aghtai, "Developing a two-level framework for residential energy management," *IEEE Trans. Smart Grid*, vol. 9, no. 3, pp. 1707–1717, 2018.

[194] Q. Hu, F. Li, X. Fang, and L. Bai, "A framework of residential demand aggregation with financial incentives," *IEEE Transactions on Smart Grid*, vol. 9, no. 1, pp. 497–505, 2016.

[195] F. Lezama, J. Soares, B. Canizes, and Z. Vale, "Flexibility management model of home appliances to support dso requests in smart grids," *Sustainable Cities and Society*, vol. 55, p. 102048, 2020.

[196] M. Elkazaz, M. Sumner, and D. Thomas, "A hierarchical centralized community energy management system using a model predictive controller," in *2020 International Conference on Smart Grids and Energy Systems (SGES)*, pp. 801–806, IEEE, 2020.

[197] D. Neves, I. Scott, and C. A. Silva, "Peer-to-peer energy trading potential: An assessment for the residential sector under different technology and tariff availabilities," *Energy*, vol. 205, pp. 118023: 1–15, Aug. 2020.

[198] M. S. Javadi, A. E. Nezhad, A. R. Jordehi, M. Gough, S. F. Santos, and J. P. Catalão, "Transactive energy framework in multi-carrier energy hubs: A fully decentralized model," *Energy*, vol. 238, p. 121717, 2022.

[199] C. García-Santacruz, P. J. Gómez, J. M. Carrasco, and E. Galván, "Multi P2P energy trading market, integrating energy storage systems and used for optimal scheduling," *IEEE Access*, vol. 10, pp. 64302–64315, 2022.

[200] M. Mehdinejad, H. Shayanfar, and B. Mohammadi-Ivatloo, "Decentralized blockchain-based peer-to-peer energy-backed token trading for active prosumers," *Energy*, vol. 244, pp. 122713: 1–15, Apr. 2022.

[201] W.-Y. Zhang, B. Zheng, W. Wei, L. Chen, and S. Mei, "Peer-to-peer transactive mechanism for residential shared energy storage," *Energy*, vol. 246, pp. 123204: 1–12, May 2022.

[202] Y. Xia, Q. Xu, S. Tao, P. Du, Y. Ding, and J. Fang, "Preserving operation privacy of peer-to-peer energy transaction based on enhanced benders decomposition considering uncertainty of renewable energy generations," *Energy*, vol. 250, p. 123567, Jul. 2022.

[203] N. G. Paterakis, O. Erdinç, I. N. Pappi, A. G. Bakirtzis, and J. P. Catalão, "Coordinated operation of a neighborhood of smart households comprising electric vehicles, energy storage and distributed generation," *IEEE Transactions on smart grid*, vol. 7, no. 6, pp. 2736–2747, 2016.

[204] C. de Mattos Affonso and M. Kezunovic, "Technical and economic impact of PV-BESS charging station on transformer life: A case study," *IEEE Transactions on Smart Grid*, vol. 10, no. 4, pp. 4683–4692, 2018.

[205] S. Haider, R. e. Z. Rizvi, J. Walewski, and P. Schegner, "Investigating peer-to-peer power transactions for reducing EV induced network congestion," *Energy*, vol. 254, pp. 124317: 1–20, Sep. 2022.

[206] Y. Chen, W. Pei, T. Ma, and H. Xiao, "Asymmetric Nash bargaining model for peer-to-peer energy transactions combined with shared energy storage," *Energy*, vol. 278, pp. 127980: 1–13, Sep. 2023.

[207] M. I. Azim, W. Tushar, and T. K. Saha, "Investigating the impact of P2P trading on power losses in grid-connected networks with prosumers," *Applied Energy*, vol. 263, p. 114687, 2020.

[208] S.-W. Park, Z. Zhang, F. Li, and S.-Y. Son, "Peer-to-peer trading-based efficient flexibility securing mechanism to support distribution system stability," *Applied Energy*, vol. 285, p. 116403, 2021.

[209] M. F. Dynge, P. C. del Granado, N. Hashemipour, and M. Korpås, "Impact of local electricity markets and peer-to-peer trading on low-voltage grid operations," *Applied Energy*, vol. 301, p. 117404, 2021.

[210] T. A. Short, *Electric power distribution handbook*. CRC press, 2003.

[211] IEEE, "Guide for loading mineral-oil-immersed transformers," *IEEE Standard*, vol. 57, pp. 91–1995, 1995.

[212] R. Yu, J. Ding, W. Zhong, Y. Liu, and S. Xie, "Phev charging and discharging cooperation in v2g networks: A coalition game approach," *IEEE Internet of Things Journal*, vol. 1, no. 6, pp. 578–589, 2014.

[213] D. J. Olsen, M. R. Sarker, and M. A. Ortega-Vazquez, "Optimal penetration of home energy management systems in distribution networks considering transformer aging," *IEEE Transactions on Smart Grid*, vol. 9, no. 4, pp. 3330–3340, 2016.

[214] M. I. Azim, S. Pourmousavi, W. Tushar, and T. K. Saha, "Feasibility study of financial P2P energy trading in a grid-tied power network," in *2019 IEEE Power & Energy Society General Meeting (PESGM)*, pp. 1–5, IEEE, 2019.

[215] A. Al-Sorour, M. Fazeli, M. Monfared, A. Fahmy, J. R. Searle, and R. P. Lewis, "Enhancing PV self-consumption within an energy community using MILP-based P2P trading," *IEEE Access*, vol. 10, pp. 93760–93772, 2022.

[216] "Pecanstreet: Energy Dataport," 2023.

[217] P. Siano, "Demand response and smart grids—a survey," *Renewable and sustainable energy reviews*, vol. 30, pp. 461–478, 2014.

[218] C. Long and L. F. Ochoa, "Voltage control of pv-rich lv networks: Oltc-fitted transformer and capacitor banks," *IEEE Transactions on Power Systems*, vol. 31, no. 5, pp. 4016–4025, 2015.

[219] M. S. H. Nizami, M. J. Hossain, and E. Fernandez, "Multiagent-based transactive energy management systems for residential buildings with distributed energy resources," *IEEE Transactions on Industrial Informatics*, vol. 16, no. 3, pp. 1836–1847, 2019.

[220] Y. Guo, M. Pan, Y. Fang, and P. P. Khargonekar, "Decentralized coordination of energy utilization for residential households in the smart grid," *IEEE transactions on smart grid*, vol. 4, no. 3, pp. 1341–1350, 2013.

[221] B. Moradzadeh and K. Tomsovic, "Two-stage residential energy management considering network operational constraints," *IEEE Transactions on Smart Grid*, vol. 4, no. 4, pp. 2339–2346, 2013.

[222] J. H. Yoon, R. Baldick, and A. Novoselac, "Dynamic demand response controller based on real-time retail price for residential buildings," *IEEE Transactions on Smart Grid*, vol. 5, no. 1, pp. 121–129, 2014.

[223] C. Vivekananthan, Y. Mishra, G. Ledwich, and F. Li, "Demand response for residential appliances via customer reward scheme," *IEEE transactions on smart grid*, vol. 5, no. 2, pp. 809–820, 2014.

[224] M. I. Azim, A. S. Gazafroudi, and M. Khorasany, "Generation-side and demand-side player-centric tradings in the LEM: Rule-empowered models and case studies," in *Trading in Local Energy Markets and Energy Communities: Concepts, Structures and Technologies*, pp. 221–239, Feb. 2023.

[225] M. I. Azim, M. R. Alam, W. Tushar, T. K. Saha, and C. Yuen, "A cooperative P2P trading framework: Developed and validated through hardware-in-loop," *IEEE Transactions on Smart Grid*, vol. 14, no. 4, pp. 2999–3015, Jul. 2023.

[226] D. Teixeira, L. Gomes, and Z. Vale, "Single-unit and multi-unit auction framework for peer-to-peer transactions," *International Journal of Electrical Power & Energy Systems*, vol. 133, pp. 107235: 1–11, Dec. 2021.

[227] L. Ali, M. I. Azim, J. Peters, V. Bhandari, A. Menon, V. Tiwari, J. Green, and S. Muyeen, "Application of a community battery-integrated microgrid in a blockchain-based local energy market accommodating P2P trading," *IEEE Access*, vol. 11, pp. 29635–29649, Mar. 2023.

[228] H. K. Lopez and A. Zilouchian, "Peer-to-peer energy trading for photo-voltaic prosumers," *Energy*, p. 125563, 2022.

[229] Y. Xia, Q. Xu, and F. Li, "Grid-friendly pricing mechanism for peer-to-peer energy sharing market diffusion in communities," *Applied Energy*, vol. 334, pp. 120685: 1–16, Mar. 2023.

[230] S. Cui, Y.-W. Wang, Y. Shi, and J.-W. Xiao, "A new and fair peer-to-peer energy sharing framework for energy buildings," *IEEE Transactions on Smart Grid*, vol. 11, no. 5, pp. 3817–3826, 2020.

[231] D. Li, J.-H. Bae, and M. Rishi, "A preference analysis for a peer-to-peer (p2p) electricity trading platform in south korea," *Energies*, vol. 15, no. 21, p. 7973, 2022.

[232] T. Chernova and E. Gryazina, "Peer-to-peer market with network constraints, user preferences and network charges," *International Journal of Electrical Power & Energy Systems*, vol. 131, pp. 106981: 1–12, Oct. 2021.

[233] V. Rigoni and A. Keane, "Open-dsopf: an open-source optimal power flow formulation integrated with opendss," in *2020 IEEE Power & Energy Society General Meeting (PESGM)*, pp. 1–5, IEEE, 2020.

[234] P. A. Garcia, J. L. R. Pereira, S. Carneiro, V. M. Da Costa, and N. Martins, "Three-phase power flow calculations using the current injection method," *IEEE Transactions on power systems*, vol. 15, no. 2, pp. 508–514, 2000.

[235] H. T. Dinh, D. Kim, and D. Kim, "Milp-based optimal day-ahead scheduling for system-centric cems supporting different types of homes and energy trading," *arXiv preprint arXiv:2202.10181*, 2022.

[236] D. Mak and D.-H. Choi, "Smart home energy management in unbalanced active distribution networks considering reactive power dispatch and voltage control," *IEEE Access*, vol. 7, pp. 149711–149723, 2019.